



# PHYLOGENY OF GENUS *CUPULADRIA* (BRYOZOA, CHEILOSTOMATA) IN THE NEOGENE OF TROPICAL AMERICA

AMALIA HERRERA-CUBILLA<sup>1</sup> AND JEREMY B. C. JACKSON<sup>1,2,3</sup>

<sup>1</sup>Center for Tropical Paleoecology and Archeology, Smithsonian Tropical Research Institute, MRC 0580-01 Box 0843–03092 Panama, Republic of Panama, <herreraa@si.edu>; <sup>2</sup>Center for Marine Biodiversity and Conservation, Scripps Institution of Oceanography, University of California, San Diego, La Jolla, CA 92093-0244, USA; and <sup>3</sup>Department of Paleobiology, MRC-121, National Museum of Natural History, PO Box 37012, Washington, DC 20013-7012, USA, <jeremybcjackson@gmail.com>

**ABSTRACT**—We used 57 morphometric characters to discriminate 17 extant and fossil *Cupuladria* species and analyzed their phylogenetic relationships in relation to extant *Discoporella* species. Data were gathered from 496 extant and fossil *Cupuladria* specimens ranging in age from early Miocene to Recent and distributed from the Caribbean to tropical eastern Pacific. A first series of discriminant analyses distinguished three morphological groups: *Cupuladria* with vicarious avicularia, *Cupuladria* without vicarious avicularia, and *Discoporella*. Further discriminant analyses identified 17 species of *Cupuladria*. Cladistic analyses of these three groups yielded four equally parsimonious trees. All of the consensus trees exhibited the same topology, dividing the 25 tropical American cupuladriids into four distinct monophyletic clades, including *Discoporella*, and are consistent with previous molecular phylogenies except that there are no molecular data for the C<sub>V2</sub> clade. Diversification of species was higher in the C<sub>V1</sub> and C<sub>V2</sub> clades than C<sub>NV</sub> clade, and involved mostly Caribbean species. *Cupuladria* with vicarious clade 1 (C<sub>V1</sub>) includes: *C. monotrema*, *C. pacificensis*, *C. exfragminis*, *C. cheethami*, *C. biporosa*, and four new species: *C. pervagata*, *C. floridensis*, *C. colonensis* and *C. dominicana*. *Cupuladria* with vicarious clade 2 (C<sub>V2</sub>) includes: *C. multesima*, *C. incognita*, and three new species *C. collyrida*, *C. veracruxiensis* and *C. planissima*. *Cupuladria* clade without vicarious (C<sub>NV</sub>) includes: *C. surinamensis*, *C. panamensis*, and one new species *C. gigas*. The stratigraphic occurrence of species is consistent with cladogram topology within clades. However hypothesized cladistic relations among clades are the reverse of their stratigraphic occurrence with younger clade C<sub>NV</sub> appearing as the hypothetical ancestor of the two older clades C<sub>V1</sub> and C<sub>V2</sub>. More extensive collections of early to middle Miocene specimens of *Cupuladria* and *Discoporella* will be required to resolve this apparent paradox.

## INTRODUCTION

CUPULADRIID BRYOZOANS in the genera *Cupuladria* and *Discoporella* are among the most diverse and abundant bryozoans in tropical American seas where they have dominated shallow-water faunas since the early Miocene (Cheetham et al., 1999; Cheetham and Jackson, 2000; O’Dea et al., 2004). This great abundance and diversity have made cupuladriids a model system for studies of diversification and extinction, life history evolution, systematics, and paleoceanographic analysis (O’Dea and Jackson, 2002; Dick et al., 2003; O’Dea et al., 2004, 2007, 2008; Herrera-Cubilla et al., 2006, 2008; O’Dea, 2006; O’Dea and Jackson, 2009; Jagadeeshan and O’Dea, 2012). In particular, the striking responses of cupuladriid faunas to the gradual isolation of the tropical eastern Pacific from the Caribbean by the uplift of the Isthmus of Panama, and attendant major changes in oceanographic conditions, have provided deep insight into the role of environmental change in driving major ecological and evolutionary events.

In the course of these studies, it has become apparent that cupuladriid species diversity based upon both morphometric and genetic analyses is several times greater than reported previously (Dick et al., 2003; Herrera-Cubilla et al., 2006, 2008; O’Dea and Jackson, 2009); a pattern previously demonstrated for other cheilostome bryozoans (Cheetham, 1986; Jackson and Cheetham, 1990, 1994; Cheetham and Jackson, 1996; Cheetham et al., 2007) and marine invertebrates generally (Knowlton, 1993; Knowlton and Jackson, 1994). Phylogenetic studies, however, have been restricted to

molecular analyses of living species with no contribution from the fossil record.

In this paper we develop a first phylogeny of the genus *Cupuladria* based on morphometric analysis of 17 living and fossil species of *Cupuladria* and eight extant species of *Discoporella*. The 17 *Cupuladria* species include all those described by Herrera-Cubilla et al. (2006) plus additional living and fossil species from the Gulf of Mexico, Greater Antilles, Honduras, Nicaragua, Panama, Colombia, and Guyana in the western Atlantic; and Mexico, Panama, and Colombia in the eastern Pacific. Morphological techniques comparable to those in our previous studies were used for species discrimination (Herrera-Cubilla et al., 2006, 2008). We used the same morphologically based approach for cladistic analysis developed by Cheetham et al. (2006, 2007). Extant *Discoporella* species (Herrera-Cubilla et al., 2008) were added to the cladistic analyses to help delineate overall generic relations within the family Cupuladriidae, but further study is required to discriminate fossil *Discoporella* species. We also visually fitted the cladogram topology to the stratigraphic ranges of species to compare their hypothesized times of divergence with the first occurrence of species in the fossil record.

## COLLECTIONS

All the specimens were collected from Neogene to Recent marine deposits in the Caribbean and tropical eastern Pacific. The stratigraphic provenance of fossil *Cupuladria* examined is summarized in Figure 1. Eighty-one percent were collected by the Panama Paleontological Project (PPP) in Panama, Costa Rica, Honduras and Nicaragua, currently housed at the

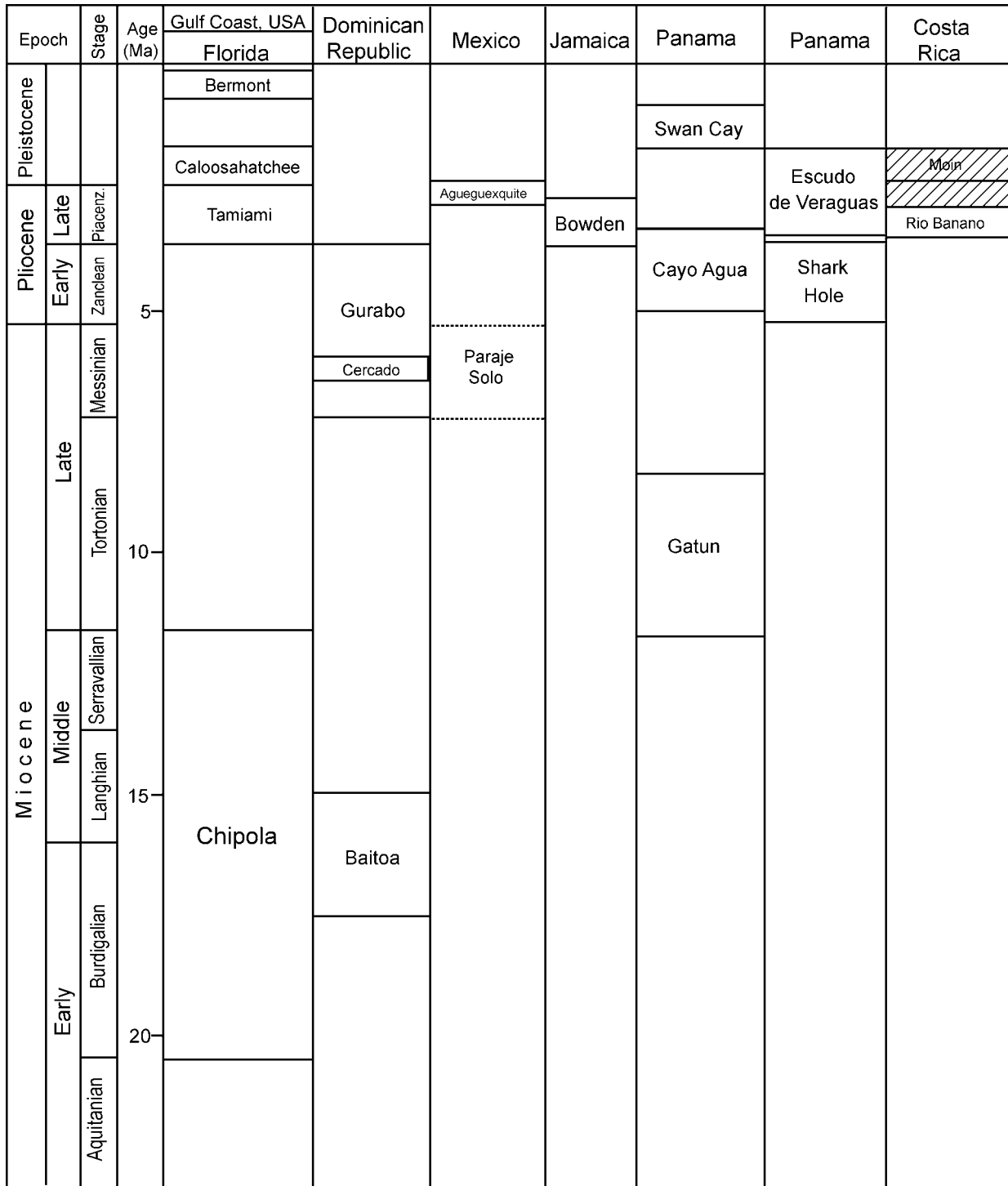


FIGURE 1—Neogene correlation chart, showing formations in tropical America from which *Cupuladria* was collected. Modified after Cheetham et al., 2007, according to Graham, 1976, Coates et al., 2005, and McNeill et al., 2012.

Smithsonian Tropical Research Institute in Panama. The remainder were obtained from the following museum collections: Neogene Paleontology of the Northern Dominican Republic Project (DR) and additional collections, Department of Paleobiology, National Museum of Natural History, Washington DC; Department of Palaeontology, the Natural History Museum, London; Section of Fossil Protists and Invertebrates, Louisiana State University, Museum of Natural Science; Department of Marine Invertebrates, Museum of Comparative

Zoology, Harvard University; Invertebrate Paleontology Division, Florida Museum of Natural History (FLMNH), University of Florida; and Museo de Historia Natural Marina de Colombia, Instituto de Investigaciones Marinas y Costeras. The museum collections include specimens from Florida, the Gulf of Mexico, the Greater Antilles, Caribbean Colombia, Guyana, and the eastern Pacific coast of Mexico.

Data for PPP fossil localities are in electronic file, LOCDBAS4.DBF, dated 20 April 2005, available on the PPP

World Wide Web site (Collins, 2005) and Coates (1999a, 1999b). Locality data for the DR Project samples are published in Saunders et al. (1986). Locality data for extant (SURVEY) specimens collected by the PPP along both coasts of Panama between 1995 and 1998 are published in Herrera-Cubilla et al. (2006, 2008). Locality data are also available for specimens borrowed from FLMNH on its Invertebrate Paleontology Database on the FLMNH World Wide Web site, dated 10 May 2010. Additional locality data are provided in the specimen descriptions in the Systematic Paleontology section.

#### TAXONOMIC CHARACTERS

We used a combination of traditional zooidal characters and non-traditional colonial characters as in our previous studies (Fig. 2; Herrera-Cubilla et al., 2006, 2008). Characters include primary information on zooidal dimensions such as width and length; colony-level characters such as size, shape, and dry weights of whole colonies; and ‘shape’ or ratio characters calculated between various pairs of the original measured characters. We used the term vicarious avicularium following Cook and Chimonides (1994, p. 254), who defined them as “large avicularia which replace and autozooid, but do not replace the distal zooidal avicularian subunit” (vibraculum). “The zoecial vibracula, although apparently inserted between the zooecia at the frontal surface . . . are not strictly interzoecial, nor are they adventitious or dependent” (Cook, 1965a, p. 156). Some new characters including autozooids (Zcp), vicarious avicularia with closure plates (Vcp), and kenozooids at the margin of the colony (Ken) (Fig. 3) were scored 0 or 1 on an individual-colony basis. All measurements were re-scaled as in previous studies  $\log_{10}(1+\text{variable})$ . Table 1 contains the full set of 57 morphological characters used for discrimination of taxa and subsequent cladistic analysis.

#### DISCRIMINATION OF SPECIES

All multivariable analyses for the morphometric discrimination of species were performed with PASW statistical software (SPSS Inc., 2009). A total of 20 separate discriminant analyses described below are numbered sequentially as DA1, DA2 . . . DA20.

*Extant species of Cupuladria and Discoporella.*—We used a sequence of two discriminant analyses to examine the morphological distances among species of *Cupuladria* and *Discoporella* for 15 extant species of the two genera from both sides of the Isthmus of Panama previously described by Herrera-Cubilla et al. (2006, 2008). The analyses were based on 54 of the 57 morphometric characters listed in Table 1, including most of the characters used in earlier analyses plus ten new characters related to the vicarious avicularia and their vibracula. The three characters Zcp, Vcp and Ken were not included because they are only present in fossils. The 54 characters were measured or scored from 258 colonies that were entered as ‘groups’ into a linear discriminant analysis (DA).

The initial DA1 clearly separated the 15 previously described species into two groups: *Cupuladria* species with vicarious avicularia (henceforth termed “vicarious *Cupuladria*”) and *Cupuladria* species without vicarious (henceforth “non-vicarious *Cupuladria*”) along with *Discoporella* species (above and below in Fig. 4.1). The two groups were different at  $p < 0.0001$  with 100 percent of colonies correctly classified and jackknife values of 98.5 percent (Table 2). Characters with the highest coefficients in the DA were: Cw, Ch, Rahw, VI, VOwVOI, and RaVawVw. We then ran a second DA2 to resolve further the cluster of non-vicarious *Cupuladria* plus *Discoporella* cluster (Fig. 4.2). This analysis clearly separated all the *Discoporella* species (above), from the non-vicarious *Cupuladria* species (below), at  $p < 0.0001$ ,

99.1 percent of colonies were correctly classified versus 90.9 percent jackknife (Table 2). The first three discriminant functions account for 92 percent of the total variance. Characters with highest coefficients were: Cw, Graden, Aw, AwAl, RaOIzI, and RaAloAl. The linear pattern exhibited by non-vicarious *Cupuladria* is due to the contribution of Cw, Graden and Aw that have the highest coefficients along the DF1.

*Recent and fossil Cupuladria species.*—Having thus confirmed the strong differences between *Cupuladria* and *Discoporella*, and between vicarious and non-vicarious *Cupuladria*, we next performed an extensive second series of DA to discriminate extant and fossil species of vicarious and non-vicarious *Cupuladria*. Here we used a modification of our earlier methods (Herrera-Cubilla et al., 2006, 2008) to incorporate part of the methodology used by Cheetham et al. (2006, 2007).

A subset of 91 well-preserved colonies of extant and fossil *Cupuladria* was chosen subjectively to maximize the range of morphological, geographic, and stratigraphic variation (present) in the whole dataset (see Cheetham et al., 2006, 2007). The principal criteria for this preliminary selection included differences among species observed previously plus variations in colony size and shape, closure plates of autozooids and vicarious avicularia, evidence for determinate growth, shape of the basal sectors, and numbers of pores. These 91 colonies were entered as ‘groups’ in a third discriminant analysis (DA3) based on all of the 52 characters observed for *Cupuladria* (opesiules, pores, related to the nearly complete cryptocyst of *Discoporella* and basal granules are absent in *Cupuladria*; see Table 1 for details). DA3 distinguished two clusters of vicarious (N=70) and non-vicarious colonies (N=21) (Fig. 5), just as for recent colonies of *Cupuladria* (Herrera-Cubilla et al., 2006, fig. 2). The clusters were different at  $p < 0.0001$ , success of classification was 100 percent versus 97 percent jackknifed. The first three discriminant functions account for 99.9 percent of the total variance. The characters with the highest coefficients were the VI, Vw, VAl, VOwVOI, OwOI, RaAloOI. Separation of vicarious from non-vicarious *Cupuladria* along DF2 is due to VAwo, Vw, and VOwVOI which have in rank order the highest coefficients.

The 70 colonies with vicarious avicularia and 21 colonies without vicarious avicularia were treated separately in a series of hierarchical cluster analyses using the average linkage method based on Euclidean distances to obtain discrete groups to begin the process of discriminating morphospecies in each group. The resulting clusters were next tested for stability in a series of DA to determine whether the groups were significantly different from each other and whether each colony was correctly assigned to its group (Jackson and Cheetham, 1994; Herrera-Cubilla et al., 2006, 2008). The resulting groups, or morphospecies, thus discriminated were used to classify batches of colonies randomly selected from the whole dataset that were entered unassigned in a second series of DAs. Correctness of classification was determined by whether a colony was assigned to its higher probability group, given the function coefficients calculated by the DA. After each DA, the process of combining groups, reassigning colonies to their highest probability groups, or leaving incorrectly classified colonies unassigned for entry in the next DA, was made manually. Classification of colonies was cross-validated by first order or higher order jackknifing. These methods are equal to those employed in previous studies (including Cheetham et al., 2006, 2007).

*Colonies with vicarious avicularia.*—Hierarchical cluster analysis of 70 colonies with vicarious avicularia based on 52 characters yielded 20 discrete groups with a Similarity Coefficient  $\leq 0.03$  plus four outliers (5.7% of total specimens). Three rounds of DAs (DA4–DA6) reduced the 20 clusters of vicarious

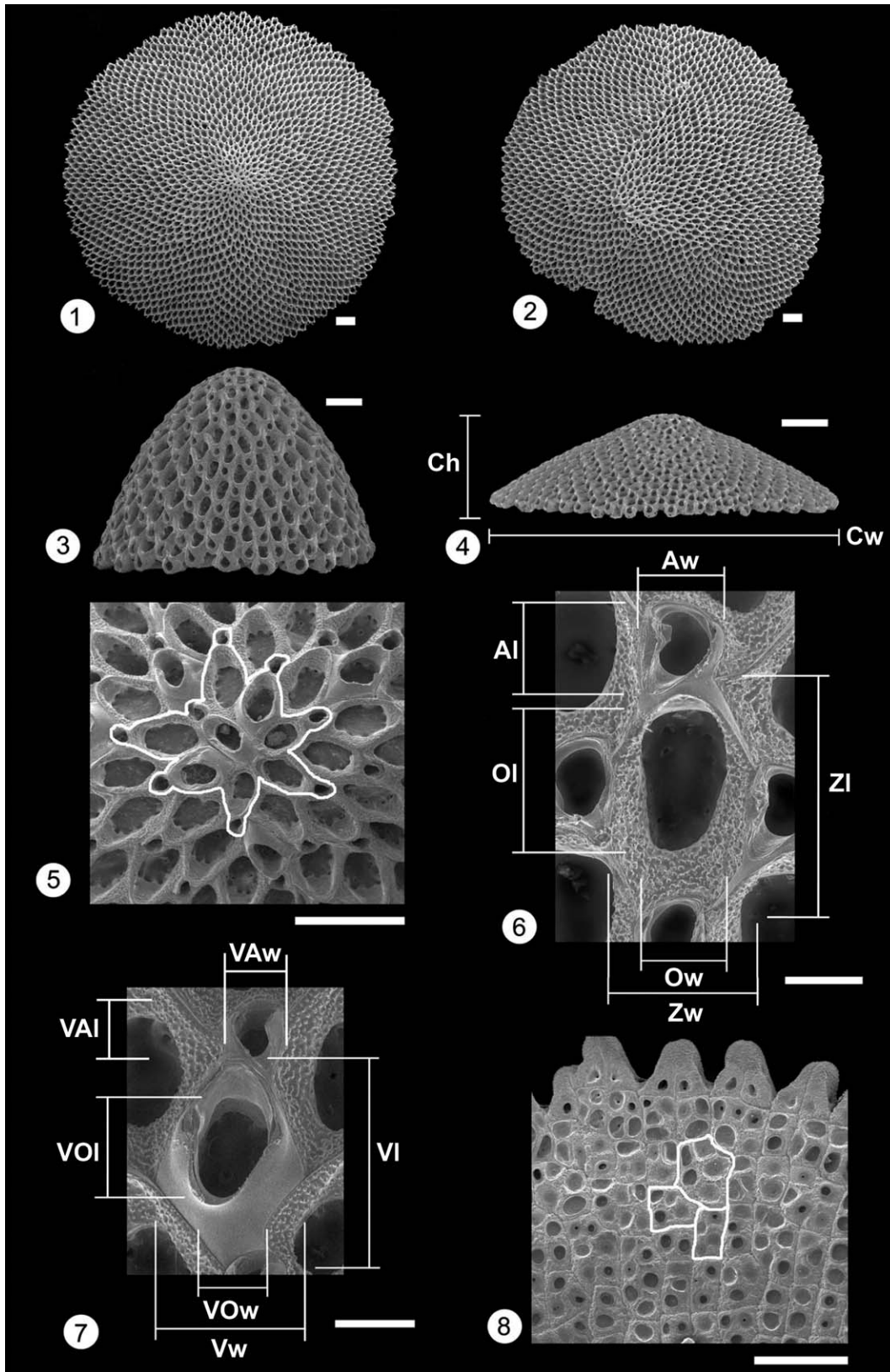


FIGURE 2—Morphological characters used for discriminant and cladistic analyses of extant and fossil cupuladriids. 1–8 characters for *Cupuladria* after Herrera-Cubilla et al., 2006: 1–4, colony size, shape and mode of reproduction; 1–2, 4, *C. biporosa* Canu and Bassler, 1923; 3, *C. panamensis*; 5–8, *C. biporosa*: 5, ancestrula and early astogeny (outlined); 6, 7, characters of autozooid and vicarious avicularium; 8, basal sectors (outlined) and pores. Colonies bar scale=1 mm, colony modules bar scale=100  $\mu$ m.



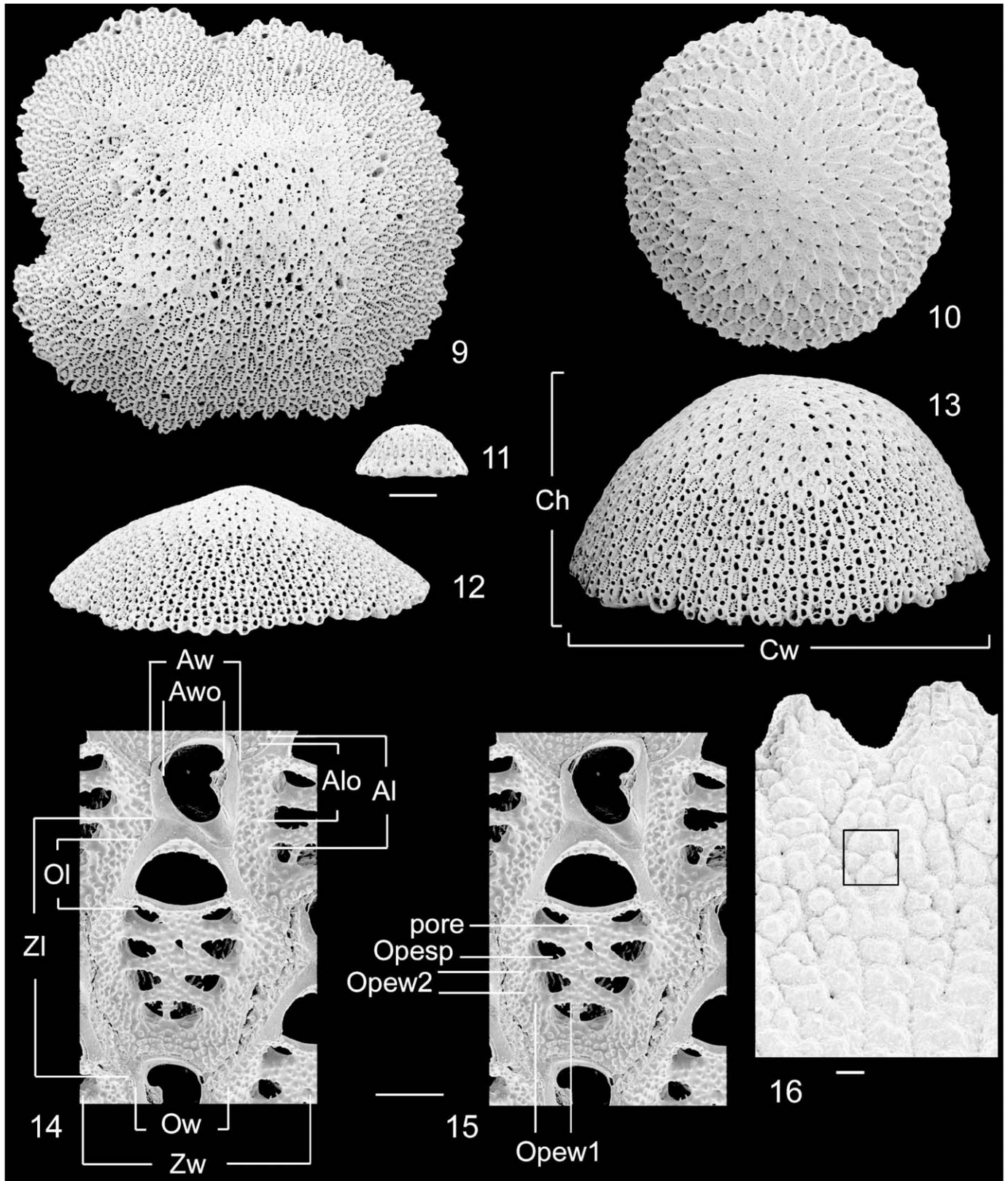


FIGURE 2—9–16 characters for *Discoporella* after Herrera-Cubilla et al., 2008: 9, 13, *D. cookae* (clonal origin); 10, *D. scutella*; 11, *D. triangula*; 12, *D. bocadeltoroensis* (aclonal origin); 14–16, *D. marcusorum*; 14, 15, characters of autozooid and vibraculum avicularium; 16, basal granular density. Colonies bar scale=1 mm, colony modules bar scale=100 μm.

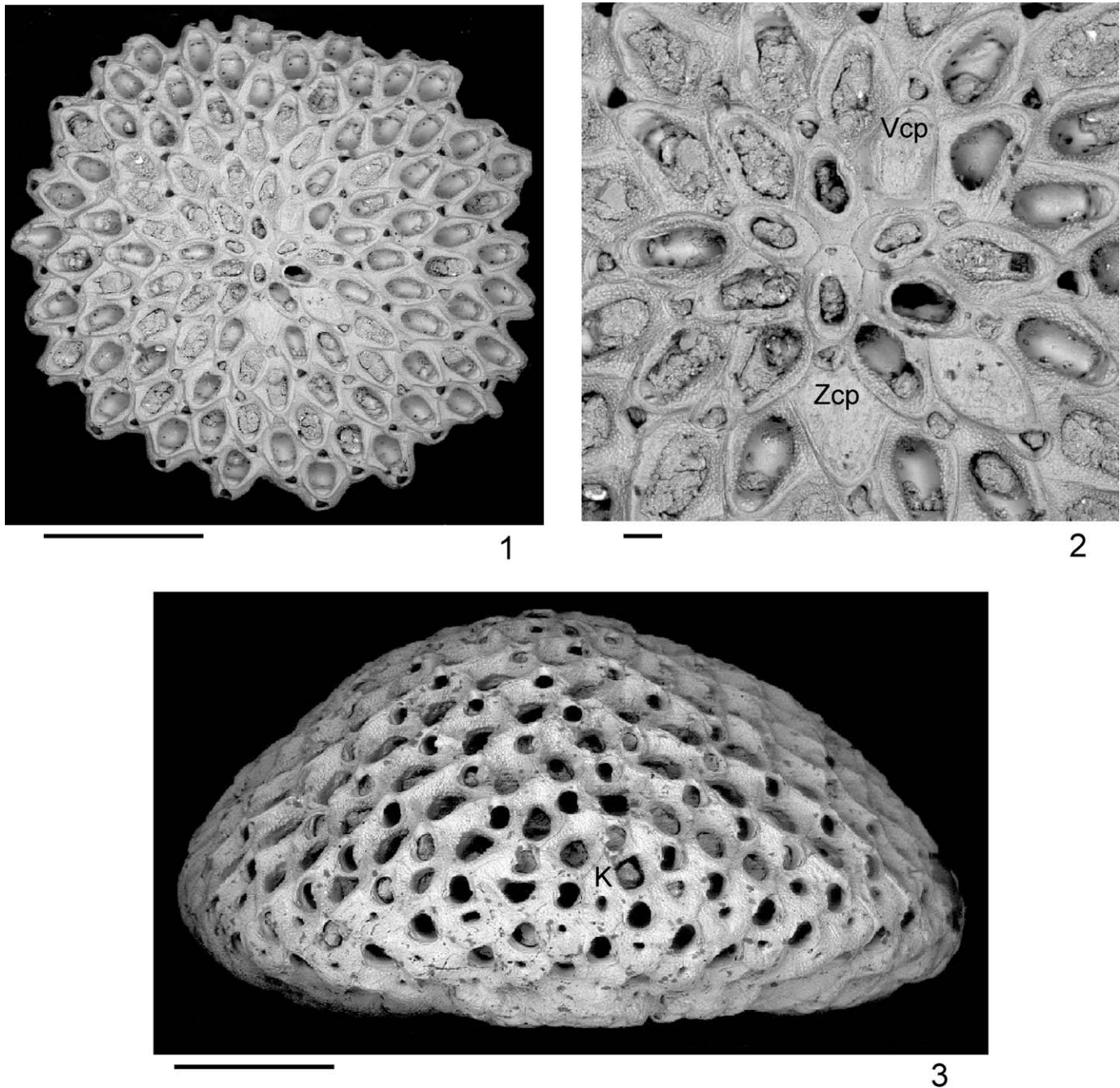


FIGURE 3—Autozooids and vicarious avicularia with closure plates, kenozooids. 1, 2 *Cupuladria veracruxiensis* n. sp., autozooids and vicarious avicularia with closure plates; 3, *C. collyrida*, holotype, USNM542561, kenozooids at the colony margin. Colonies bar scale=1 mm, colony modules bar scale=100  $\mu$ m. For details on these characters see Table 1.

specimens to 14 morphospecies. All the groups were different at  $p < 0.0001$  and 100 percent of vicarious morphospecies were correctly classified versus 99 percent jackknifed. Next, to initiate the process of classification of the remaining specimens, three batches of vicarious colonies were entered un-assigned into consecutive DAs. The first batch of 80 specimens were added to DA6, and then submitted to three rounds of additional DA (DA7–DA9) whereby 99 percent of the cases were correctly classified versus 94 percent jackknifed. Addition of a second batch of 59 specimens including fossils 4 Ma yielded 98 percent of the cases correctly classified versus 94 percent jackknifed (DA10). Finally the third batch of 22 colonies, including fossils from Florida and

recent specimens from the Caribbean coast of Colombia, yielded 98 percent of the cases correctly classified versus 93 percent jackknifed (DA11) for all 231 vicarious colonies (Fig. 6, Table 3). The characters with the highest coefficients were in rank order: Rahw, Ch, RaZV, Psec, Cw, Ol, Csur, RaAloAl, and Asec (see Table 1 for details).

*Colonies without vicarious avicularia.*—Only 30 characters were used to cluster the 21 specimens without vicarious avicularia, since all the characters related with vicarious avicularia were absent. This analysis yielded five discrete groups with a Similarity Coefficient  $\leq 0.09$  plus two outliers (9.5% of total specimens). Four subsequent rounds of DA (DA12–DA15)



TABLE 1—Full set of morphological characters used in the discrimination of taxa and cladistic analysis.

| Abbreviation                 | Character name   |
|------------------------------|--|
| 1. Cw <sup>1αβ</sup>         | Colony diameter  |
| 2. Ch <sup>1αβ</sup>         | Colony height  |
| 3. Rahw <sup>1αβ</sup>       | Colony height-diameter ratio   |
| 4. Csur <sup>1αβ</sup>       | Colony surface area  |
| 5. Ci <sup>1αβ</sup>         | Calcification index  |
| 6. RaZV <sup>1αβ</sup>       | Autozooid-vicarious avicularium ratio and mode of reproduction: fraction of the eight units, from the first generation of the colony, that are autozooids. In the absence of an ancestrula (e.g., origin by fragmentation) we scored as the integer 2. |
| 7. Zl <sup>1αβ</sup>         | Autozooid length   |
| 8. Zw <sup>1αβ</sup>         | Autozooid width  |
| 9. ZwZl <sup>1αβ</sup>       | Autozooid width-length ratio   |
| 10. Ol <sup>1αβ</sup>        | Opesia length  |
| 11. Ow <sup>1αβ</sup>        | Opesia width   |
| 12. OwOl <sup>1αβ</sup>      | Autozooid opesia width-length ratio  |
| 13. Al <sup>1αβ</sup>        | Autozooid vibraculum length  |
| 14. Aw <sup>1αβ</sup>        | Autozooid vibraculum width   |
| 15. AwAl <sup>1αβ</sup>      | Autozooid vibraculum width-length ratio  |
| 16. Alo <sup>1αβ</sup>       | Autozooid vibraculum opesia length   |
| 17. Awo <sup>1αβ</sup>       | Autozooid vibraculum opesia width  |
| 18. AwoAlo <sup>1αβ</sup>    | Autozooid vibraculum opesia width-length ratio   |
| 19. RaOIZl <sup>1αβ</sup>    | Ratio opesia length-autozooid length   |
| 20. RaOwZw <sup>1αβ</sup>    | Ratio opesia width-autozooid width   |
| 21. RaAlZl <sup>1αβ</sup>    | Ratio autozooid vibraculum length-autozooid length   |
| 22. RaAwZw <sup>1αβ</sup>    | Ratio autozooid vibraculum width-autozooid width   |
| 23. RaAloAl <sup>1αβ</sup>   | Ratio autozooid vibraculum opesia length-autozooid vibraculum length   |
| 24. RaAwoAw <sup>1αβ</sup>   | Ratio autozooid vibraculum opesia width-autozooid vibraculum width   |
| 25. RaAloOl <sup>1αβ</sup>   | Ratio autozooid vibraculum opesia length-autozooid opesia length   |
| 26. RaAwoOw <sup>1αβ</sup>   | Ratio autozooid vibraculum opesia width-autozooid opesia width   |
| 27. Zcp <sup>2β</sup>        | Presence/absence of closure plates in autozooids   |
| 28. Vcp <sup>2β</sup>        | Presence/absence of closure plates in vicarious avicularia   |
| 29. Nope <sup>1α</sup>       | Number of opesiules  |
| 30. Opew <sup>1α</sup>       | Opesiule maximum average diameter (calculated on Opew1 and Opew2 measured on the bigger opesiule found per autozooid)  |
| 31. OpeSp <sup>1α</sup>      | Opesiule median number of spines per autozooid   |
| 32. Npor <sup>1α</sup>       | Number of pores in autozooid frontal shield  |
| 33. NV <sup>1αβ</sup>        | Number of vicarious avicularia   |
| 34. Vl <sup>1αβ</sup>        | Length of vicarious avicularium  |
| 35. Vw <sup>1αβ</sup>        | Width of vicarious avicularium   |
| 36. VwVl <sup>2αβ</sup>      | Vicarious avicularium width-length ratio   |
| 37. VOl <sup>1αβ</sup>       | Length of the vicarious avicularium opesia   |
| 38. VOw <sup>1αβ</sup>       | Width of the vicarious avicularium opesia  |
| 39. VOwVOl <sup>2αβ</sup>    | Vicarious avicularium opesia width-length ratio  |
| 40. VAl <sup>1αβ</sup>       | Vicarious avicularium vibraculum length  |
| 41. VAw <sup>1αβ</sup>       | Vicarious avicularium vibraculum width   |
| 42. VAwVAl <sup>2αβ</sup>    | Vicarious avicularium vibraculum width-length ratio  |
| 43. VAlo <sup>2αβ</sup>      | Vicarious avicularium vibraculum opesia length   |
| 44. VAwo <sup>2αβ</sup>      | Vicarious avicularium vibraculum opesia width  |
| 45. VAwoVAlo <sup>2αβ</sup>  | Vicarious avicularium vibraculum opesia width-length ratio   |
| 46. RaVOlVl <sup>1αβ</sup>   | Ratio vicarious avicularium opesia length-vicarious avicularium length   |
| 47. RaVOwVw <sup>1αβ</sup>   | Ratio vicarious avicularium vibraculum opesia width-vicarious avicularium width  |
| 48. RaVAIVl <sup>1αβ</sup>   | Ratio vicarious avicularium vibraculum length-vicarious avicularium length   |
| 49. RaVAwVw <sup>1αβ</sup>   | Ratio vicarious avicularium vibraculum width-vicarious avicularium width   |
| 50. RaVAloVAl <sup>2αβ</sup> | Ratio vicarious avicularium vibraculum opesia length-vicarious avicularium vibraculum length   |
| 51. RaVAwoVAw <sup>2αβ</sup> | Ratio vicarious avicularium vibraculum opesia width-vicarious avicularium vibraculum width   |
| 52. RaVAloVOl <sup>2αβ</sup> | Ratio vicarious avicularium vibraculum opesia length-vicarious avicularium opesia length   |
| 53. RaVAwoVOw <sup>2αβ</sup> | Ratio vicarious avicularium vibraculum opesia width-vicarious avicularium opesia width   |
| 54. Asec <sup>1αβ</sup>      | Basal sector area  |
| 55. Psec <sup>1αβ</sup>      | Number of pores per sector   |
| 56. Graden <sup>1α</sup>     | Basal granule density near the margin on the basal side of the colony  |
| 57. Ken <sup>2β</sup>        | Presence/absence of kenozooids in the margin of the colony   |

<sup>1</sup> Characters used in Herrera-Cubilla et al. (2006, 2008).

<sup>2</sup> Characters added in this study.

<sup>α</sup> Characters used in the first series of discriminant analyses.

<sup>β</sup> Characters used in the second series of discriminant analyses.

reduced the five clusters of non-vicarious specimens to four putative morphospecies with 100 percent of colonies correctly classified versus 95 percent jackknifed. Next, 55 of the remaining non-vicarious colonies were added unassigned to the colonies from DA15. After four rounds of DA (DA16–DA19), one species group represented by only two fossil specimens was merged into another group from which it was not different at  $p < 0.0001$ . This reduced the number of groups discriminated to three with 100 percent of cases correctly classified versus 99 percent jackknifed. Next a second batch of 30 colonies was submitted to the same procedure bringing the total to 106 for the last DA20 resulting in

99.1 percent of colonies correctly classified versus 99.1 percent jackknifed (Fig. 7, Table 3). The characters with the highest coefficients were in rank order: Csur, Cw, Ch, and Rahw (see Table 1 for details).

The 14 vicarious and three non-vicarious groups (hereafter morphospecies or species) of *Cupuladria* are considered equivalent to biological species distinguished in previous studies of different cheilostome genera using similar morphometric methods for which genetic data was also available (Jackson and Cheetham, 1990, 1994; Herrera-Cubilla et al., 2006, 2008).

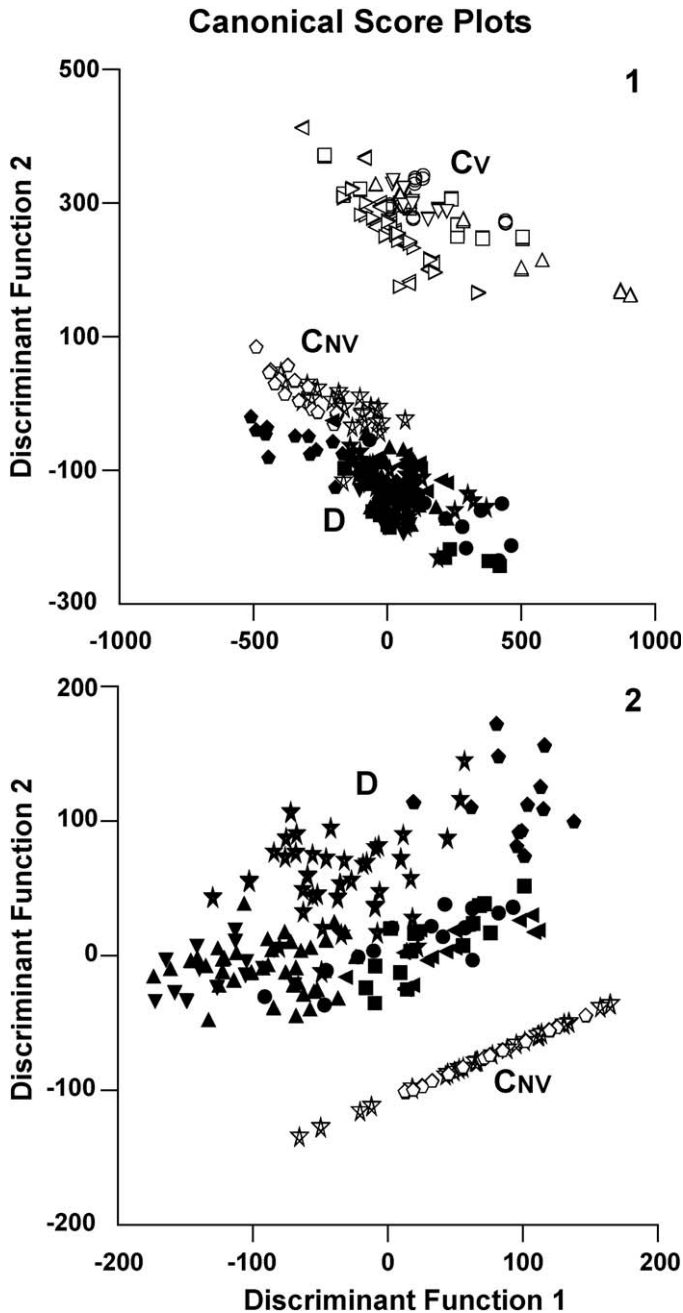


FIGURE 4—Canonical score plots done on 15 species of extant *Cupuladria* and *Discoporella* described in Herrera-Cubilla et al., 2006, 2008. All colonies were entered as ‘groups’. 1, first discriminant analysis (DA1) separates vicarious *Cupuladria* species (above) from non-vicarious *Cupuladria* and *Discoporella* species (below); 2, second discriminant analysis (DA2) separates non-vicarious *Cupuladria* (below) from *Discoporella* (above). The species are: □ *C. biporosa*, ○ *C. cheethami*, △ *C. exfragminis*, ▽ *C. pacificiensis*, ◁ *C. multesima*, ▷ *C. incognita*, ☆ *C. surinamensis*, ◊ *C. panamensis*, ■ *D. scutella*, ● *D. peltifera*, ▲ *D. terminata*, ▼ *D. triangula*, ◀ *D. bocasdeltoroensis*, ★ *D. marcusorum*, ◆ *D. cookae*.

CLADISTIC ANALYSIS

We constructed cladistic phylogenies for 25 cupuladriid species, including all 17 recent and fossil *Cupuladria* species discriminated above plus eight recent *Discoporella* species. The later include the seven species previously described from Panama (Herrera-Cubilla et al., 2008) and *Discoporella* sp. nov. P1 (from Jagadeeshan and O’Dea, 2012). The 57

TABLE 2—Results of linear discriminant analysis done on 15 species of *Cupuladria* and *Discoporella* described in A. Herrera-Cubilla et al. (2006, 2008). The analysis was based on a total of 54 rescaled characters, and all colonies were entered as “groups”. For details see text.

| <i>Cupuladria</i> vs. <i>Discoporella</i> : DA1                   |             |            |
|---|-------------|------------|
| Difference between groups:  |             |            |
| N=258, Wilks’ Lambda=0.000, Chi-square=53,006.86, $p < 0.0001$    |             |            |
| DF  | Eigen value | Cumulative |
| 1   | 70,981.27   | 43.1       |
| 2   | 46,116.34   | 71.1       |
| 3   | 34,583.30   | 92.0       |
| 4   | 6,107.37    | 95.7       |
| Percent of cases correctly classified: 100%                       |             |            |
| Jackknifed classification: 98.5%                                  |             |            |
| <i>Cupuladria</i> without vicarious vs. <i>Discoporella</i> : DA2 |             |            |
| Difference between groups:  |             |            |
| N=192, Wilks’ Lambda=0.000, Chi-square=18,402.96, $p < 0.0001$    |             |            |
| DF  | Eigen value | Cumulative |
| 1   | 10,386.56   | 64.3       |
| 2   | 5,630.72    | 99.2       |
| Percent of cases correctly classified: 99.1%                      |             |            |
| Jackknifed classification: 90.9%                                  |             |            |

morphological characters listed in Table 1 were coded for cladistic analysis using the same procedure as in earlier studies of cheilostome phylogeny (Jackson and Cheetham, 1994; Cheetham et al., 2006, 2007).

We used analysis of variance (ANOVA) on the 496 colonies distributed among 26 taxa, including the outgroup, to test for the statistical ability of each of the characters to distinguish among the species. These included all 231 vicarious and 106 non-vicarious *Cupuladria* specimens used for species discrimination plus 156 specimens of *Discoporella* and three of *Antropora*. All the ANOVAs yielded F-values significant at  $p < 0.0001$ .

We then used the post-hoc Duncan’s Multiple Range Test (DMRT) to identify which of the species-groups have means that do not differ at the default significance level of  $p < 0.05$  to

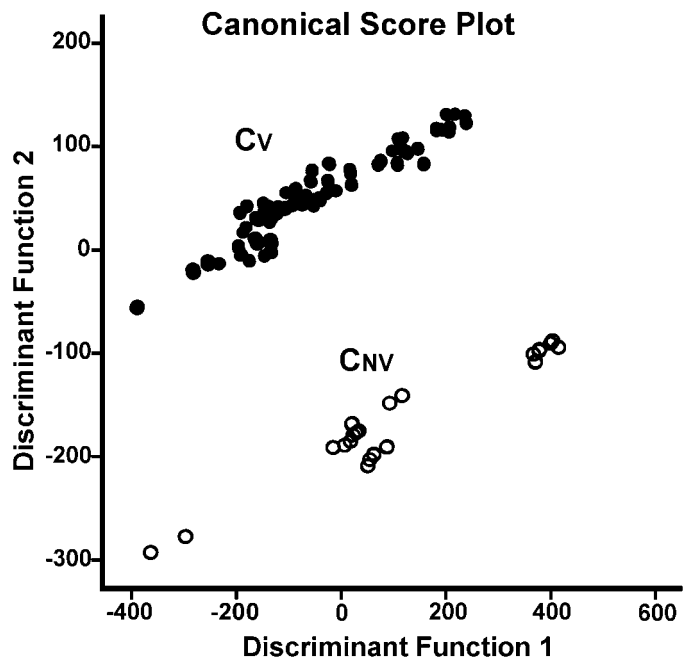


FIGURE 5—Canonical score plot for 91 extant and fossil colonies of *Cupuladria* entered as ‘groups’ based on 52 characters. Colonies with vicarious avicularia (solid circles), colonies without vicarious avicularia (open circles). See text for details.



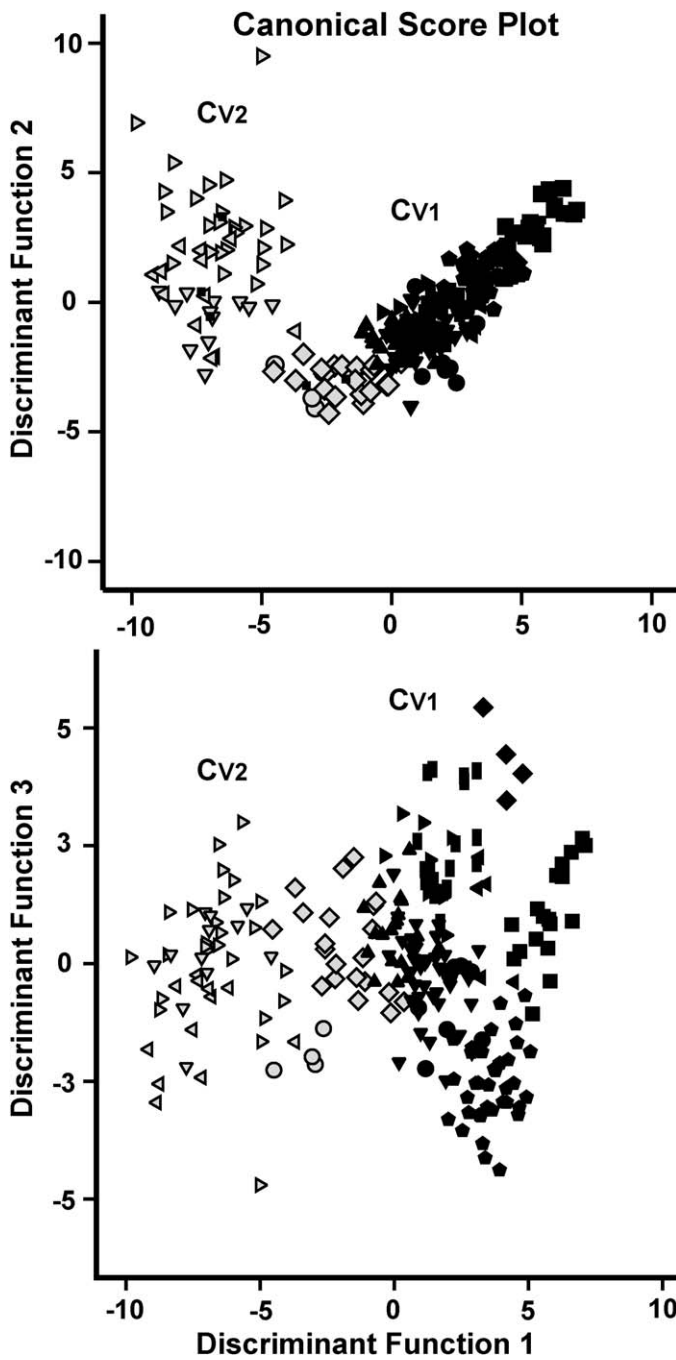


FIGURE 6—Canonical score plots for extant and fossil Vicarious *Cupuladria*. The species are: ● *C. monotrema*, ▲ *C. pacificensis*, ▼ *C. pervagata*, ▲ *C. cheethami*, ► *C. biporosa*, ◆ *C. exfragminis*, ◆ *C. floridensis*, ◆ *C. colonensis*, ■ *C. dominicana*, ○ *C. collyrida*, ◆ *C. veracruxiensis*, ▼ *C. incognita*, ▼ *C. planissima*, ◀ *C. multesima*, ■ Group centroid.

form homogeneous subsets (SPSS Inc., 2009). Coded states of each character were assigned rank-order values from zero to nine, with the difference between successive states (ranks) equal to two for non-overlapping subsets or one with an overlap of one. This procedure is analogous to gap coding but based upon ranges rather than gaps (Cheetham et al., 2007, p. 15, fig. 7). We used letters to assign rank-order values for the few characters for which the number of character subsets exceeded 10 (see online Supplemental Data file). All of the coded characters

TABLE 3—Results of linear discriminant analysis done on total extant and fossil *Cupuladria* species with and without vicarious. For details see text.

| <i>Cupuladria</i> species with vicarious:                   |             |                     |
|---|-------------|---------------------|
| DA11  |             |                     |
| Difference between groups:                                  |             |                     |
| N=231, Wilks' Lambda=0.000, Chi-square=1,907.15, $p<0.0001$ |             |                     |
| DF  | Eigen value | Cumulative Variance |
| 1   | 17.19       | 61.6                |
| 2   | 3.98        | 75.9                |
| 3   | 2.45        | 84.6                |
| 4   | 1.86        | 91.3                |
| 5   | 1.16        | 95.4                |
| Percent of cases correctly classified: 97.9%                |             |                     |
| Jackknifed classification: 93.2%                            |             |                     |
| <i>Cupuladria</i> species without vicarious:                |             |                     |
| DA20  |             |                     |
| Difference between groups:                                  |             |                     |
| N=106, Wilks' Lambda=0.079, Chi-square=257.25, $p<0.0001$   |             |                     |
| DF  | Eigen value | Cumulative Variance |
| 1   | 4.50        | 77.7                |
| 2   | 1.29        | 100.0               |
| Percent of cases correctly classified: 99.1%                |             |                     |
| Jackknifed classification: 99.1%                            |             |                     |

successfully separated species into one or more subsets in the following DMRTs (Appendix 1).

The oldest known specimens of cupuladriids consist of badly worn fragments unsuitable for morphological measurements and are therefore inadequate to use as the outgroup for cladistic analysis. These specimens (NHM, D-41382-4) collected from the Eocene Bartonian, Bende-Ameki Formation, Nigeria Africa, have features similar to both *Cupuladria* and *Discoporella* (Fig. 8). They resemble *Cupuladria* on the frontal surface in lacking a bar forming subopercular opesia, denticles, or spines. In

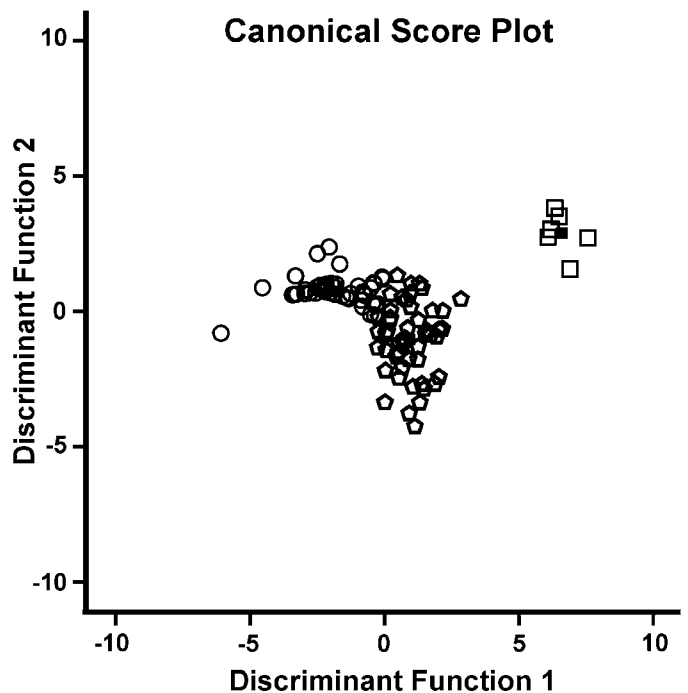


FIGURE 7—Canonical score plot for extant and fossil non-Vicarious *Cupuladria*. The species are: ○ *C. surinamensis*, ◡ *C. panamensis*, □ *C. gigas*, ■ Group centroid.

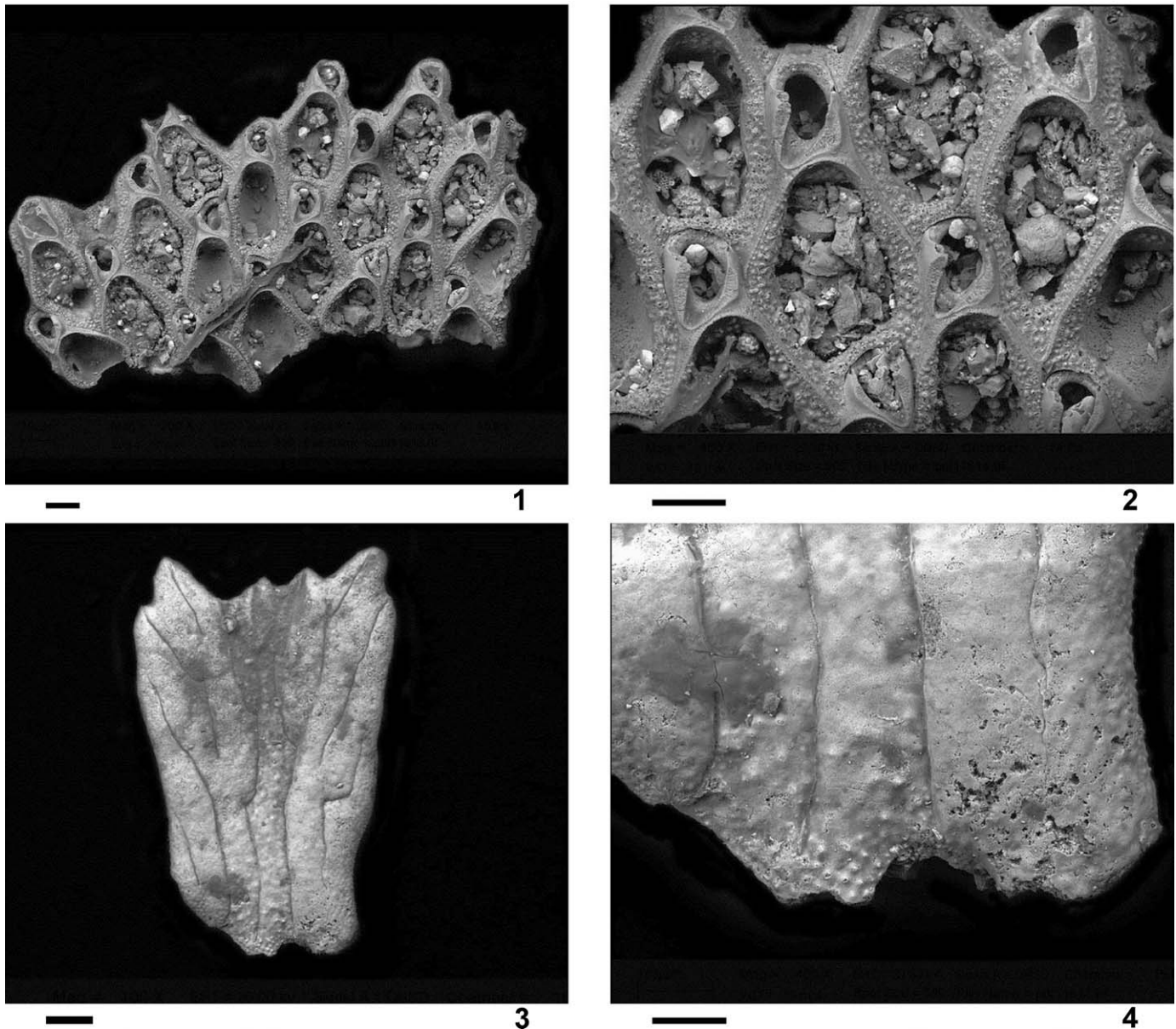


FIGURE 8—Cupuladriid specimen from Ameki formation Nigeria Africa middle Eocene, in the department of Paleontology's collection of the NHM. The morphology shows a *Cupuladria* 'like' specimen in frontal view and *Discoporella* basal view. Photo courtesy of P. D. Taylor.

contrast, they resemble *Discoporella* on the basal surface of the colony in the possession of tubercles and grooves. A similar mix of characters occurs in specimens of roughly the same age from Egypt: *Cupuladria numulitophila* n.sp (early Eocene, Priabonian, Maadi Fm., Gabal Homret Shaibun east of Beni Suef), and *Cupuladria fayumensis* n. sp (early Eocene, Priabonian, Qasr el-Sagha Fm., Fayum area) (Ziko A., 1985) that also occur only as worn fragments unsuitable for morphological analysis.

Because of this lack of suitable fossil material, we used the extant encrusting anascan *Antropora leucocypha*, Marcus, 1937 (Calloporidae) from the Perlas Archipelago in the Gulf of Panama as the outgroup for cladistic analysis. Its most important trait is the presence of internal brooding chambers (Marcus, 1937; Cook, 1968; Winston, 1982), which also occur in the Cupuladriidae.

Hastings (1930, p. 709, fig. 17) described the position of an internal sac-bearing embryo in *Antropora tinctoria*, but was unable

to conclude if such sac represented a true ovicell (for a discussion on the similarity between *A. leucocypha* and *A. tinctoria* see the systematic paleontology section). Tilbrook (1998) also described seven species of *Antropora* with small indistinct or vestigial endozooidal ovicells. Subsequently, Ostrovsky and colleagues demonstrated that cupuladriids incubate embryos within an internal sac or immersed ovicell and concluded that cupuladriids are nested within calloporids based upon their type of internal brooding and simple zooidal morphology (Ostrovsky et al., 2009).

Cladograms were calculated from the characters coded by DMRT entered as ordered states in PAUP\* 4.0b10 (Swofford, 2000). The routine Branch and Bound search was used to look for the most parsimonious trees.

Four equally parsimonious trees were obtained (Fig. 9) with length 485, consistency index 0.59, and retention index 0.86. Nine of the 57 characters were uninformative for parsimony (*Ci*,

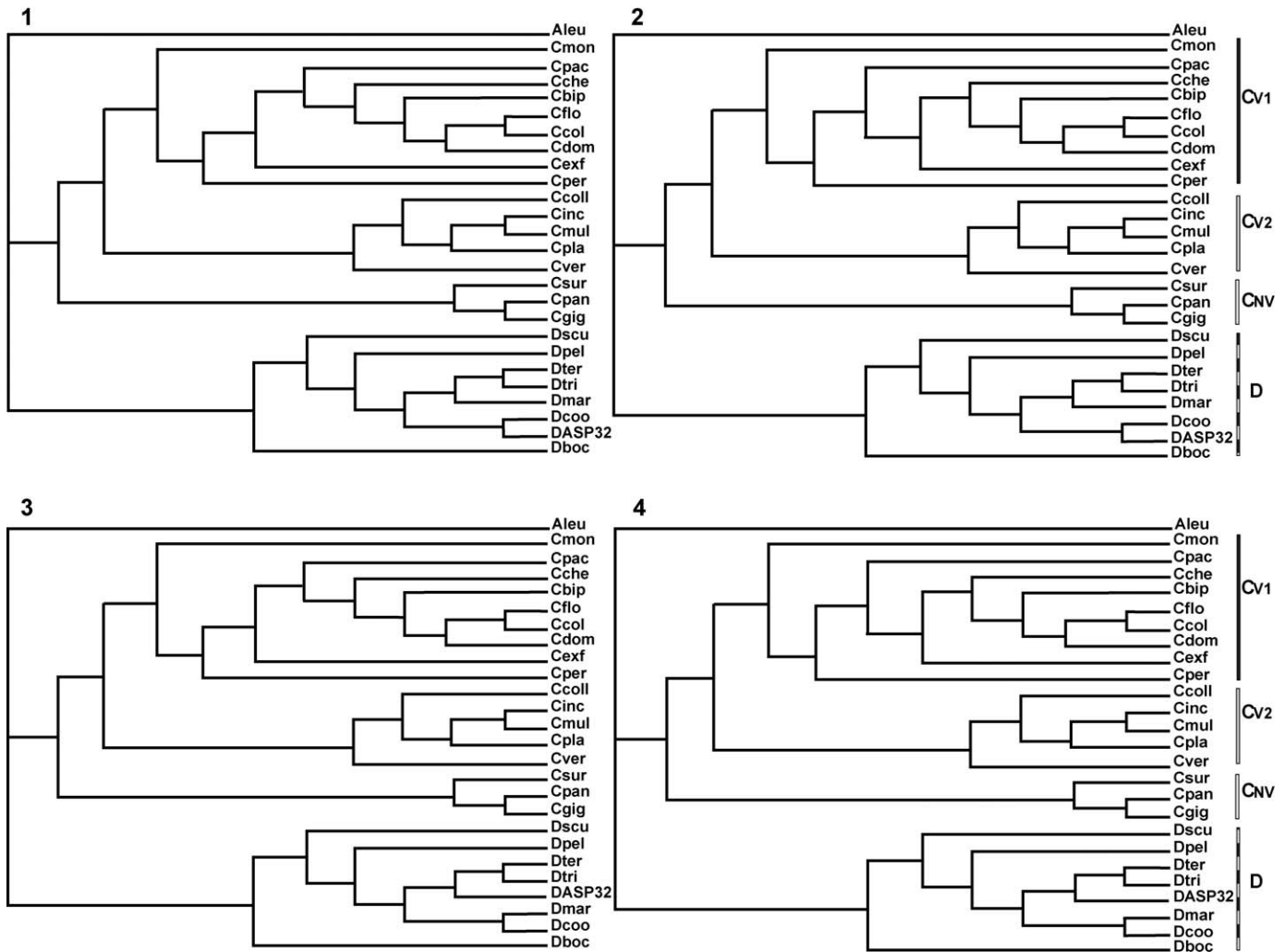


FIGURE 9—Four equally parsimonious trees obtained with branch and bound search routine in PAUP\*, and routed to *A. leucocypha* (Calloporidae, Anasca); length 485, consistency index 0.59, and retention index 0.86. Species are grouped in four monophyletic groups: vicarious *Cupuladria* clade 1 ( $C_{V1}$ ), vicarious *Cupuladria* clade 2 ( $C_{V2}$ ), non-vicarious *Cupuladria* clade ( $C_{NV}$ ), and *Discoporella* (D).

ZwZI, Aw, AwAl, RaAlZI, RaAwZw, RaAloAl, RaAwoOw, Vcp). All four trees divided the 25 tropical American cupuladriids into four distinct morphological clades that are well supported by the discriminant analysis (Figs. 4–7), as well as the bootstrap support tree based on 1,000 pseudoreplicates of the original cladistic data illustrated in Figure 11A. The extant and fossil *Cupuladria* clades are: non-vicarious *Cupuladria* ( $C_{NV}$ ), *Cupuladria* clade 2 ( $C_{V2}$ ), and *Cupuladria* clade 1 ( $C_{V1}$ ); and beneath the extant *Discoporella* species (D). *Discoporella* is paraphyletic to *Cupuladria*. Within *Cupuladria*,  $C_{V1}$  and  $C_{V2}$  are sister groups both of which are apparently derived from the  $C_{NV}$  clade.

We used the command ‘ConTree’ to calculate strict, semi strict and 50 percent majority-rule consensus trees that had the same topology. The strict consensus tree (Fig. 10) closely resembles the bootstrap support tree (Fig. 11A) with good support for the grouping ( $C_{NV} + [C_{V1} + C_{V2}]$ ). The  $C_{NV}$  clade is strongly supported. In contrast, the  $C_{V1}$  clade collapses into a five branched unresolved polytomy, but with reasonably good support for (*C. cheethami* + [*C. biporosa* + [*C. dominicana* + [*C. floridensis* + *C. colonensis*]]]). The  $C_{V2}$  clade retains its previous topology but is less well supported than the  $C_{NV}$  clade.

Twelve of the 48 characters informative for parsimony with a consistency index between 0.7–1.0 and the lowest frequency of change were chosen for their potential ability to distinguish morphologically defined clades. The basal node of the  $C_{NV}$  versus  $C_{V1}$  and  $C_{V2}$  clades reflects differences in area of the basal sectors (Asec). The basal node of the  $C_{V1}$  and  $C_{V2}$  clades is defined by differences in the size of the opesia of vicarious avicularia (Vow) as well as the shape and strength of the vicarious avicularium vibraculum and its opesia (VAwVAL, VAwoVALo, RaVAwVw, RaVAloVAL, RaVAwoVAw, RaVAloVOI). Relevant characters for the *Discoporella* clade include those related to the hydrostatic mechanism (RaOlZI), colony strength (Zcp), autozooid size (Zw), and autozooid vibraculum strength (RaAwoAw).

We visually fit the strict consensus cladogram to the stratigraphic ranges of tropical American *Cupuladria* species (Fig. 10). Black circles represent data from this study. Gray circles indicate occurrences from O’Dea and Jackson, 2009. Open triangles indicate occurrences from Canu and Bassler (1923). The stratigraphic congruence within each of the groups of *Cupuladria* is largely consistent with cladogram topology. However, the hypothesized ancestry of the non-vicarious clade



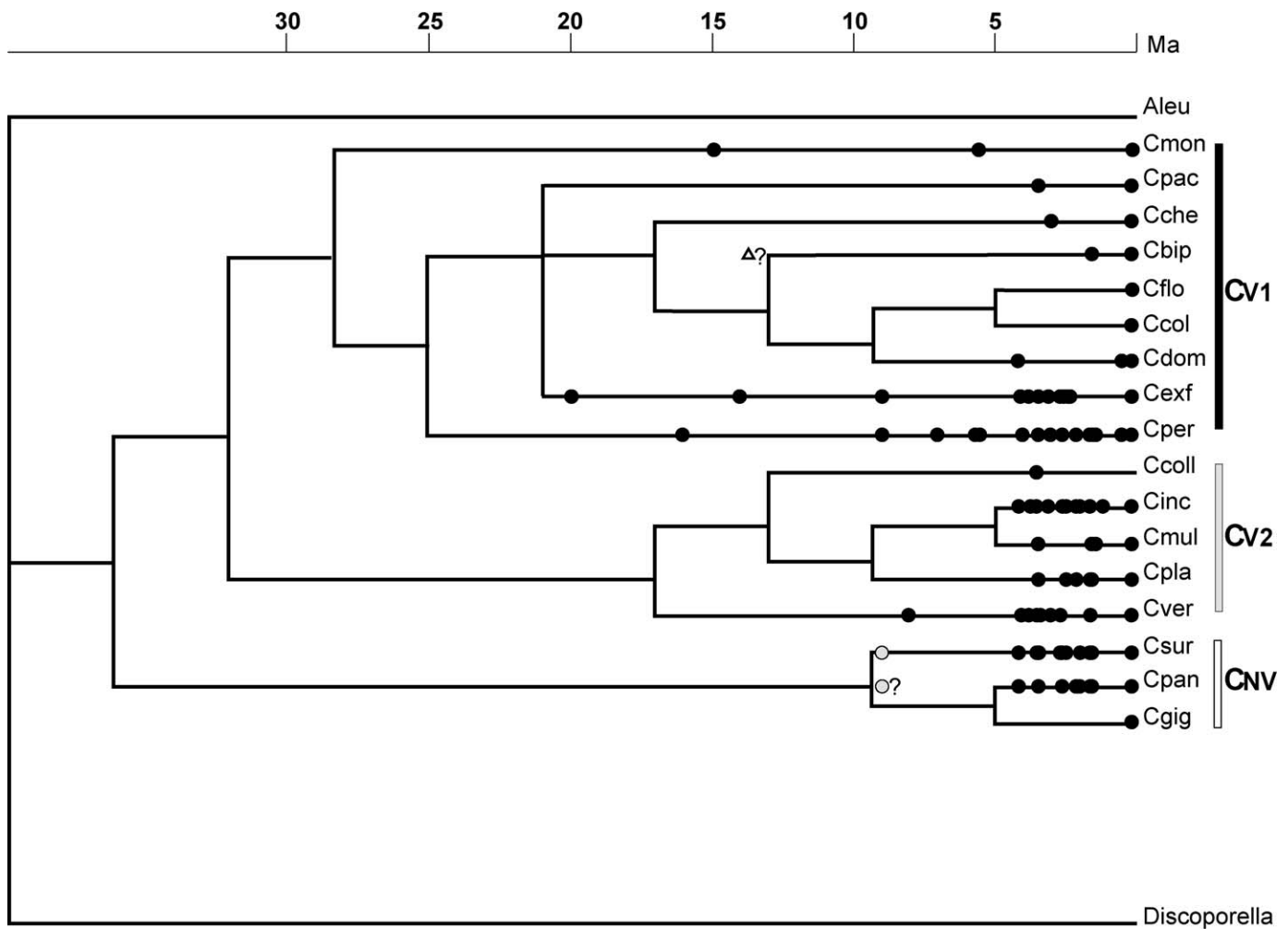


FIGURE 10—Strict consensus tree cladogram visually fitted to the stratigraphic ranges of tropical American *Cupuladria* species.

of *Cupuladria* ( $C_{NV}$ ) in relation to the two vicarious *Cupuladria* clades ( $C_{V1}$  and  $C_{V2}$ ) is stratigraphically inconsistent.

#### DISCUSSION

**Morphological characters.**—Cupuladriid autozooids are responsible for feeding and reproduction whereas autozooidal vibracula serve to support and position the colony as well as to provide limited locomotion (Cook, 1965a, 1965b; McKinney and Jackson, 1989). The function of vicarious avicularia is difficult to assess since they have not been observed in motion, however our personal observations of their placement in damaged portions of colonies and the shape of their setae suggests they may be involved in regeneration and defense (see also Cook, 1965b). All of the characters with a consistency index of 1 are related to regeneration, defense, the hydrostatic mechanism of the autozooids, and the strength of the colony and autozooids vibracula.

Characters related to vicarious avicularia were especially useful to discriminate species and delineate cladistic relationships among the vicarious *Cupuladria* clades. Avicularia have evolved many times across a broad spectrum of cheilostome taxa (Winston, 1984; Cheetham et al., 2006) and bryozoologists distinguish several types based on their position and shape (Winston, 1984). Vicarious avicularia in cupuladriids replace an autozooid in position, and they appear to arise by intramural budding in both the  $C_{V1}$  and  $C_{V2}$  clades. In the former, they have been observed in proximity to damaged portions of colonies

where they may act to maintain colonial integrity. In contrast, in  $C_{V2}$  they appear during early astogeny and are generally restricted to the central part of the colony.

Other morphological characters of particular interest include the area of basal sectors (Asec) that has a consistency index of only 0.7 but a high coefficient in the final discriminant analysis of vicarious *Cupuladria* species (DA11). The shape of the basal sectors also changes noticeably from rectangular in the  $C_{V1}$  clade to radial in the  $C_{V2}$  clades (except *C. veracruxiensis*) and the  $C_{NV}$  clade. In general, the basal sectors are also related in *Cupuladria* to occurrence of kenozooidal chambers. These change in the number of internal layers from 1 to 2 in  $C_{V1}$ , 3 to 6 in  $C_{V2}$ , and just 1 in  $C_{NV}$  (Herrera-Cubilla et al., 2006). Both basal sectors and kenozooidal chambers are absent in *Discoporella*.

The ratio of opesia-autozooid length (RaOIZl) is important cladistically because *Discoporella* autozooids have a nearly complete cryptocyst except for a number of opesiules along each side, while those in *Cupuladria* have a wide open front. This difference in cryptocyst development and size of opesia may be related to egg size, which is larger in *Cupuladria* than in *Discoporella* (Cook, 1965b). Recent measurements of the diameter of the embryos of *C. exfragminis* and *D. marcorum* yielded 0.223 mm and 0.157 mm (Ostrovsky et al., 2009; figs. 2, 4, respectively). However we did not find significant difference in autozooid area between the species of *Cupuladria* and

*Discoporella* used in this work ( $N=25$ , Mann-Whitney  $U=67$ ,  $Z=-0.058$ ,  $p=0.954$ ). Differences in  $ZI$  and  $Zw$  were also not significant. Other useful characters within the  $C_{NV}$  and *Discoporella* clades are: autozooid size ( $Zw$ ), closure plates in autozooids ( $Zcp$ ), which in *Discoporella* occurs at the center of the colony, and the strength of the autozooidal vibraculum (RaAwoAw).

Only three of the nine characters uninformative for parsimony were among the characters with highest coefficient in DAs for species discrimination. These include Aw, AwAl, and RaAloAl in DA2 done to further resolve the non-vicarious *Cupuladria* plus *Discoporella* clusters. This last character was also among those with highest coefficient in the final DA11 performed to classify vicarious *Cupuladria* colonies.

**Cladistic analyses of morphological versus molecular characters.**—The results of both the discriminant (Figs. 4–7) and cladistic (Figs. 9–11) analyses yielded a subdivision of tropical American cupuladriids which is in good agreement with two previous molecular phylogenetic analyses with respect to separation of genera and major clades within genera (Dick et al., 2003; Jagadeeshan and O’Dea, 2012). There are discrepancies, however, in the resolution of topologies between the two types of analyses that appear to reflect differences in the numbers of taxa studied. We examined 25 species whereas the two previous studies included 10 and 14 species respectively. For example, we analyzed three species within the  $C_{NV}$  clade whereas Dick et al. (2003, fig. 4) analyzed only *C. surinamensis*, Cadée, 1975, that appeared at the basal node of the *Discoporella* clade. The topology of this clade was better resolved by Jagadeeshan and O’Dea (2012, fig. 2) who also included *C. gigas* in their analysis. Similarly, Jagadeeshan and O’Dea sampled only *C. incognita*, Herrera-Cubilla et al. 2006, from the  $C_{V2}$  clade resulting in its placement as a sister species of *C. exfragminis*, whereas the phylogeny based on morphological characters placed these two species in two distinct clades.

**Correspondence between phylogeny and the fossil record.**—The relationships among sister clades in both the molecular and morphologically based phylogenies are stratigraphically incongruent by 20 Ma (compare Figs. 10 and 11). This is despite quantitative estimates of the probability of completeness of the fossil record of nearly 100 percent and near maximum probability of the occurrence of ancestors of  $PA=0.5$  (Foote, 1996; Cheetham and Jackson, 1998, 2000). Resolution of this issue will require cladistic reexamination of eight or more Eocene to Recent principally eastern Atlantic species traditionally assigned to *Cupuladria* but intermediate in a number of characters between *Discoporella* and *Cupuladria* (Lagaaij, 1963; Cook, 1965a, 1965b, 1985; Boardman et al., 1970; Cadée, 1975). As we have seen, the oldest cupuladriid known (NHM D41382-4, Bende Ameki, Nigeria, middle Eocene) resembles *Cupuladria* on the frontal surface in lacking the development of a cryptocyst, denticles, or spines, but possesses tubercles and grooves on the basal surface of the colony similar to *Discoporella* (Fig. 8). The other seven species also have basal grooves with tubercles and varying complete development of a cryptocyst. All of them also appear to lack vicarious avicularia, which is consistent with our results (Fig. 10).

In contrast, the fossil record of the  $C_{V1}$  clade extends back to the early Miocene Chipola Formation along the northern coast of the Gulf of Mexico and that of the  $C_{V2}$  clade to the (?) late Miocene Paraje Solo Formation, Veracruz, Mexico (Fig. 10). Diversification was slow until the early Pliocene, although this may be at least partially an artifact of the sparseness of the Miocene fossil record as for other well-studied clades (Jackson and Cheetham, 1994; Cheetham and Jackson, 1995). The fossil record of eastern Pacific cupuladriids is also scanty and unstudied. Nevertheless, it is of great interest that the only two

recent species of *Cupuladria* encountered in our very extensive eastern Pacific dredge samples have a Caribbean fossil record that extends back to the Pliocene for *C. pacificiensis* and to the early Miocene for *C. exfragminis* (Fig. 10).

This apparent lack of a uniquely eastern Pacific clade of *Cupuladria* has two important implications. First, the radiation of *Cupuladria* in tropical America appears to have occurred almost entirely within the Caribbean and Gulf of Mexico, as was also the case for the cheilostomes *Metrarabdotos* and *Stylopoma*. Second, the two pairs of most closely related species on opposite sides of the Isthmus of Panama diverged within the Caribbean, long before the final isolation of the two oceans 3.5 Ma, and became allopatric only after the two Pacific species had finally gone extinct within the Caribbean. *Discoporella marcusorum* and *D. cookae* exhibit a similar evolutionary history (O’Dea and Jackson, 2009). Extinction in both cases did not occur until the late Pliocene, about 2 Ma after final closure of the Seaway and the collapse in Caribbean planktonic productivity (O’Dea et al., 2007; O’Dea and Jackson, 2009). The predominantly clonal life histories of eastern Pacific species of cupuladriids are closely tied to the high productivity in the eastern Pacific (O’Dea et al., 2004, 2008).

#### SYSTEMATIC PALEONTOLOGY

Order CHEILOSTOMATIDA Busk, 1852

Suborder FLUSTRINA Smitt, 1867

Superfamily CALLOPOROIDEA Norman, 1903

Family CALLOPORIDAE Norman, 1903

Genus ANTROPORA Norman, 1903

ANTROPORA LEUCOCYPHA Marcus, 1937

1937 *Crassimarginatella leucocypha* MARCUS, p. 46.

1982 *Antropora leucocypha* (MARCUS); WINSTON, p. 123.

**Description.**—Colony encrusting gastropod shells, pink to magenta in color, unilaminar to bilaminar. Autozooids irregularly oval, cryptocyst very narrow distally, slightly wider and crenulated proximally. Triangular spaces between autozooids, avicularia not observed and ovicell endozooidal.

**Material.**—USNM593679-593681, La Guarda channel. See Appendix 2 for morphological measurements.

**Occurrence.**—La Guarda channel, Las Perlas Archipelago, Gulf of Panama, Panama.

**Remarks.**—*Antropora leucocypha* was originally described from the Atlantic, but is very similar to the eastern Pacific (EP) species *A. tincta* from which can only be distinguish by the frequency of kenozooids, size of avicularia and shape of the avicularian mandible (Cook, 1968; Winston, 1982). According to PPP and DR records, its stratigraphic range is from middle Miocene to the present with occurrence in both the western Atlantic and Pacific.

Family CUPULADRIIDAE Lagaaij, 1952

Genus CUPULADRIA Canu and Bassler, 1919

CUPULADRIA MONOTREMA (Busk, 1884)

1994 *Cupuladria monotrema* (Busk), COOK AND CHIMONIDES, p. 261.

**Description.**—Colonies are conical, with maximum observed diameter 6.8 mm, the central area of the colony is occupied mostly by vicarious avicularia up to the fifth astogenetic generation, but occasionally autozooids are present. Vicarious avicularia opesia auriform, and gymnocyst well developed. Cryptocyst of autozooids in central area straight sided, lateral septula not visible, while cryptocyst of autozooids in periphery descend steeply. The autozooids are hexagonal in shape, and the

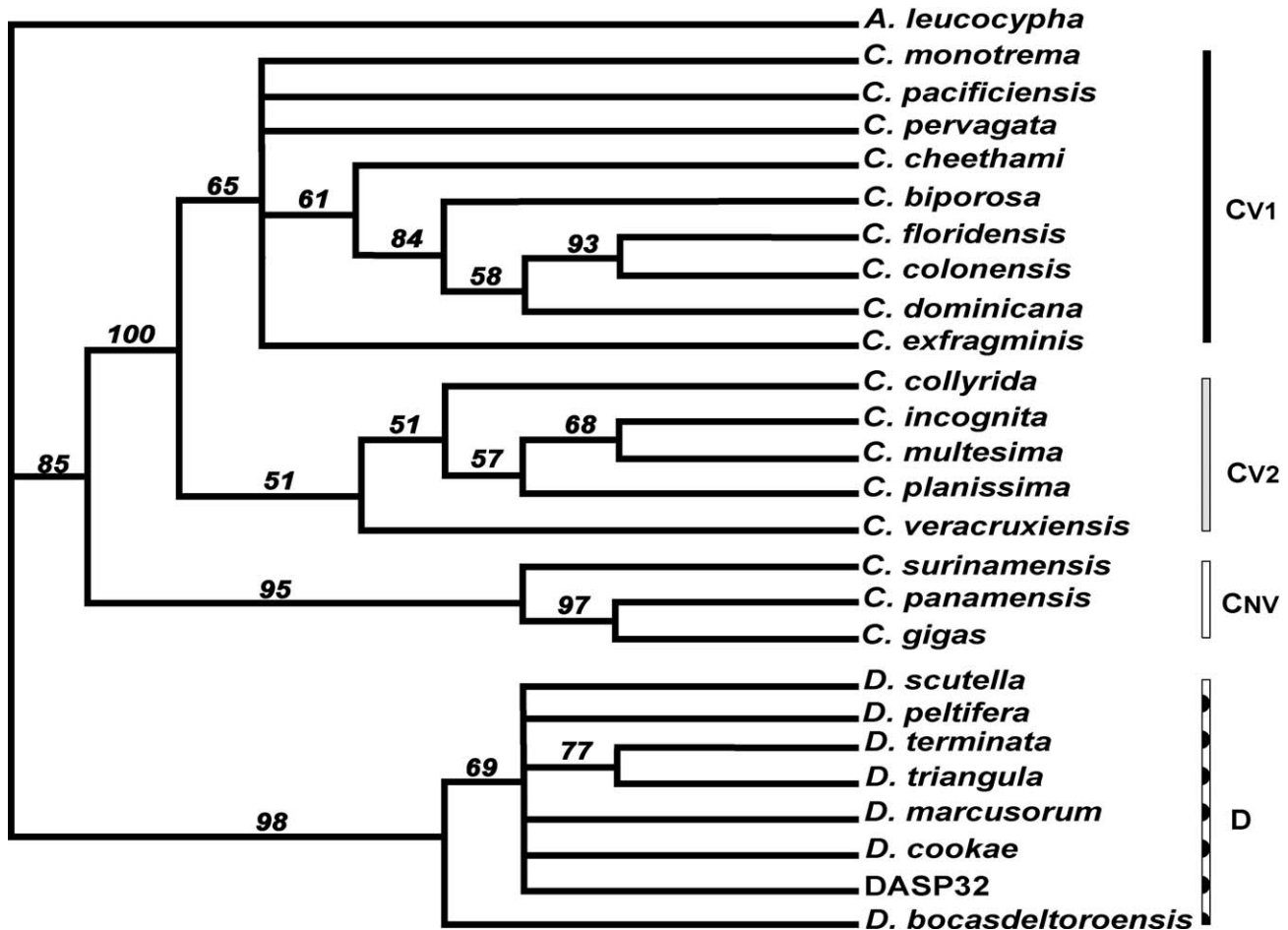


FIGURE 11—Comparison between molecular versus morphological phylogenies of Cupuladriidae. A, this study, bootstrap support tree, based on 1000 pseudoreplicates of the original cladistic data.

basal sectors are rectangular with one but occasionally two pores per basal sector.

**Material.**—USNM593682, PPP1284; USNM593683, NMB15962; USNM593684–593688, Guyana shelf, Luymes CICAR 23 st. 54. See Appendix 2 for morphological measurements.

**Occurrence.**—?Middle Miocene, east Deer I., Bocas del Toro, Panama. Messinian to Zanclean, Gurabo Formation, Rio Gurabo, Dominican Republic. Recent, Guyana shelf, Guyana.

CUPULADRIA PACIFICIENSIS Herrera-Cubilla et al., 2006  
Figures 12, 13

1950 *Cupuladria canariensis* OSBURN, p. 33, pl. 3, figs. 2, 3  
(in part?).

**Description.**—Colonies conical, with a maximum observed diameter of 7.6 mm, the central area of the colony is occupied mostly by autozooids. In general cryptocyst of autozooids descend moderately but septula still visible, autozooids are hexagonal in shape. Vicarious avicularia are scattered through the zone of astogenetic change (Herrera-Cubilla et al., 2006), with gymnocyst well developed, opesia auriform in shape. The basal sectors are rectangular with 3–6 pores per basal sector. In the central area of the colony of few fossil specimens have been observed autozooids and vicarious avicularia with closure plates, and autozooids whose cryptocysts are thickened by secondary calcification.

**Types.**—Hypotype USNM542592, PPP334.

**Material.**—USNM593689–593694, PPP365, 635, 639, 2038, 2026; USNM593695, GM98–69, 9°18.6' Lat., 80°20' Lon., Gulf de los Mosquitos, Bocas del Toro, Panama; USNM593696, SB95–9, 9°31' Lat., 78°44.3' Lon., San Blas, Panama; USNM593697, SB95–11, 9°30.2' Lat., 78°54.9' Lon., San Blas, Panama; USNM593698–593699, SB95–20, 9°36.9' Lat., 78°59.2' Lon., San Blas, Panama; USNM593700, GC97–65, 7°10.9' Lat., 81°39.9' Lon., Gulf of Chiriquí, Panama; USNM593701, GP97–1, 8°36.1' Lat., 78°34.9' Lon., Gulf of Panama, Panama; USNM593702, GP97–9, 7°32.8' Lat., 78°10.6' Lon., Gulf of Panama, Panama; USNM593703–593704, BT98–19, 9°22.5' Lat., 82°10' Lon., Bocas del Toro, Panama; USNM523170–523172 designated by Herrera-Cubilla et al., 2006.

See Appendix 2 for morphological measurements.

**Occurrence.**—Early Pliocene, Cayo Agua Formation, Punta Norte to Punta Tiburon, Bocas del Toro, Panama. Late Pliocene, Escudo de Veraguas Formation, northern coast, Bocas del Toro, Panama; late Pliocene, Moin Formation, Lomas del Mar, eastern sequence, Limon, Costa Rica; late Pliocene, Lomas del Mar, western reef track sequence, Limon, Costa Rica. Recent, Gulf of Panamá and Chiriquí EP.

**Remarks.**—The vicarious avicularia vibracula opesia width (VAwo) are less than 0.1 mm and the ratio autozooid vibracula opesia length–autozooid vibracula length (RaAloAl) less than 0.75 mm like in *C. exfragminis*, *C. biporosa* and *C. cheethami*. Three Caribbean specimens of late Pliocene age were discriminated as *C. pacificiensis* probably because the process of extinction did not occur until that time (see Discussion). However



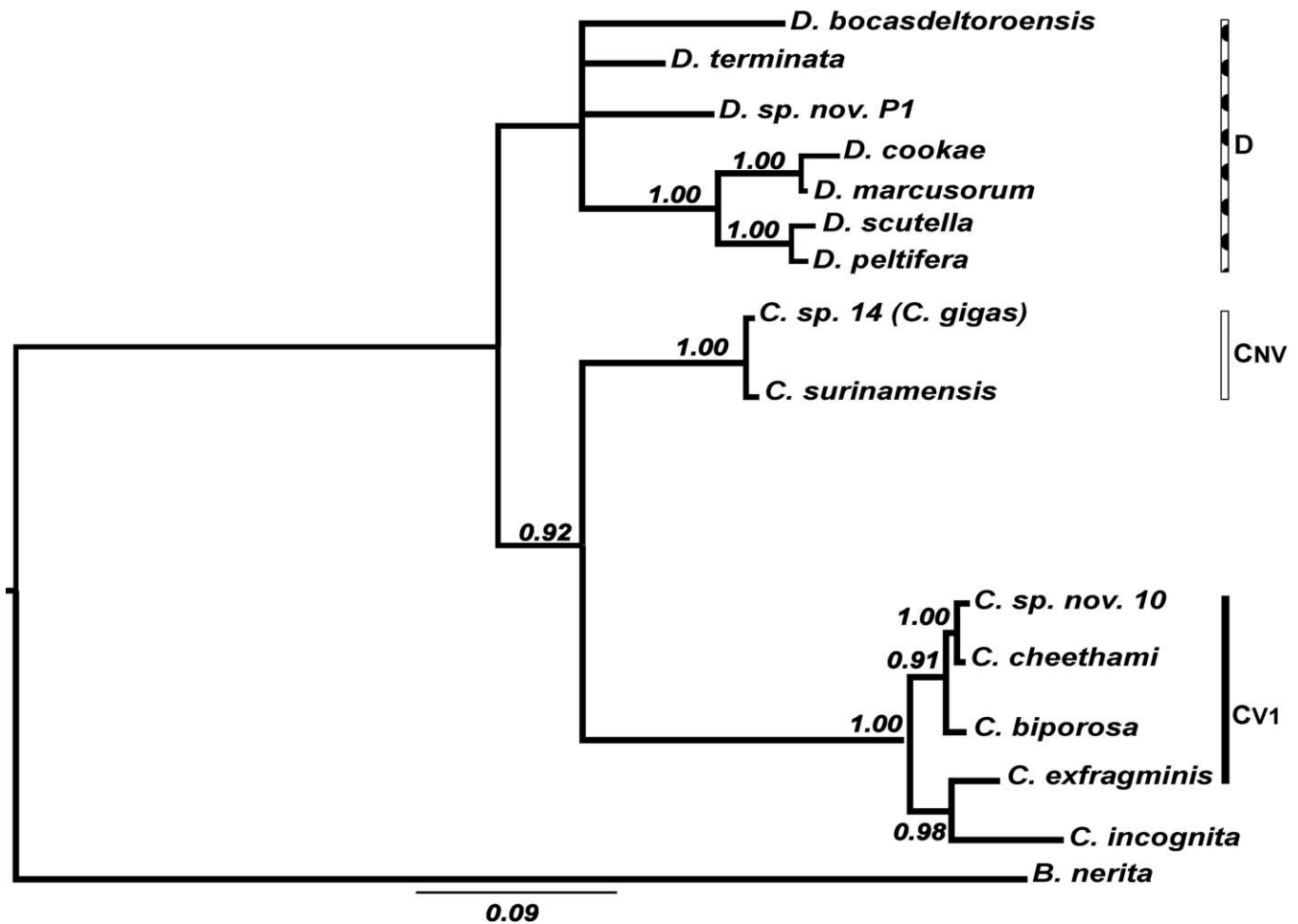


FIGURE 11—B, Bayesian inference phylogeny (Jagadeeshan and O’Dea, 2012).

five recent specimens could not be discriminated from their cognate species from the opposite ocean, a difficulty also encountered in a previous study (Herrera-Cubilla et al., 2006).

CUPULADRIA EXFRAGMINIS Herrera-Cubilla et al., 2006  
 Figures 14–19

1950 *Cupuladria canariensis* OSBURN, p. 33, pl. 3, figs. 2, 3 (in part?).

**Description.**—Colonies have an irregular conical shape, with a maximum observed diameter of 9.3 mm, the central area of the colony is occupied mostly by autozooids. In general cryptocyst of autozooids descend moderately but septula still visible, autozooids are hexagonal. Vicarious avicularia are scattered through the zone of astogenetic change with gymnocyst well developed, opesia auriform in shape, and like in *C. pacificiensis* VAwo are less than 0.1 mm. The basal sectors are rectangular with 2–5 pores per basal sector. Closure plates are absent in autozooids and vicarious avicularia in all specimens examined. One of five specimens from the Chipola formation possesses a few autozooids thickened by secondary calcification.

**Types.**—Hypotypes USNM542593 NMB17830; USNM542594, PPP204; USNM542595, PPP1306.

**Material.**—USNM593705, Chipola Formation, Shoal River, FL, U.S.A.; USNM593706–593712, PPP1306, 350, 345, 204, 69, 65; USNM593713, NMB18105; USNM593714, Solarte I., western Tip, Bocas del Toro, Panama; USNM593715–

USNM593716, PPP68, 2169; USNM593717, Shell creek De Soto Co., FL, U.S.A.; USNM593718, Bastimentos I., Bocas del Toro, Panama; USNM593719–593720, NMB18388, 18084; USNM593721, PPP3257; USNM593722, GP97–1, 8°36.1’ Lat., 78°34.9’ Lon., Gulf of Panama, Panama; USNM593723–593724, GC97–89, 8°0.03’ Lat., 82°2.3’ Lon., Gulf of Chiriqui, Panama; USNM593725, Caroline Sta. 56, Sto. Domingo, Dominican Republic; USNM523173–523175 designated by Herrera-Cubilla et al. (2006).

**Other material.**—UF44633, Chipola formation, Tenmile creek 02, Florida U.S.A.; UF53535, Richardson Rd. Shell Pit 01B, Florida, U.S.A.; UF47715, 49626 Macaspahlt Shell Pit, Florida, U.S.A.; UF51907, 27564 Bermont Formation, Leisey Shell Pit, Florida, U.S.A.; LSUMG-I9314, E Destin FL, U.S.A. (Gulf of Mexico); MHNMC IB88, 11°19’86” Lat., 74°5’ 28” Lon. 20 m depth, Caribe, Colombia; MHNMC IB96, 9°41’47” Lat., 76°5’71” Lon., 71 m depth, Caribe, Colombia.

See Appendix 2 for morphological measurements.

**Occurrence.**—Early Miocene, Chipola Formation, Tenmile Creek 02, Florida, U.S.A. middle Miocene, Chipola Formation, Shoal River, Florida, U.S.A. Late Miocene, Gatun Formation, Sabanita to Payardi, Colon, Panama. Early Pliocene, Cayo Agua Formation, Punta Piedra Roja, western sequence, Bocas del Toro, Panama. Late Pliocene, Solarte I., western tip, Bocas del Toro, Panama; late Pliocene, Cayo Agua Formation, Punta Norte to Punta Tiburon, Bocas del Toro Panama, late Pliocene, Escudo de Veraguas Formation, northern coast, Bocas del Toro, Panama;

late Pliocene, Bastimentos I., Bocas del Toro Panama; late Pliocene, Rio Banano Formation, Limon, Costa Rica; late Pliocene, Moin Formation, Pueblo Nuevo, Limon, Costa Rica; late Pliocene, Lomas del Mar, western reef track sequence, Limon, Costa Rica; late Pliocene to early Pleistocene, Macasphalt Shell Pit, Florida, U.S.A. Pliocene, Tamiami Formation, Richardson Rd. Shell Pit 01B, Florida, U.S.A.; Pliocene, Shell creek, DeSoto Co., Florida, U.S.A. Pleistocene, Bermont Formation, Leisey Shell Pit, Florida, U.S.A.; Pleistocene, Bermont Formation, South Bay 04, Florida, U.S.A. Recent Gulf of Panama and Chiriqui EP.

*Remarks.*—Like in *C. pacificiensis* four Caribbean specimens from late Pliocene to Pleistocene were discriminated as *C. exfragminis*, probably for the same reasons pointed above. As well as four Recent specimens from the same region, finding the same difficulty to discriminate them from their cognate species.

CUPULADRIA PERVAGATA new species  
Figures 20, 21

*Diagnosis.*—Autozooids have the ratio autozooid vibracula opesia length-autozooid vibracula length (RaAloAl)  $\geq 0.75$  mm. Colonies are conical, average height diameter ratio 0.19 mm, average diameter 5.7 mm.

*Description.*—Colonies are conical, with maximum observed diameter of 7.7 mm. The central area of the colony is formed mostly by autozooids and in the majority of the colonies examined their cryptocysts are not thickened by secondary calcification. In general cryptocyst of autozooids descend moderately but septula still visible. Vicarious avicularia are scattered throughout the zone of astogenetic change with gymnocyst well developed, opesia auriform in shape and VAwo less than 0.1 mm (for details see text). Basal sectors are rectangular or irregular in shape with 2–5 pores per sector.

*Etymology.*—Pervagata, Latin “widespread, common” with reference to its widespread geographical and stratigraphical distribution.

*Types.*—Holotype, USNM542565, BT98–19, 9°22.5' Lat., 82°10' Lon., Bocas del Toro; Panama; Paratypes: USNM542566, CMN95–5, 14°30' Lat., 82°29' Lon., Cayos Miskitos, Nicaragua; USNM542567, PPP709; USNM542568, PPP196; USNM542569, PPP1306; USNM542570, NMB16942.

*Material.*—USNM593726, NMB16935; USNM593727, PPP1306; USNM593728–593730, NMB17175, 15863, 15864; USNM593731–593736, PPP379, 350, 334, 709, 69, 311; USNM593737, NMB18105; USNM593738, PPP370, USNM593739–593740, 593742, Bowden Formation, Jamaica; USNM593741, Puerto Limon, Costa Rica; USNM593743–593747, PPP634, 2038, 2024, 631, 944; USNM593748, GM98–90, 8°57.4' Lat., 80°50' Lon., Bocas del Toro, Panama; USNM593749–593750, BT98–19, 9°22.5' Lat., 82°10' Lon., Bocas del Toro; Panama; USNM593751–593752, Eolis station FL U.S.A.; USNM593753, CMN95–5, 14°30' Lat., 82°29' Lon., Cayos Miskitos, Nicaragua; USNM593754, CMN95–11, 14°29' Lat., 82°47.4' Lon., Cayos Miskitos, Nicaragua; USNM593755, PB99–225, 9°39.1' Lat. 79°37.9' Lon., Colon, Panama.

*Other material.*—BZ5603 Basal Moin Formation Puerto Limon, Costa Rica; UF57526, Caloosahatchee Formation, Florida, U.S.A.; UF51907 Bermont Formation, South Bay 04, Florida, U.S.A.; MHNMC–IB88, 11°19'86" Lat., 74°5'28" Lon., Caribbean Colombia.

See Table 4 for morphological measurements.

*Occurrence.*—Middle Miocene, Baitoa Formation, Rio Yaque Norte, Dominican Republic. Late Miocene, Gatun Formation, Sabanita to Payardi, Colon, Panama; late Miocene, Cercado Formation, Rio Mao, Dominican Republic; Messinian to Zanclean, Gurabo Formation, Rio Gurabo, Dominican Republic. Early Pliocene, Shark Hole Point Formation, Valiente Peninsula,

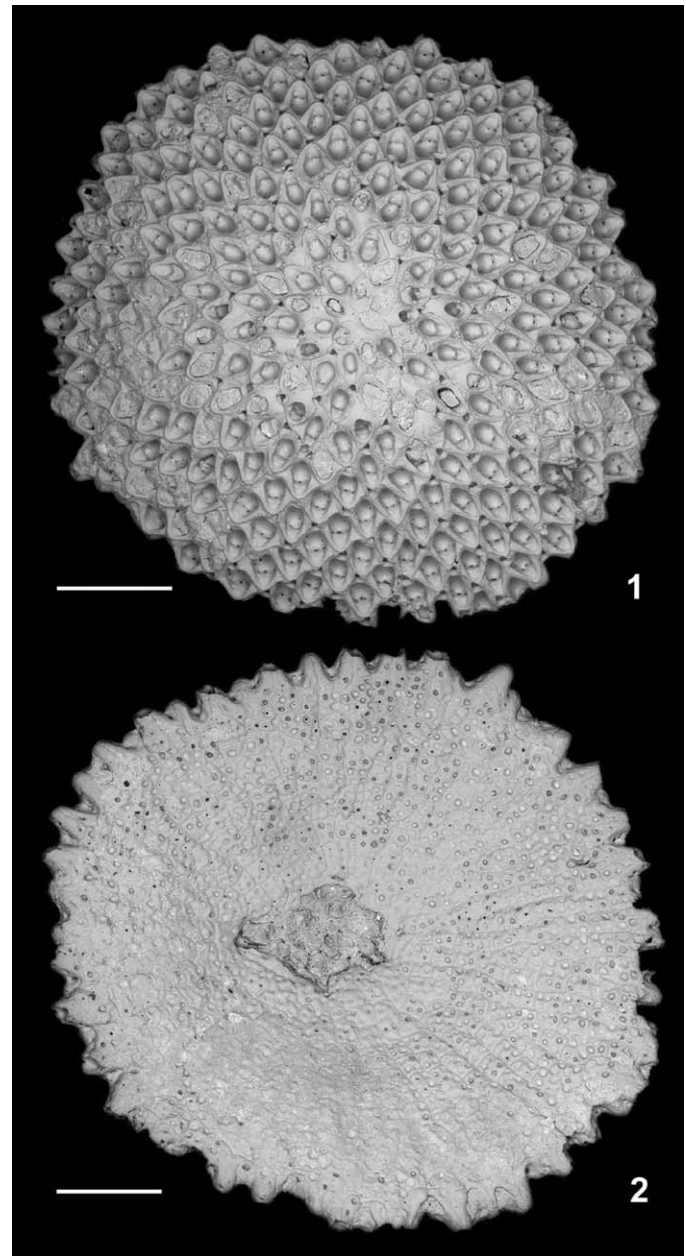


FIGURE 12—*Cupuladria pacificiensis*. 1, 2, hypotype, USNM542592, PPP334, Cayo Agua Formation, early Pliocene, Bocas del Toro, Panama: 1, colony frontal view; 2, colony basal view. Scale bar=1 mm.

Bruno Bluff to Plantain Cay, Bocas del Toro, Panama; early Pliocene, Cayo Agua Formation, Punta Piedra Roja, western sequence, Bocas del Toro, Panama; early Pliocene, Cayo Agua Formation, Punta Norte, western side, Bocas del Toro, Panama; early Pliocene, Cayo Agua Formation, Punta Norte to Punta Tiburon, Bocas del Toro, Panama. Late Pliocene, Escudo de Veraguas Formation, northern coast, Bocas del Toro, Panama; late Pliocene, Cayo Agua Formation, Bocas del Toro, Panama; late Pliocene, Solarte Island., western tip, Bocas del Toro, Panama; late Pliocene, Rio Banano Formation, Santa Rita, Limon, Costa Rica; late Pliocene, Moin Formation; Lomas del Mar, eastern sequence, Limon, Costa Rica; late Pliocene, Moin Formation, Pueblo Nuevo Cemetery, Limon, Costa Rica; late Pliocene, Lomas del Mar, western reef track sequence, Limon, Costa Rica. Pliocene, Puerto Limon, Costa Rica; Pliocene, basal Moin Formation, Puerto Limon, Costa Rica; Pliocene, Bowden



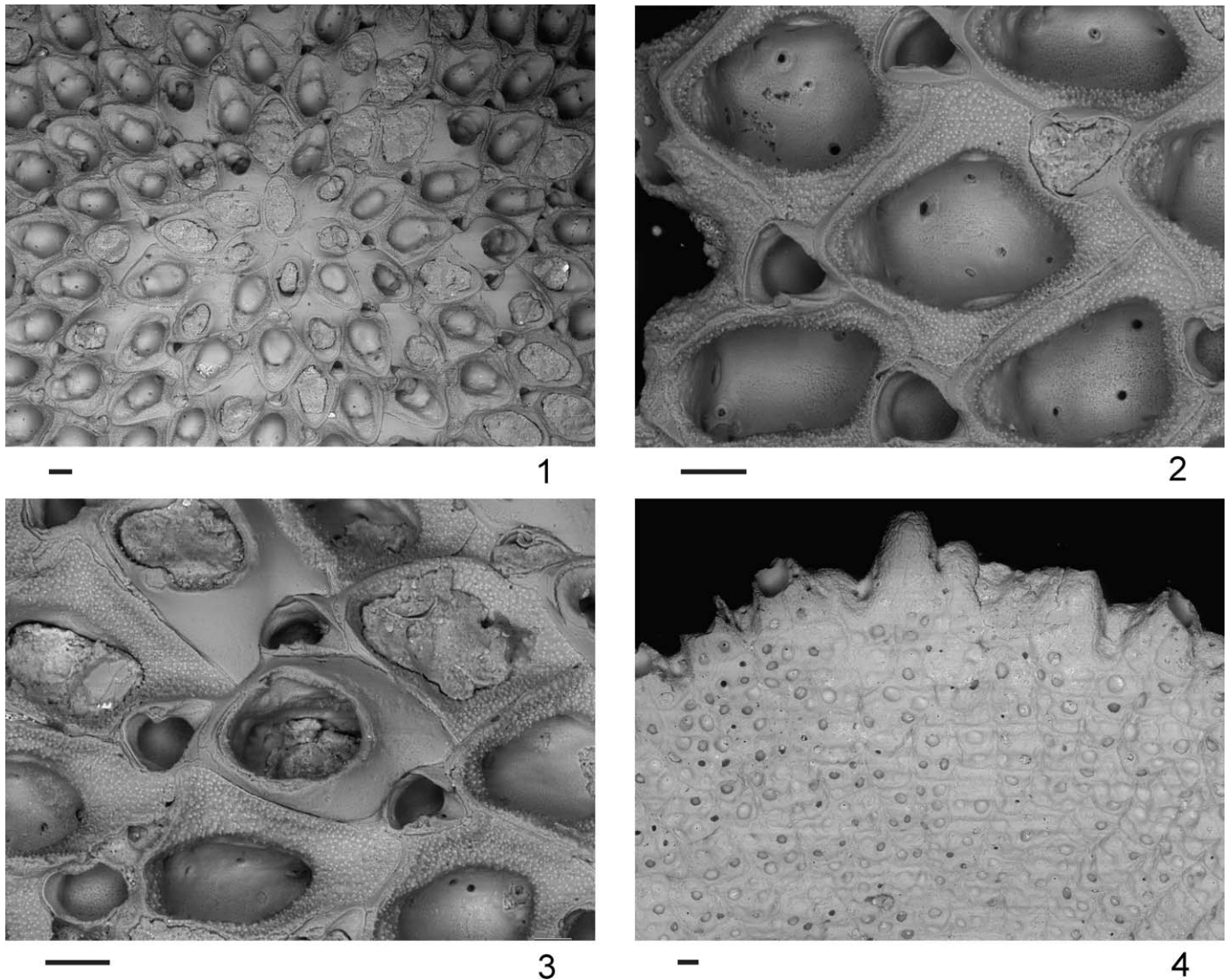


FIGURE 13—*Cupuladria pacificiensis*. 1–4, hypotype, USNM542592, PPP334, Cayo Agua Formation, early Pliocene, Bocas del Toro, Panama: 1, colony center showing autozooids and vicarious avicularia; 2, view of the autozoooid and autozoooid vibraculum; 3, closer view of vicarious avicularium and vicarious avicularium vibraculum; 4, view of the basal sectors and pores. Scale bar=100  $\mu$ m.

Formation, Jamaica. Pleistocene, Caloosahatchee Formation, Florida, U.S.A.; Pleistocene, Bermont Formation, south bay 04, Florida, U.S.A. Recent from Florida to Caribbean Colombia.

**Remarks.**—*Cupuladria pervagata* has a widespread stratigraphic range and geographic distribution in the Caribbean Neogene, and is part of the  $C_{V1}$  group. *Cupuladria pervagata* is morphologically similar to *C. pacificiensis* and *C. biporosa*. Its colony size is similar to *C. pacificiensis* but is flatter in shape. Recent specimens of both species have a central area of the colony formed mostly by autozooids whose cryptocysts are not thickened by secondary calcification, but this feature has been observed only sporadically in fossils. Autozooids and vicarious avicularia with closure plates also occur sometimes in fossil specimens, as has been observed in other species of the  $C_{V1}$  and  $C_{V2}$  clades (see Table 4 and Appendix 2). Autozooids and vicarious opesia size and basal sector area are similar in the two species, although the number of pores per sector is 3–6 in *C. pacificiensis* versus 2–5 in *C. pervagata*. The main difference between the two species is in the ratio of the length of the opesia of autozoooid vibracula to the length of autozoooid vibracula (RaAloA1). This character showed a high coefficient to

discriminate species in DA11 (see above). The ratio for *C. pervagata* is  $\geq 0.75$  mm (similar to *C. monotrema*, *C. dominicana*, *C. colonensis* and *C. floridensis*) versus 0.67 for *C. pacificiensis*. This feature may be related to the strength of the vibracula mechanism of living cupuladriid colonies, which show a high degree of coordination to maintain them above the sediment surface and to right themselves when turned upside down (Cook, 1963; Cook and Chimonides, 1978; Winston, 1988). *Cupuladria pervagata* corresponds to *C. sp. nov. aff. biporosa* in the PPP collection of cupuladriids from the SWC analyzed in O’Dea and Jackson, 2009.

CUPULADRIA CHEETHAMI Herrera-Cubilla et al., 2006

**Description.**—Colonies are conical, with maximum observed diameter of 9.1 mm. The central area of the colony is formed mostly by autozooids. In general cryptocyst of autozooids descend moderately but septula still visible. Vicarious avicularia are scattered throughout the zone of astogenetic change with gymnocyst well developed, opesia auriform in shape and VAwo less than 0.1 mm (for details see text). Autozooids are hexagonal.



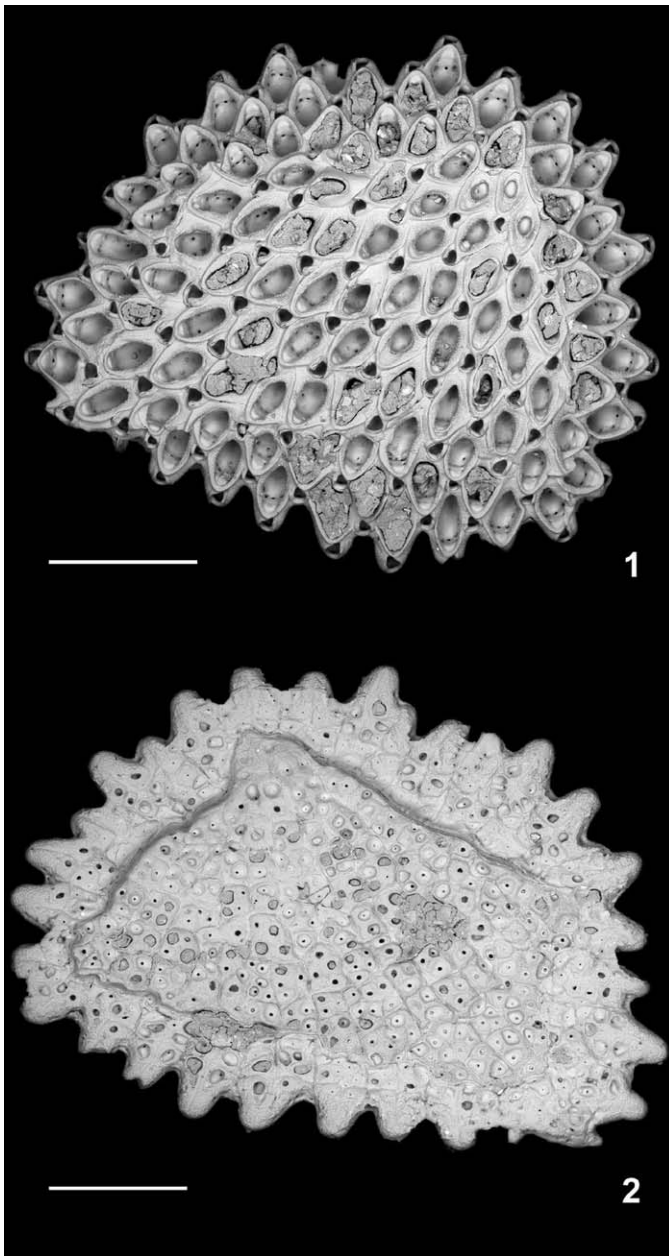


FIGURE 14—*Cupuladria exfragminis*. 1, 2, UF44633, Chipola Formation, early Miocene, Florida, U.S.A.: 1, colony frontal view; 2, colony basal view. Scale bar=1 mm.

The autozooids and vicarious avicularia of this species are notably longer than any other species in the  $C_{V1}$  clade. Basal sectors are rectangular in shape with 3–4 pores per sector. In none of the specimens examined have been observed autozooids and vicarious avicularia with closure plates.

**Material.**—USNM593756, PPP210; USNM593757, CMN95–9, 14°42' Lat., 82°54' Lon., Cayos Miskitos, Nicaragua; USNM523167–523169 designated by Herrera-Cubilla et al., 2006. See Appendix 2 for morphological measurements.

**Occurrence.**—Late Pliocene, Solarte Island western tip, Bocas del Toro, Panama. Recent, Panama and Central America.

CUPULADRIA BIPOROSA Canu and Bassler, 1923

1923 *Cupuladria biporosa* CANU AND BASSLER, p. 9, pl. 47, figs. 1, 2, Miocene, Santo Domingo.

1965b *Cupuladria biporosa* (Canu and Bassler), COOK, p.203, pl. 1, figs. 2, 4, 6.

**Description.**—Colonies are conical, with maximum observed diameter of 12 mm. The central area of the colony is formed mostly by autozooids that are thickened by secondary calcification, although not completely closed, cryptocyst straight sided and septula not visible. Vicarious avicularia are scattered throughout the zone of astogenetic change with gymnocyst well developed, opesia auriform in shape and VAwo less than 0.1 mm (for details see text). Autozooids are hexagonal. Basal sectors are rectangular in shape with 3–5 pores per sector. In none of the specimens examined have been observed vicarious avicularia with closure plates.

**Material.**—USNM593758, PPP963; USNM593759, BT99–130, 9°28.43' Lat., 82°20' Lon., Bocas del Toro, Panama; USNM593760–593761, LC98–29, 9°9.4' Lat., 81°00' Lon., Laguna de Chiriqui, Bocas del Toro, Panama; USNM593762–593763, SB95–18, 9°31.9' Lat., 78°56.5' Lon., San Blas, Panama; USNM593764, Pepperfish key, Gulf of Mexico, 29°23'00" Lat.; 83°41'45" Lon. U.S.A.

See Appendix 2 for morphological measurements.

**Occurrence.**—Late Pliocene, Moin Formation, Lomas del Mar, eastern sequence, Limon, Costa Rica. Recent, from Gulf of Mexico to Panama.

**Remarks.**—Seventy percent of the colonies identified as *C. biporosa* have the cryptocyst of the autozooids of the central area thickened by secondary calcification. Cook (1965b) was the first to discuss this feature, commenting that thickening was observed sometimes in colonies of this species. We have also sporadically observed thickening (one to two colonies) in fossil specimens of: *C. pacificensis*, *C. exfragminis*, and *C. pervagata*; and in one recent specimen of *C. dominicana*.

#### CUPULADRIA FLORIDENSIS new species

Figures 22, 23

**Diagnosis.**—Autozooids have the largest ratio autozooid vibracula opesia length–autozooid vibracula length (RaAloAl) of 0.78 mm; and vicarious the largest ratio vicarious avicularia vibracula opesia length–vicarious avicularia vibracula length (RaVALoVAL) of 0.76 mm in average. Colonies are large with a dome shape, average height to diameter ratio 0.28 mm, average diameter 13.4 mm.

**Description.**—Colonies have a maximum observed diameter of 18.4 mm. The central area of the colony is formed mostly by autozooids, cryptocyst descend moderately but septula still visible. Vicarious avicularia are scattered throughout the zone of astogenetic change with gymnocyst well developed, opesia auriform in shape, and VAwo  $\geq 0.1$  mm (for details see text). Autozooids are hexagonal. Basal sectors are rectangular in shape with 3–5 pores per sector.

**Etymology.**—The name floridensis refers to state of Florida U.S.A., where the first specimens were found.

**Types.**—Holotype USNM542571, New Orleans off coast, 28°32' Lat., 93°24'42" Lon., LA U.S.A.; Paratypes: USNM542572 Dry Tortugas, Florida keys, FL, U.S.A.; USNM542573 Nassau, Bahamas; USNM542574 Punta San Blas, Colon, Panama.

**Material.**—USNM593765–593767, Dry Tortugas, Florida keys, FL, U.S.A.; USNM593768–593769, New Orleans off coast, 28°32' Lat., 93°24'42" Lon., LA, U.S.A.; USNM593770, Albatross Station 2823.

**Other material.**—MCZ100101, Florida keys, 25°13'18" Lat., 80°12'42" Lon., FL, U.S.A.; LSUMG-19314, E Destin, Gulf of Mexico, FL, U.S.A.; NHM.1971.3, 18°41'60" Lat., 110°57' 0" Lon. Mexico; MHNMC IB88, 11°19' 86" Lat., 74°5' 28" Lon., Caribbean, Colombia; MHNMC IB96, 9°41'47" Lat., 76°5'71" Lon., Caribbean, Colombia.

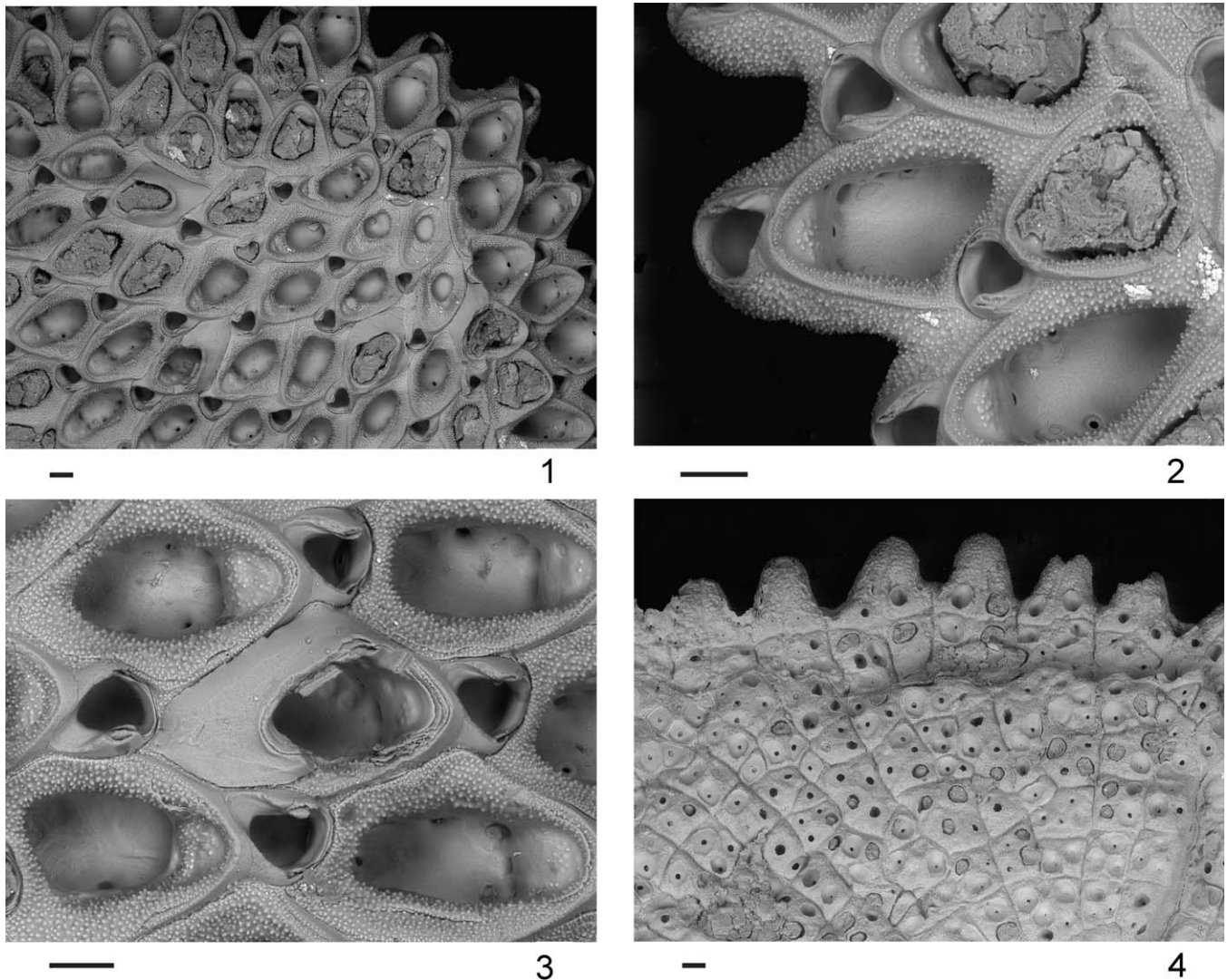


FIGURE 15—*Cupuladria exfragminis*. 1–4, UF44633, Chipola Formation, early Miocene, Florida, U.S.A.: 1, close-up of the colony showing autozooids and vicarious avicularia; 2, view of the autozoooid and autozoooid vibraculum; 3, closer view of vicarious avicularium and vicarious avicularium vibraculum; 4, view of the basal sectors and pores. Scale bar=100  $\mu$ m.

See Table 4 for morphological measurements.

**Occurrence.**—Recent from Gulf of Mexico to Colombia.

**Remarks.**—This species like *C. colonensis* and *C. dominicana* has a  $VAwo \geq 0.1$  mm (for details see text); and the diagnostic characters mentioned above such as  $RaAloAl$  have been important in the discrimination of species; while those related to the strength of the vicarious avicularia vibracula such as  $RaValoVAI$  have been important to define this clade (see text). Besides along with *C. dominicana* have the largest ratio autozoooid vibracula opesia width-autozoooid opesia width ( $RaAwoOw$ ) of 0.68 mm in average, in comparison to *C. colonensis* which is 10 percent smaller.

Three specimens collected from Mexico eastern Pacific were discriminated as *C. floridensis*.

CUPULADRIA COLONENSIS new species

Figures 24, 25

**Diagnosis.**—Autozooids have the ratio autozoooid vibracula opesia width-autozoooid opesia width ( $RaAwoOw$ ) of 0.62 mm in

average. Colonies are large and conical with average height to diameter ratio 0.27 mm, average diameter 16.9 mm.

**Description.**—Colonies conical with maximum observed diameter 18.1 mm. The central area of the colony is formed mostly by autozooids, cryptocyst descend moderately but septula still visible. Vicarious avicularia are scattered throughout the zone of astogenetic change with gymnocyst well developed, opesia auriform in shape, and  $VAwo \geq 0.1$  mm (for details see text). Autozooids are hexagonal. Basal sectors rectangular or irregular with 3–4 pores per sector.

**Etymology.**—The name colonensis refers to the Province of Colon where the large specimens were found.

**Types.**—Holotype USNM542575, Punta San Blas, Colon, Panama, Paratypes: USNM542576 Dry Tortugas, Florida keys, FL, U.S.A.; USNM542577 Pepperfish key, 29°23'00" Lat.; 83°41'45" Lon, Gulf of Mexico, FL, U.S.A.

**Material.**—USNM593771, Pepperfish key, Gulf of Mexico, FL U.S.A. See Table 4 for morphological measurements.

**Occurrence.**—Recent Gulf of Mexico and Panama.

**Remarks.**—*Cupuladria colonensis* has one of the smaller ratio autozoooid vibracula opesia width-autozoooid opesia width



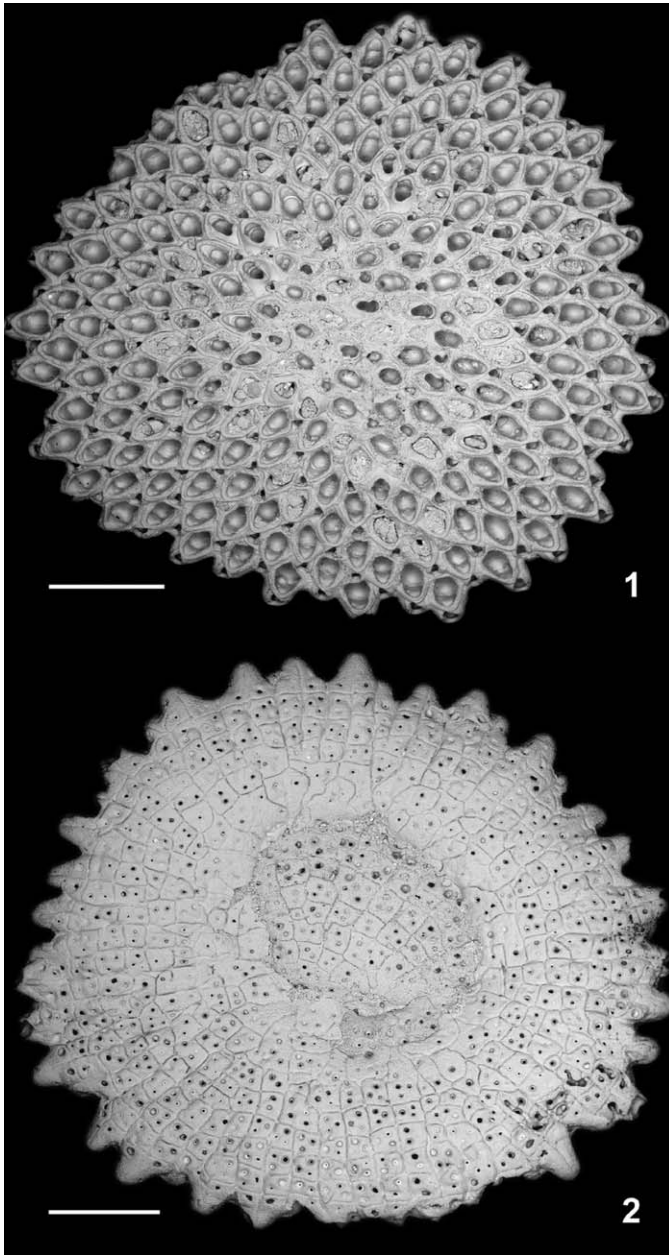


FIGURE 16—*Cupuladria exfragminis*. 1, 2, hypotype, USNM542595, PPP1306, Gatun Formation, late Miocene, Colon, Panama: 1, colony frontal view; 2, colony basal view. Scale bar=1 mm.

(RaAwoOw) of 0.62 mm in the  $C_{V1}$  clade along with *C. Cheethami* with 0.5 mm, however the ratio vicarious avicularia vibracula opesia length-vicarious avicularia vibracula length (RaVAloVAI) of 0.75 mm in average, are similar to *C. dominicana*.

CUPULADRIA DOMINICANA new species  
Figures 26, 27

**Diagnosis.**—Autozooids have the ratio autozooid vibracula opesia width-autozooid opesia width (RaAwoOw) of 0.68 mm; and vicarious the ratio vicarious avicularia vibracula opesia length-vicarious avicularia vibracula length (RaVAloVAI) of 0.75 mm in average. Colonies are conical with average height diameter ratio of 0.27 mm, and average diameter 9.7 mm.

**Description.**—Colonies conical with maximum observed diameter 13.4 mm. The central area of the colony is formed mostly by autozooids, cryptocyst descend moderately but septula still visible. Vicarious avicularia are scattered throughout the zone of astogenetic change with gymnocyst well developed, opesia auriform in shape, and VAwo  $\geq 0.1$  mm (for details see text). Autozooids hexagonal. Basal sectors rectangular or irregular in shape with 3–4 pores per sector.

**Etymology.**—The name *Dominicana* refers to “native or inhabitant of the Dominican Republic”, where the first specimens were found.

**Types.**—Holotype USNM542578, northeast coast Sto. Domingo, 19°10'15" Lat., 69°27'20" Lon. to 19°10'15" Lat., 69°28'5" Lon., Dominican Republic. Paratypes: USNM542579, LCH95–7, 15°59.3' Lat., 86°30' Lon., Cayos Cochinos, Honduras; USNM542580, CMN95–9, 14°42' Lat., 82°54' Lon., Cayos Miskitos, Nicaragua.

**Material.**—USNM593772, NMB17830; USNM593773, SB95–20, 9°36.37' Lat., 78°59.2' Lon., San Blas, Panama; USNM593774–593776, North East coast Sto. Domingo 19°10'15" Lat., 69°27'20" Lon. to 19°10'15" Lat., 69°28'5" Lon., Dominican Republic; USNM593777, Caroline Sta. 56, Sto. Domingo 19°10'15" Lat., 69°27'20" Lon. to 19°10'15" Lat., 69°28'5" Lon., Dominican Republic; USNM593778–593779, LCH95–11, 15°58.62' Lat., 86°30' Lon., Cayos Cochinos, Honduras; USNM593780, LCH95–18, 15°58' Lat., 86°26.46' Lon., Cayos Cochinos, Honduras; USNM593781, CMN95–9, 14°42' Lat., 82°54' Lon., Cayos Miskitos, Nicaragua; USNM593782–593783, CMN95–11, 14°29' Lat., 82°47.4' Lon., Cayos Miskitos, Nicaragua.

**Other material.**—UF50495, Bermont Formation, Belle Glade 01, FL, U.S.A.; MCZ100097, Dry Tortugas, Florida keys, FL, U.S.A.; MHNMC-IB88, 11°19'86" Lat., 74°5'28" Lon., Caribe, Colombia.

See Table 4 for morphological measurements.

**Occurrence.**—Early Pliocene, Cayo Agua Formation, Bocas del Toro, Panama. Pleistocene, Bermont Formation, Belle Glade 01, FL, U.S.A. Recent, from Gulf of Mexico to Colombia.

**Remarks.**—*Cupuladria dominicana* is similar to *C. floridensis* in several autozooid and vicarious features like RaAwoOw and RaVAloVAI (for details see text), but they differ in the width of vicarious vibracula opesia (VAwo), which is smaller than *C. floridensis* and *C. colonensis*. The cryptocyst of the autozooids of the central area were thickened by secondary calcification in one colony of this species.

CUPULADRIA COLLYRIDA new species

Figures 28, 29

**Diagnosis.**—Autozooids have a RaAloAI of 0.83 mm, colonies have a circular-dome shape, and determinate growth with vicarious avicularia occupying the central area, average height diameter ratio 0.53 mm, and average diameter 3.4 mm.

**Description.**—Colonies circular-dome shape, with maximum observed diameter 3.7 mm. Central area of the colony occupied by vicarious avicularia up to the second astogenetic generation with gymnocyst well developed and opesia auriform in shape. Autozooids hexagonal with cryptocyst straight sided and septula not visible. Growth determinate, cessation of growth marked by presence of kenozooids at colony margin, which is formed by almost entirely calcified autozooids leaving a single pore open and vibracula still functional. Basal sectors radial with 2–4 pores per sector.

**Etymology.**—Collyrida, Latin “roll/cake” with reference to the dinner roll shape of the zoarium.

**Types.**—Holotype, USNM542561, Pliocene, Bowden Formation, Jamaica.



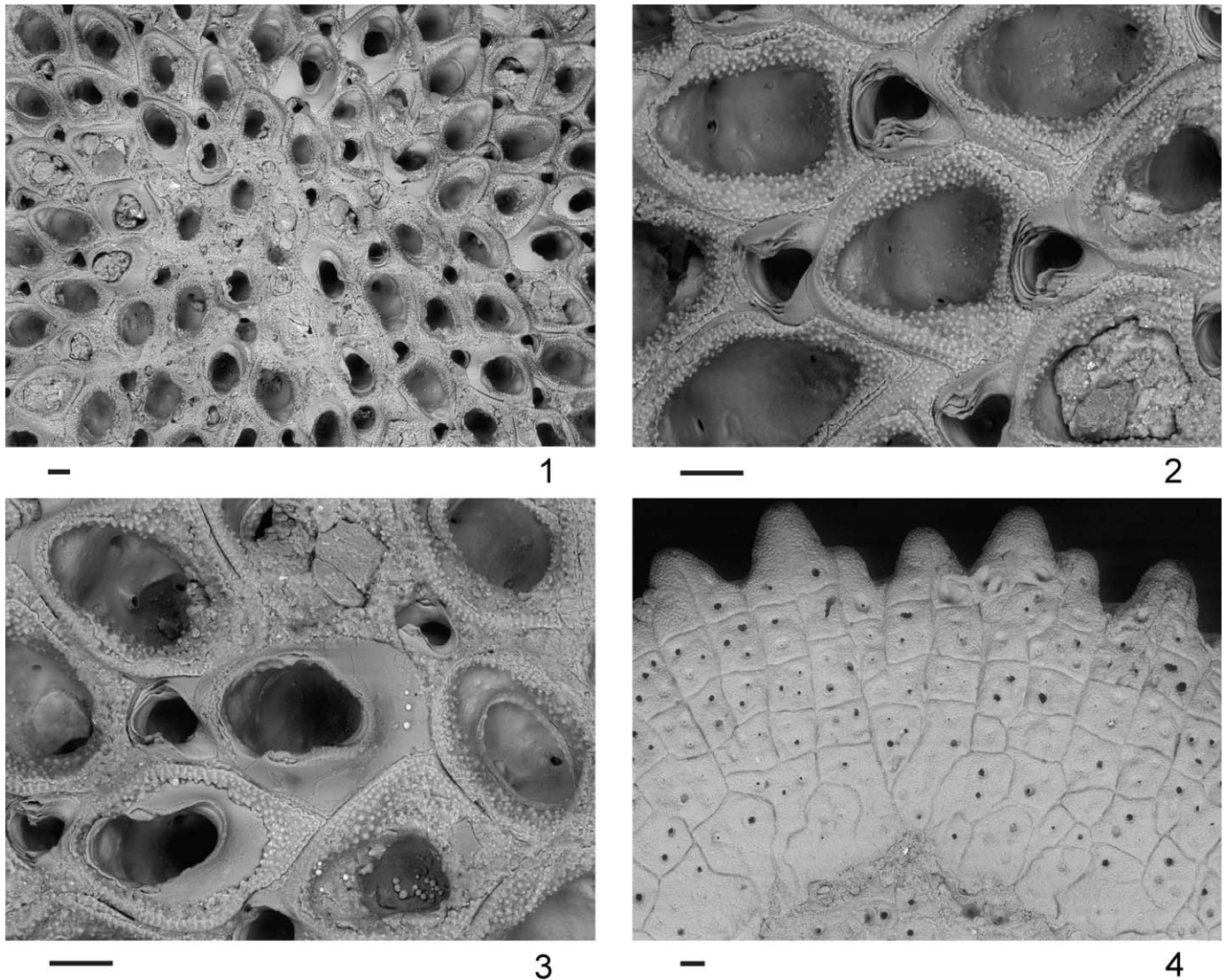


FIGURE 17—*Cupuladria exfragminis*. 1–4, hypotype, USNM542595, PPP1306, Gatun Formation, late Miocene, Colon, Panama: 1, colony center showing autozooids and vicarious avicularia; 2, view of the autozooid and autozooid vibraculum; 3, closer view of vicarious avicularium and vicarious avicularium vibraculum; 4, view of the basal sectors and pores. Scale bar=100  $\mu$ m.

**Material.**—BZ3249 Bowden Formation, Jamaica. See Table 4 for morphological measurements.

**Occurrence.**—Pliocene, Bowden Formation, Jamaica.

**Remarks.**—*Cupuladria collyrida* has the largest ratio autozooid vibracula opesia length-autozooid vibracula length (RaAloAl) in both  $C_{V1}$  and  $C_{V2}$  clades; only *C. gigas* in the  $C_{NV}$  clade has a similar ratio. The determinate growth observed in this species is a trait that has been more characteristic of extant *Discoporella* from the Caribbean side of the Isthmus of Panama (Herrera-Cubilla et al., 2008).

CUPULADRIA INCOGNITA Herrera-Cubilla et al., 2006

**Description.**—Colonies conical with maximum observed diameter of 6.8 mm, living colonies are blue-black. Central area of the colony occupied by vicarious avicularia with gymnocyst well developed and opesia auriform in shape. Autozooids hexagonal, with cryptocyst straight sided and well developed centrally, septula not visible. Basal sectors radial with 7–23 pores.

**Types.**—Hypotype USNM593785, PPP342.

**Material.**—USNM593784, 593786, PPP357, 709; USNM593787, NMB17841, USNM593788, PPP368; USNM593789, Bowden Formation, Jamaica; USNM593790, Puerto Limon, Costa Rica; USNM593791, PPP1253; USNM593792–593794, Bastimentos I., Bocas del Toro, Panama; USNM593795–593799, PPP178, 2171, 362, 640, USNM593800, NMB18080; USNM593801, BA98–125, 9°25.3' Lat., 82°20.4' Lon., Bahía Almirante, Bocas del Toro, Panama; USNM593802, GM98–74, 9°21.18' Lat., 80°12' Lon., Golfo de los Mosquitos, Bocas del Toro, Panama; USNM593803, GM98–90, 8°57.4' Lat., 80°50' Lon., Golfo de los Mosquitos, Bocas del Toro, Panama; USNM593804, PB99–225, 9°39.1' Lat., 79°37.9' Lon., Costa Arriba, off Islas Farallones, Colon, Panama; USNM523163 designated by Herrera-Cubilla et al., 2006.

**Other material.**—UF75958, Bowden Formation, St. Thomas Parish, Jamaica; BZ5603, Basal Moin Formation Puerto Limon, Costa Rica.

See Appendix 2 for morphological measurements.

**Occurrence.**—Early Pliocene Cayo Agua Formation, Punta Piedra Roja, western sequence, Bocas del Toro, Panama; early

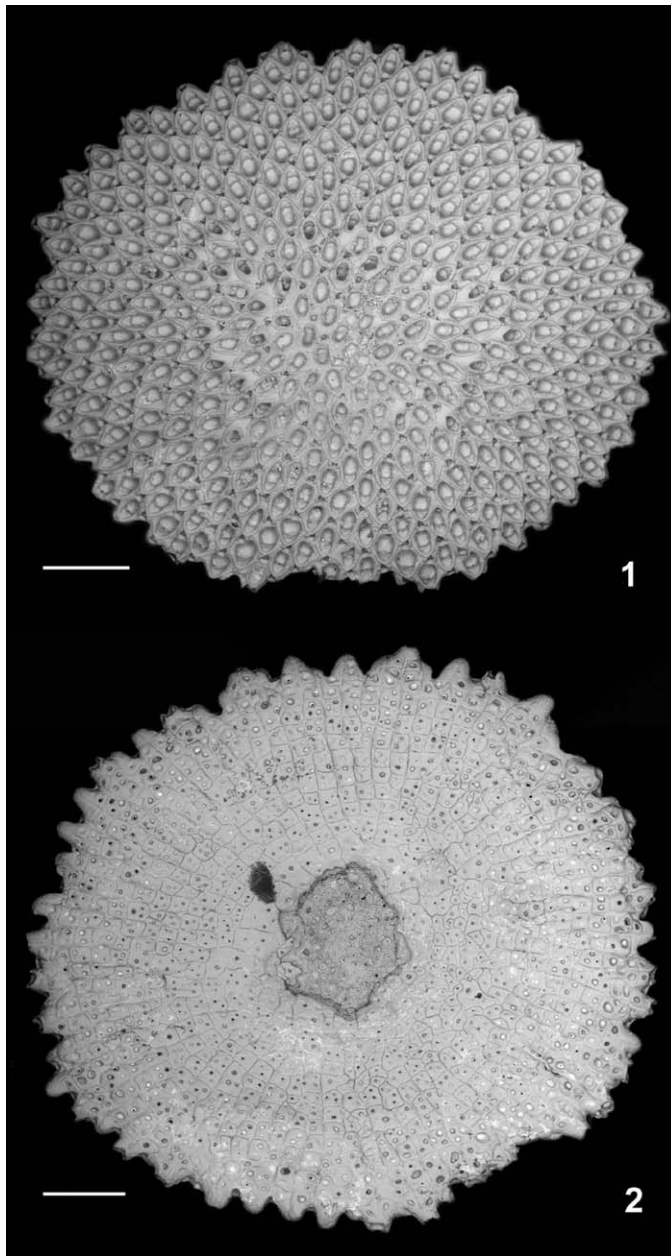


FIGURE 18—*Cupuladria exfragminis*. 1, 2, hypotype, USNM542593, PPP65, Cayo Agua Formation, late Pliocene, Bocas del Toro, Panama: 1, colony frontal view; 2, colony basal view. Scale bar=1 mm.

Pliocene, Cayo Agua Formation, Punta Norte to Punta Tiburon, Bocas del Toro, Panama; early Pliocene, Bowden Formation, St. Thomas Parish, Jamaica. Late Pliocene, Escudo de Veraguas Formation, northern coast, Bocas del Toro, Panama; late Pliocene, Escudo de Veraguas Formation, Bocas del Toro, Panama; late Pliocene, Bastimentos Island, Fish Hole, western sequence, Bocas del Toro, Panama; late Pliocene, Bastimentos Island, Bocas del Toro, Panama; late Pliocene, Rio Banano Formation, Santa Rita, Limon, Costa Rica; late Pliocene, Moin Formation, Lomas del Mar, eastern sequence, Limon, Costa Rica; late Pliocene, Lomas del Mar, western reef track sequence, Limon, Costa Rica; late Pliocene, basal Moin Formation, Puerto Limon, Costa Rica. Pliocene, Puerto Limon, Costa Rica, Pliocene, Bowden Formation, Jamaica. Recent: Bocas del Toro, Colon and San Blas, Panama.

#### CUPULADRIA MULTESIMA Herrera-Cubilla et al., 2006

*Description*.—Colonies have a dome shape with maximum observed diameter of 5.6 mm, live colonies are brown. Central area of the colony occupied by vicarious avicularia with gymnocyst well developed and opesia auriform in shape. Autozooids hexagonal, with cryptocyst straight sided and well developed centrally, septula not visible. Basal sectors radial with 4–9 pores.

*Types*.—Hypotype USNM593805, PPP370.

*Material*.—USNM593806–593807, PPP2024, 2221; USNM593808, 593811–593812, SB95–18, 9°31.9' Lat., 78°56.5' Lon., San Blas, Panama; USNM593809, 593814, BT98–36, 9°13.5' Lat., 81°53' Lon., Bocas del Toro, Panama; USNM593810, GM98–69, 9°18.6' Lat., 80°20' Lon., Bocas del Toro, Panama; USNM593813, SB95–20, 9°36.9' Lat., 78°59.2' Lon., San Blas, Panama; USNM523158, 523160 designated by Herrera-Cubilla et al., 2006.

See Appendix 2 for morphological measurements.

*Occurrence*.—Late Pliocene, Escudo de Veraguas Formation, northern coast; late Pliocene, Swan Cay Formation, north of Isla Colon, Bocas del Toro, Panama; late Pliocene, Lomas del Mar, western reef track sequence, Limon, Costa Rica. Recent: Bocas del Toro to San Blas, Panama.

#### CUPULADRIA PLANISSIMA new species

Figures 30, 31

*Diagnosis*.—Vicarious avicularia occupy the central area, and have the vicarious avicularia vibracula width-length ratio (VAwVAI) of 0.82 mm in average, colonies are conical with basal side completely flat and basal sectors radial, average height diameter ratio 0.44 mm, average diameter 3.4 mm.

*Description*.—Colonies have a dome shape, with maximum observed diameter 5 mm. Central area of colony occupied by vicarious avicularia up to the second astogenetic generation; with gymnocyst well developed and opesia auriform in shape. Autozooids hexagonal with cryptocyst descending moderately and septula still visible. Basal side of colony not concave but completely flat. Basal sectors radial with 4–14 pores per sector.

*Etymology*.—Planissima Latin “flat, level” with reference to the planar basal side of the colony.

*Types*.—Holotype USNM542581, Bastimentos I., Bocas del Toro, Panama; Paratypes: USNM542582–542583, PPP2026, 335.

*Material*.—USNM593815, NMB18105; USNM593816, Bastimentos I., Bocas del Toro, Panama; USNM593817–593818, PPP635, 963; USNM593819, BT98–36, 9°13.5' Lat., 81°53' Lon., Bocas del Toro, Panama; USNM593820, GM98–69, 9°18.6' Lat., 80°20' Lon., Bocas del Toro, Panama; USNM593821, SB95–18, 9°31.9' Lat., 78°56.5' Lon., San Blas, Panama; USNM593822, BT98–5, 9°30.4' Lat., 82°20' Lon., Bocas del Toro, Panama.

*Other material*.—BZ5603, Basal Moin Formation Puerto Limon, Costa Rica. See Table 4 for morphological measurements.

*Occurrence*.—Early Pliocene, Cayo Agua Formation, Punta Norte to Punta Tiburon, Bocas del Toro, Panama. Late Pliocene, Bastimentos Island., Bocas del Toro, Panama; late Pliocene, Rio Banano Formation, Limon, Costa Rica; late Pliocene, Moin Formation, Lomas del mar eastern sequence, Limon, Costa Rica; late Pliocene, Lomas del Mar, western reef track sequence, Limon, Costa Rica; late Pliocene, basal Moin Formation, Puerto Limon, Costa Rica. Recent: Bocas del Toro and San Blas, Panama.

*Remarks*.—*Cupuladria planissima* has the smaller vicarious avicularia vibracula width-length ratio (VAwVAI) of the  $C_{V2}$  clade; and it also differs from *C. multesima* and *C. incognita* in the moderate development of the cryptocyst.



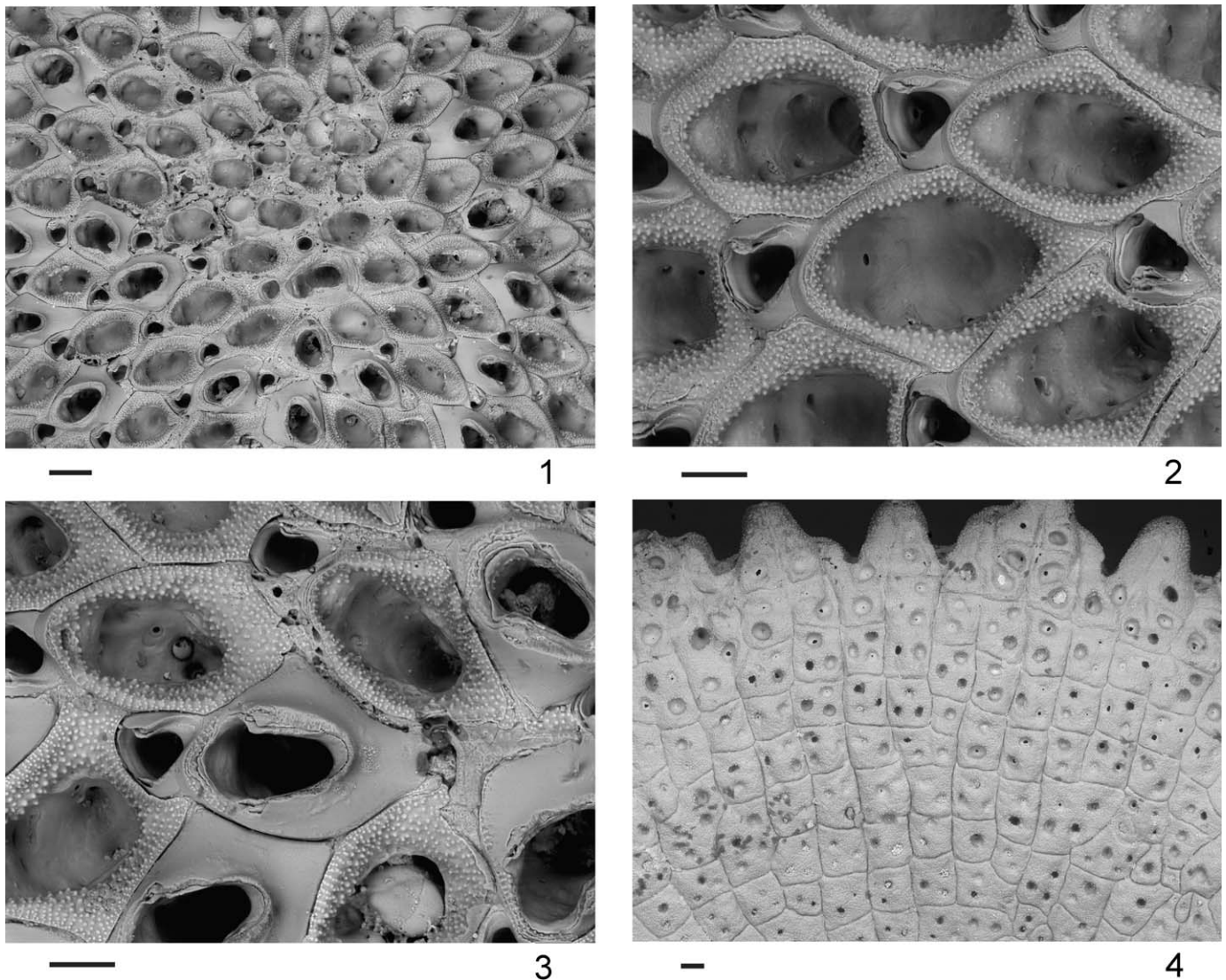


FIGURE 19—*Cupuladria exfragminis*. 1–4, hypotype, USNM542593, PPP65, Cayo Agua Formation, late Pliocene, Bocas del Toro, Panama: 1, colony center showing autozooids and vicarious avicularia; 2, view of the autozoid and autozoid vibraculum; 3, closer view of vicarious avicularium and vicarious avicularium vibraculum; 4, view of the basal sectors and pores. Scale bar=100  $\mu$ m.

CUPULADRIA VERACRUZIENSIS new species

Figures 32, 33

**Diagnosis.**—Autozooids have the opesia length (OL) of 0.27 mm in average; the colonies are conical, with vicarious avicularia occupying the central area, basal sectors rectangular or irregular in shape, average height diameter ratio 0.18 mm, average diameter 4 mm.

**Description.**—Colonies are conical, with maximum observed diameter 6.1 mm. Central area of colony occupied by vicarious avicularia up to the sixth astogenetic generation; with gymnocyst well developed and opesia auriform in shape. Autozooids hexagonal, with cryptocyst descending moderately and septula still visible. Basal sectors rectangular or irregular in shape with 2–6 pores per sector.

**Etymology.**—Named for the state of Veracruz (from Latin: Vera Crux), Mexico where the oldest specimen was collected.

**Types.**—Holotype USNM542562, PPP2171. Paratypes: USNM542563, Fowey lighthouse, Key Biscayne Florida U.S.A.; USNM542564, TU638.

**Material.**—USNM593823–593827, PPP379, 63, 196;

USNM593828–593829, TU638, TU1046; USNM593830, NMB18105; USNM593831–593833, PPP695, 678, 2174; USNM593834, CMN95–5, 14°30' Lat., 82°29' Lon., Cayos Miskitos, Nicaragua.

**Other material.**—D34528, Paraje Solo Formation, Veracruz, Mexico; UF53535, Richardson road shell pit, FL, U.S.A.; UF47715, Macasphalt shell pit, FL, U.S.A.; MCZ100096, Marquesas Key, FL, U.S.A.; MHNMC–IB88, 11°19'86" Lat., 74°5'28" Lon. Caribbean, Colombia.

See Table 4 for morphological measurements.

**Occurrence.**—(?)Late Miocene, Paraje Solo Formation, Veracruz, Mexico. Early Pliocene, Shark Hole Point Formation, Valiente peninsula, from Bruno bluff to Plantain cays, Bocas del Toro, Panama; early Pliocene, Cayo Agua Formation, Punta Norte western side, Bocas del Toro, Panama. Late Pliocene, Escudo de Veraguas Formation, northern coast, Bocas del Toro, Panama; late Pliocene, Rio Banano Formation, Limon, Costa Rica. Pliocene Agueguexquite Formation, Coatzacoalcos, Veracruz, Mexico; Pliocene, Richardson road shell pit 01B, Florida,



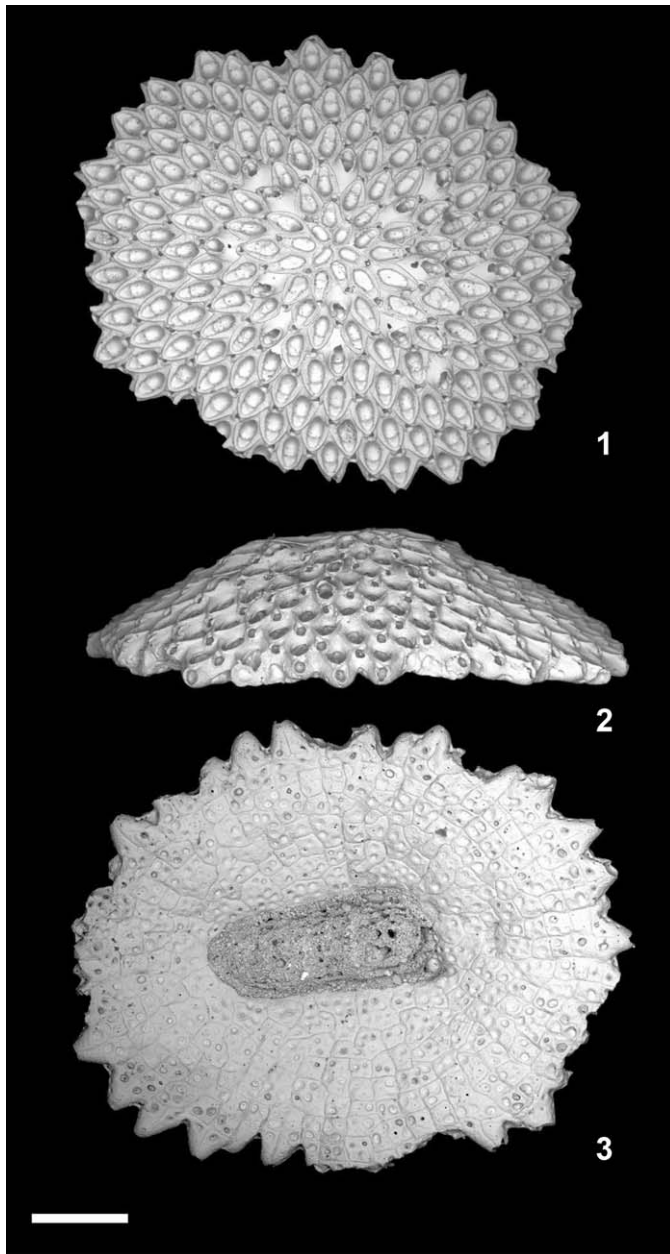


FIGURE 20—*Cupuladria pervagata* n. sp. 1–3, holotype, USNM542565, BT98–19, Recent, Bocas del Toro, Panama: 1, colony frontal view; 2, colony side view; 3, colony basal view. Scale bar=1 mm.

U.S.A.; Pliocene, Macasphalt shell pit, Florida, U.S.A. Recent: Florida, Nicaragua, Caribbean Colombia.

**Remarks.**—*Cupuladria veracruxiensis* has the largest opesia length (Ol) in the  $C_{V2}$  clade, and differs also from the rest of their members in the shape of the basal sectors, which are rectangular instead of radial. Some specimens have autozoid and vicarious avicularia with closure plates.

#### CUPULADRIA SURINAMENSIS Cadée, 1975

**Description.**—Autozooids have a length (Zl) of 0.53 mm in average; the colonies are conical, with maximum observed diameter of 10 mm. The central area of the colony is formed exclusively by autozooids. Autozooids are hexagonal, their cryptocyst descend steeply and septula are visible. Vicarious

avicularia not observed. Basal sectors are radial with 2–17 pores. Few specimens have autozooids with closure plates.

**Types.**—Hypotypes USNM542586–542588, PPP640, 212, 352.

**Material.**—USNM593835–593836, PPP326; USNM593837, NMB17830; USNM593838–593844, PPP340, 335, 212, 210, 722, 709, 368; USNM593845, 593847, NMB17841, 18388; USNM593846, 593849, Bastimentos I., Bocas del Toro, Panama; USNM593848, 593850–593853, PPP635, 178, 362, 2024; USNM593854–593856, BT98–46, 9°8′ Lat., 81°33.2′ Lon., Escudo de Veraguas, Bocas del Toro, Panama; USNM593857–593858, SB95–12, 9°32.5′ Lat., 78°57.8′ Lon., San Blas, Panama; USNM593859, GM98–50, 8°57′ Lat., 81°30′ Lon., Escudo de Veraguas, Panama; USNM593860, GM98–73, 9°16.7′ Lat., 80°12′ Lon., Golfo de los Mosquitos, Panama; USNM593861, GM98–74, 9°21.18′ Lat., 80°12′ Lon., Golfo de los Mosquitos, Panama; USNM593862, GM98–89, 8°55′ Lat., 80°50′ Lon., Golfo de los Mosquitos, Panama; USNM593863–593865, BT98–102, 9°20.7′ Lat., 82°7′ Lon., Bocas del Toro, Panama; USNM593866, BT98–125, 9°25.3′ Lat., 82°20.4′ Lon., Bahía de Almirante, Panama; USNM593867, BT98–128, 9°27.78′ Lat., 82°18.37′ Lon., Bahía de Almirante, Panama; USNM593868–593869, LCH95–2, 15°56.4′ Lat., 86°29.9′ Lon., Cayos Cochinos, Honduras; USNM593870, LCH95–11, 15°58.62′ Lat., 86°30′ Lon., Cayos Cochinos, Honduras; USNM593871–593872, CMN95–9, 14°42′ Lat., 82°54′ Lon., Cayos Miskitos, Nicaragua; USNM593873–593875, CMN95–11, 14°29′ Lat., 82°47.4′, Cayos Miskitos, Nicaragua.

**Other material.**—BZ3249, Basal Moin Formation Puerto Limon, Costa Rica; NHM1975.9.4.2, 6°14.5′ Lat., 53°25′ Lon., Guyana. See Appendix 2 for morphological measurements.

**Occurrence.**—Early Pliocene, Cayo Agua Formation, Punta Piedra Roja, western sequence, Bocas del Toro, Panama; early Pliocene, Cayo Agua Formation, Punta Norte to Punta Tiburon, Bocas del Toro, Panama; early Pliocene, Cayo Agua Formation, Bocas del Toro, Panama. Late Pliocene, Escudo de Veraguas Formation, northern coast, Bocas del Toro, Panama; late Pliocene, Escudo de Veraguas Formation, Bocas del Toro, Panama; late Pliocene, Solarte Island, western tip, Bocas del Toro, Panama; late Pliocene, Bastimentos Island, Bocas del Toro, Panama; late Pliocene, Rio Banano Formation, Santa Rita, Limon, Costa Rica; late Pliocene, Santa Rita, Limon, Costa Rica; late Pliocene, Moin Formation, Lomas del Mar, eastern sequence, Limon, Costa Rica; late Pliocene, Lomas del Mar, western reef track sequence, Limon, Costa Rica. Pliocene, Bowden Formation, Jamaica. Recent, Central America and Guyana.

#### CUPULADRIA PANAMENSIS Herrera-Cubilla et al., 2006

**Description.**—Autozooids have a length (Zl) of 0.56 mm in average; the colonies have a dome shape, with maximum observed diameter of 10.3 mm. The central area of the colony is formed exclusively by autozooids. Autozooids are hexagonal; cryptocyst descends moderately but septula still visible. Vicarious avicularia not observed. Basal sectors are radial with 5–24 pores. Few specimens have autozooids with closure plates.

**Types.**—Hypotypes USNM542589, CMN95–5, 14°30′ Lat., 82°29′ Lon., Cayos Miskitos, Nicaragua; USNM542590, Escudo de Veraguas Formation, Bocas del Toro, Panama; USNM542591, PPP2170.

**Material.**—USNM593876–593877, PPP350, 212; USNM593878, Escudo de Veraguas formation, Bocas del Toro, Panama; USNM593879, PPP2174; USNM593880–593881, NMB18084; USNM593882–593885, PPP2024, 2038, 942; USNM593886–593887, SB95–4, 9°34′ Lat., 78°35′ Lon., San Blas, Panama; USNM593888–593889, SB95–7, 9°31′ Lat., 78°45′ Lon., San Blas, Panama; USNM593890–593891, SB95–9, 9°31′ Lat., 78°44.3′ Lon., 67 m depth, brown sandy mud, San Blas, Panama; USNM593892, GM98–50, 8°57′ Lat., 81°30′ Lon., Escudo de Veraguas, Panama; USNM593893–593894, GM98–

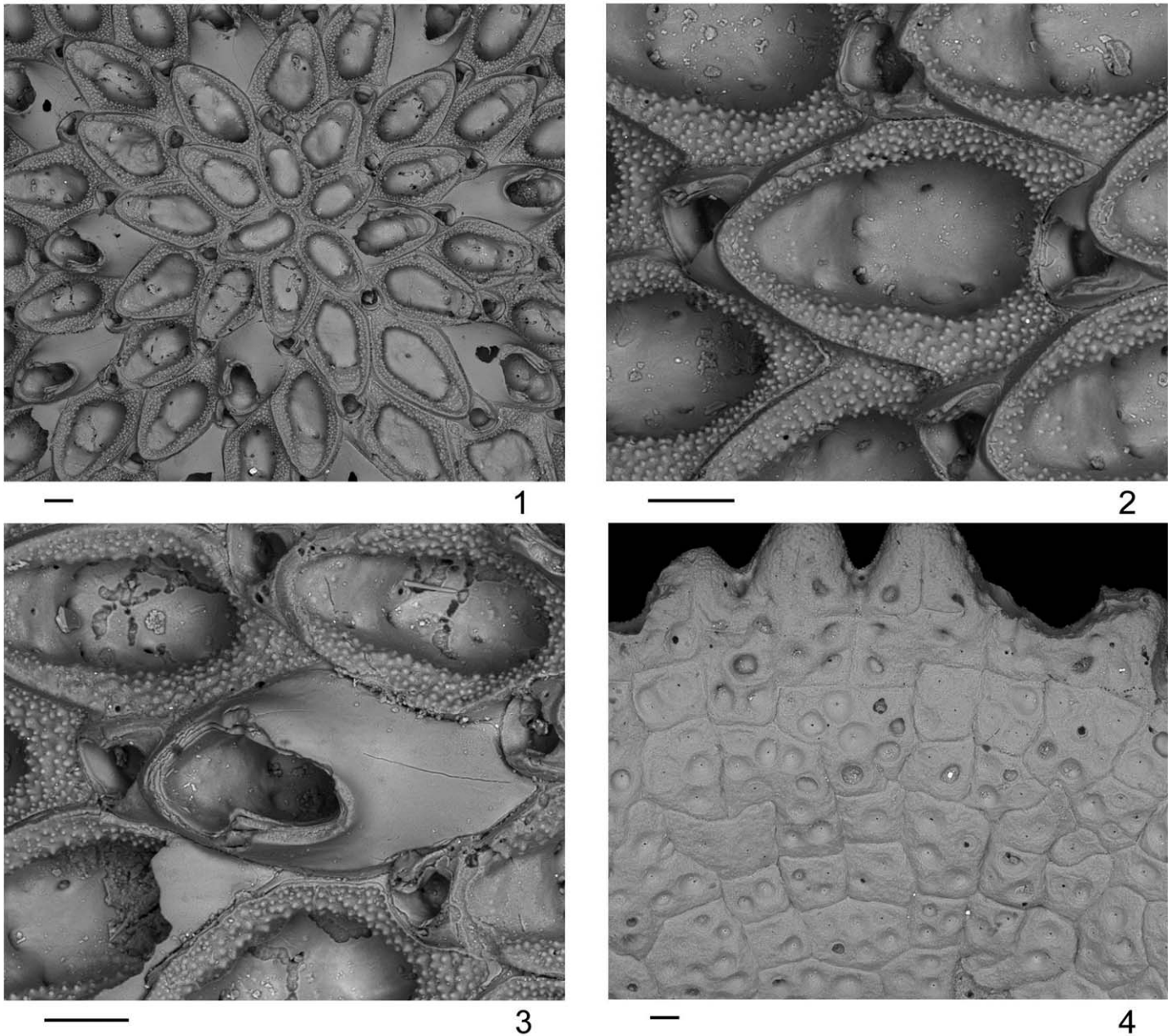


FIGURE 21—*Cupuladria pervagata* n. sp. 1–4, holotype, USNM542565, BT98–19, Recent, Bocas del Toro, Panama: 1, colony center showing autozooids and vicarious avicularia; 2, view of the autozoid and autozoid vibraculum; 3, closer view of vicarious avicularium and vicarious avicularium vibraculum; 4, view of the basal sectors and pores. Scale scale=100  $\mu$ m.

73, 9°16.7' Lat., 80°12' Lon., Golfo de los Mosquitos, Panama; USNM593895–593896, GM98–74, 9°21.18' Lat., 80°12' Lon., Golfo de los Mosquitos, Bocas del Toro, Panama; USNM593897–593898, 593910, GM98–90, 8°57.4' Lat., 80°50' Lon., Bocas del Toro, Panama; USNM593899–593901, 593908–593909, GM98–78, 9°28.93' Lat., 80° Lon., Golfo de los Mosquitos, Bocas del Toro, Panama; USNM593902–593907, SB95–20, 9°36.9' Lat., 78°59.2' Lon., San Blas, Panama; USNM593911, LCH95–2, 15°56.4' Lat., 86°29.9' Lon., Cayos Cochinos, Honduras; USNM593912–593913, LCH95–11, 15°58.62' Lat., 86°30' Lon., Cayos Cochinos, Honduras; USNM593914–593916, CMN95–9, 14°42' Lat., 82°54' Lon., Cayos Miskitos, Nicaragua; USNM593917–593919, PB99–225, 9°39.1' Lat., 79°37.9' Lon., Colon, Panama; USNM523179, 523182 designated by Herrera-Cubilla et al., 2006.

*Other material.*—BZ5603, Basal Moin Formation Puerto Limon, Costa Rica. See Appendix 2 for morphological measurements.

*Occurrence.*—Early Pliocene, Cayo Agua Formation, Punta Piedra Roja, western sequence, Bocas del Toro, Panama. Late Pliocene, Solarte Island, western tip, Bocas del Toro, Panama; late Pliocene, Escudo de Veraguas Formation, northern coast, Bocas del Toro, Panama; late Pliocene, basal Moin Formation, Puerto Limon, Costa Rica; late Pliocene, Moin Formation, Limon, Costa Rica; late Pliocene, Moin Formation, Lomas del Mar, eastern sequence, Limon, Costa Rica; late Pliocene, Lomas del Mar, western reef track sequence, Limon, Costa Rica.

Recent, Central America to Panama.

*Remarks.*—*Cupuladria panamensis* has the largest zooid size (Z1) in the C<sub>NV</sub> clade, while *C. surinamensis* is intermediate.



TABLE 4—Measurements (in mm) of zoarial and zooidal characters for the eight new species described. Refer to Table 1 for character names.

| Characters | <i>C. pervagata</i> n. sp. |        |       |        |        | <i>C. floridensis</i> n. sp. |         |        |         |        | <i>C. colonensis</i> n. sp. |         |         |         |        | <i>C. dominicana</i> n. sp. |        |        |         |        |
|------------|----------------------------|--------|-------|--------|--------|------------------------------|---------|--------|---------|--------|-----------------------------|---------|---------|---------|--------|-----------------------------|--------|--------|---------|--------|
|            | N                          | Mean   | Min   | Max    | SD     | N                            | Mean    | Min    | Max     | SD     | N                           | Mean    | Min     | Max     | SD     | N                           | Mean   | Min    | Max     | SD     |
| Cw         | 41                         | 5.664  | 3.500 | 7.700  | 0.862  | 18                           | 13.361  | 9.550  | 18.400  | 2.891  | 4                           | 16.875  | 15.650  | 18.050  | 1.115  | 18                          | 9.713  | 6.275  | 13.400  | 1.860  |
| Ch         | 41                         | 1.111  | 0.200 | 1.900  | 0.467  | 18                           | 3.672   | 2.000  | 5.000   | 0.939  | 4                           | 4.500   | 3.800   | 5.500   | 0.770  | 18                          | 2.647  | 1.850  | 4.200   | 0.708  |
| Rahw       | 41                         | 0.193  | 0.040 | 0.322  | 0.075  | 18                           | 0.278   | 0.187  | 0.409   | 0.062  | 4                           | 0.267   | 0.222   | 0.313   | 0.042  | 18                          | 0.272  | 0.201  | 0.362   | 0.046  |
| Csur       | 41                         | 27.925 | 9.685 | 49.982 | 8.294  | 18                           | 167.248 | 87.945 | 298.633 | 70.030 | 4                           | 254.739 | 213.872 | 285.531 | 34.064 | 18                          | 87.563 | 35.906 | 157.016 | 34.242 |
| Ci         | 41                         | 0.094  | 0.047 | 0.271  | 0.034  | 18                           | 0.087   | 0.057  | 0.125   | 0.021  | 4                           | 0.117   | 0.073   | 0.141   | 0.031  | 18                          | 0.088  | 0.055  | 0.123   | 0.022  |
| RaZV       | 41                         | 0.680  | 0.125 | 1.000  | 0.194  | 18                           | 2.000   | 2.000  | 2.000   | 0.000  | 4                           | 0.688   | 0.375   | 0.875   | 0.217  | 18                          | 0.549  | 0.250  | 0.875   | 0.192  |
| Zl         | 41                         | 0.474  | 0.399 | 0.572  | 0.049  | 18                           | 0.446   | 0.382  | 0.541   | 0.037  | 4                           | 0.452   | 0.403   | 0.509   | 0.046  | 18                          | 0.470  | 0.395  | 0.570   | 0.048  |
| Zw         | 41                         | 0.329  | 0.239 | 0.408  | 0.039  | 18                           | 0.308   | 0.228  | 0.363   | 0.038  | 4                           | 0.324   | 0.269   | 0.362   | 0.044  | 18                          | 0.310  | 0.242  | 0.395   | 0.045  |
| OI         | 41                         | 0.316  | 0.260 | 0.381  | 0.035  | 18                           | 0.322   | 0.257  | 0.405   | 0.034  | 4                           | 0.308   | 0.262   | 0.363   | 0.046  | 18                          | 0.329  | 0.264  | 0.391   | 0.035  |
| Ow         | 41                         | 0.167  | 0.133 | 0.254  | 0.024  | 18                           | 0.186   | 0.141  | 0.215   | 0.022  | 4                           | 0.196   | 0.171   | 0.210   | 0.017  | 18                          | 0.171  | 0.134  | 0.203   | 0.022  |
| Al         | 41                         | 0.207  | 0.173 | 0.248  | 0.017  | 18                           | 0.226   | 0.164  | 0.272   | 0.023  | 4                           | 0.229   | 0.205   | 0.247   | 0.020  | 18                          | 0.223  | 0.192  | 0.260   | 0.020  |
| Aw         | 41                         | 0.167  | 0.141 | 0.224  | 0.016  | 18                           | 0.180   | 0.130  | 0.230   | 0.022  | 4                           | 0.181   | 0.160   | 0.198   | 0.016  | 18                          | 0.164  | 0.132  | 0.202   | 0.018  |
| Alo        | 41                         | 0.158  | 0.114 | 0.198  | 0.017  | 18                           | 0.176   | 0.134  | 0.202   | 0.015  | 4                           | 0.176   | 0.160   | 0.188   | 0.014  | 18                          | 0.173  | 0.136  | 0.209   | 0.020  |
| Awo        | 41                         | 0.110  | 0.091 | 0.145  | 0.012  | 18                           | 0.125   | 0.099  | 0.150   | 0.014  | 4                           | 0.122   | 0.110   | 0.136   | 0.011  | 18                          | 0.115  | 0.099  | 0.139   | 0.012  |
| Zcp        | 41                         | 0.024  | 0.000 | 1.000  | 0.156  | 18                           | 0.000   | 0.000  | 0.000   | 0.000  | 4                           | 0.000   | 0.000   | 0.000   | 0.000  | 18                          | 0.000  | 0.000  | 0.000   | 0.000  |
| Vcp        | 41                         | 0.024  | 0.000 | 1.000  | 0.156  | 18                           | 0.000   | 0.000  | 0.000   | 0.000  | 4                           | 0.000   | 0.000   | 0.000   | 0.000  | 18                          | 0.000  | 0.000  | 0.000   | 0.000  |
| NV         | 41                         | 15.780 | 1.000 | 49.000 | 11.385 | 18                           | 69.778  | 11.000 | 141.000 | 42.379 | 4                           | 77.000  | 50.000  | 131.000 | 36.670 | 18                          | 52.056 | 6.000  | 134.000 | 32.310 |
| VI         | 41                         | 0.423  | 0.296 | 0.517  | 0.049  | 18                           | 0.430   | 0.364  | 0.506   | 0.041  | 4                           | 0.460   | 0.408   | 0.511   | 0.046  | 18                          | 0.449  | 0.365  | 0.515   | 0.037  |
| Vw         | 41                         | 0.292  | 0.190 | 0.363  | 0.036  | 18                           | 0.292   | 0.258  | 0.340   | 0.023  | 4                           | 0.283   | 0.258   | 0.312   | 0.022  | 18                          | 0.303  | 0.266  | 0.343   | 0.023  |
| VOI        | 41                         | 0.229  | 0.179 | 0.285  | 0.023  | 18                           | 0.277   | 0.246  | 0.328   | 0.022  | 4                           | 0.284   | 0.268   | 0.303   | 0.017  | 18                          | 0.260  | 0.221  | 0.289   | 0.021  |
| VOw        | 41                         | 0.128  | 0.087 | 0.182  | 0.018  | 18                           | 0.156   | 0.127  | 0.199   | 0.017  | 4                           | 0.144   | 0.137   | 0.161   | 0.012  | 18                          | 0.149  | 0.127  | 0.177   | 0.014  |
| VAl        | 41                         | 0.174  | 0.112 | 0.217  | 0.022  | 18                           | 0.209   | 0.146  | 0.254   | 0.028  | 4                           | 0.211   | 0.179   | 0.243   | 0.029  | 18                          | 0.201  | 0.170  | 0.240   | 0.019  |
| VAw        | 41                         | 0.138  | 0.095 | 0.176  | 0.019  | 18                           | 0.164   | 0.126  | 0.193   | 0.016  | 4                           | 0.156   | 0.129   | 0.171   | 0.020  | 18                          | 0.153  | 0.133  | 0.176   | 0.012  |
| VAlO       | 41                         | 0.125  | 0.077 | 0.154  | 0.017  | 18                           | 0.157   | 0.123  | 0.198   | 0.017  | 4                           | 0.160   | 0.127   | 0.194   | 0.031  | 18                          | 0.150  | 0.124  | 0.180   | 0.015  |
| VAWo       | 41                         | 0.088  | 0.058 | 0.108  | 0.014  | 18                           | 0.109   | 0.085  | 0.129   | 0.012  | 4                           | 0.106   | 0.090   | 0.124   | 0.014  | 18                          | 0.102  | 0.084  | 0.121   | 0.010  |
| Asec       | 41                         | 0.059  | 0.026 | 0.094  | 0.015  | 18                           | 0.058   | 0.044  | 0.079   | 0.007  | 4                           | 0.059   | 0.048   | 0.069   | 0.008  | 18                          | 0.058  | 0.047  | 0.078   | 0.009  |
| Psec       | 41                         | 3.240  | 2.000 | 5.000  | 0.712  | 18                           | 3.863   | 2.915  | 5.031   | 0.579  | 4                           | 3.542   | 3.217   | 4.000   | 0.356  | 18                          | 3.934  | 2.722  | 4.477   | 0.434  |
| Ken        | 41                         | 0.000  | 0.000 | 0.000  | 0.000  | 18                           | 0.000   | 0.000  | 0.000   | 0.000  | 4                           | 0.000   | 0.000   | 0.000   | 0.000  | 18                          | 0.000  | 0.000  | 0.000   | 0.000  |

CUPULADRIA GIGAS new species  
Figures 34, 35

*Diagnosis*.—Autozooids have a length (Zl) of 0.49 mm in average, colonies large and conical, average height diameter ratio 0.41 mm, average diameter 19.7 mm.

*Description*.—Colonies conical, with maximum observed diameter 21.5 mm. The central area of the colony is formed exclusively by autozooids. Autozooids are hexagonal, their cryptocyst descend steeply and septula are visible. Vicarious avicularia absent. Basal sectors have a radial shape with 7–20 pores per sector. Autozooids with closure plates not observed.

*Etymology*.—Gigas, Latin 'a giant' with reference to the large size of the zoarium.

*Types*.—Holotype USNM542584, Paratype: USNM542585, 9°18.26' Lat., 82°11.98' Lon., Bahía de Almirante, Bocas del Toro, Panama.

*Material*.—USNM593920–593923, Bahía de Almirante, Bocas del Toro, Panama. See Table 4 for morphological measurements.

*Occurrence*.—Recent Bocas del Toro Panama.

*Remarks*.—This species has the smallest zooid size (Zl) in the C<sub>NV</sub> clade, but the largest RaAloAl of 0.83 mm in average (for details see text); and also the largest zoaria observed in members of this clade.

Genus DISCOPORELLA d'Orbigny, 1852

All the recent species from the Caribbean: *D. scutella*, *D. peltifera*, *D. terminata*, *D. triangula* and *D. bocasdeltoensis*, and: *D. marsorum* and *D. cookae*, from the EP coasts of Panama are described in Herrera-Cubilla et al., 2008.

The new species DASP32 was collected in the Gulf of Chiriqui, GC97–65, 7°10.9' Lat., 81°39.9' Lon., February 1997, H. Fortunato coll., fine mud, 142 m depth. It corresponds to *Discoporella* sp. nov. P1 in Jagadeeshan and O'Dea, 2012.

ACKNOWLEDGMENTS

A. Cheetham made helpful comments on the manuscript. Our thanks to colleagues and institutions who provided collection

material that have enriched this manuscript: H. Lessios, R. Collin, R. Robertson, A. O'Dea and F. Rodriguez (Smithsonian Tropical Research Institute); J. Sanner (National Museum of Natural History); K. Sindemark (Swedish Museum of Natural History); M. C. Boyett (Harvard University); L. Smith (Louisiana State University); C. W. Poag (Scientist Emeritus U.S. Geological Survey); M. S. Jones, P. Taylor (Natural History Museum); P. G. Weaver (NC Museum of Natural Sciences); P. Florez (Instituto de Investigaciones Marinas y Costeras); R. W. Portell (Florida Museum of Natural History). Also to J. Ceballos and R. Chong for their valuable help with the SEM and the preparation of crispy plates and figures. Financial support has been provided by STRI S&E 2008 Fund to J.B.C. Jackson, STRI S&E 2009 to A. Herrera-Cubilla, and SENACYT Project 78 2010 to A. Herrera-Cubilla.

ACCESSIBILITY OF SUPPLEMENTAL DATA

Supplemental data deposited in Dryad repository: <http://doi.org/10.5061/dryad.49k85>.

REFERENCES

- BUSK, G. 1852. Catalogue of marine Polyzoa in the collection of the British Museum, Pt. 1, British Museum, London, p. 1–54.
- BUSK, G. 1884. Report on the Polyzoa collected by H.M.S. Challenger during the years 1873–1876. Part 1. The Cheilostomata. Report on the Scientific results of the Voyage of the H.M.S. "Challenger", Zoology 10: 1–216.
- CADÉE, G. C. 1975. Lunilitiform Bryozoa from the Guyana Shelf. Netherlands Journal of Sea Research, 9 (3–4): 320–343.
- CANU, F. AND R. S. BASSLER. 1919. Fossil Bryozoa from the West Indies, contributions to the geology and paleontology of the West Indies. Publication of the Carnegie Institution of Washington, 291:73–102.
- CANU, F. AND R. S. BASSLER. 1923. North American later Tertiary and Quaternary Bryozoa. Bulletin of the United States Natural Museum, 125:1–302.
- CHEETHAM, A. H. 1986. Tempo of evolution in a Neogene bryozoan: rates of morphologic change within and across species boundaries. Paleobiology, 12:190–202.
- CHEETHAM, A. H. AND J. B. C. JACKSON. 1995. Process from pattern: tests for selection versus random change in punctuated bryozoan speciation, p. 184–207. In D. H. Erwin and R. L. Anstey (eds.), New Approaches to Speciation in the Fossil Record. Columbia University Press.



TABLE 4—Extended.

| <i>C. collyrida</i> n. sp. |        |        |        |       | <i>C. veracruxiensis</i> n. sp. |        |       |        |        | <i>C. planissima</i> n. sp. |        |       |        |        | <i>C. gigas</i> n. sp. |         |         |         |        |
|----------------------------|--------|--------|--------|-------|---------------------------------|--------|-------|--------|--------|-----------------------------|--------|-------|--------|--------|------------------------|---------|---------|---------|--------|
| N                          | Mean   | Min    | Max    | SD    | N                               | Mean   | Min   | Max    | SD     | N                           | Mean   | Min   | Max    | SD     | N                      | Mean    | Min     | Max     | SD     |
| 4                          | 3.425  | 3.000  | 3.700  | 0.299 | 21                              | 4.140  | 3.000 | 6.050  | 1.058  | 12                          | 3.438  | 1.500 | 5.000  | 0.962  | 6                      | 19.717  | 17.550  | 21.450  | 1.517  |
| 4                          | 1.800  | 1.600  | 2.000  | 0.231 | 21                              | 0.757  | 0.100 | 1.600  | 0.433  | 12                          | 1.500  | 0.600 | 2.350  | 0.562  | 6                      | 7.950   | 7.300   | 9.200   | 0.771  |
| 4                          | 0.527  | 0.432  | 0.571  | 0.066 | 21                              | 0.179  | 0.033 | 0.355  | 0.084  | 12                          | 0.441  | 0.200 | 0.629  | 0.122  | 6                      | 0.405   | 0.350   | 0.490   | 0.053  |
| 4                          | 13.445 | 10.336 | 14.612 | 2.081 | 21                              | 15.421 | 7.085 | 30.593 | 8.138  | 12                          | 13.279 | 2.584 | 25.148 | 6.914  | 6                      | 394.018 | 338.755 | 448.634 | 49.946 |
| 4                          | 0.140  | 0.097  | 0.168  | 0.031 | 21                              | 0.076  | 0.031 | 0.107  | 0.016  | 12                          | 0.105  | 0.064 | 0.153  | 0.031  | 6                      | 0.113   | 0.101   | 0.122   | 0.008  |
| 4                          | 0.250  | 0.250  | 0.250  | 0.000 | 21                              | 0.286  | 0.000 | 0.750  | 0.238  | 12                          | 0.094  | 0.000 | 0.625  | 0.186  | 6                      | 1.500   | 1.000   | 2.000   | 0.548  |
| 4                          | 0.355  | 0.318  | 0.387  | 0.030 | 21                              | 0.398  | 0.356 | 0.462  | 0.026  | 12                          | 0.381  | 0.317 | 0.423  | 0.030  | 6                      | 0.491   | 0.469   | 0.523   | 0.020  |
| 4                          | 0.325  | 0.296  | 0.362  | 0.030 | 21                              | 0.288  | 0.233 | 0.348  | 0.029  | 12                          | 0.288  | 0.261 | 0.322  | 0.022  | 6                      | 0.367   | 0.321   | 0.404   | 0.028  |
| 4                          | 0.223  | 0.200  | 0.241  | 0.017 | 21                              | 0.272  | 0.223 | 0.321  | 0.027  | 12                          | 0.245  | 0.195 | 0.280  | 0.023  | 6                      | 0.355   | 0.334   | 0.381   | 0.017  |
| 4                          | 0.136  | 0.120  | 0.161  | 0.018 | 21                              | 0.154  | 0.140 | 0.186  | 0.012  | 12                          | 0.135  | 0.113 | 0.162  | 0.014  | 6                      | 0.231   | 0.201   | 0.246   | 0.017  |
| 4                          | 0.172  | 0.139  | 0.183  | 0.022 | 21                              | 0.179  | 0.142 | 0.222  | 0.021  | 12                          | 0.185  | 0.149 | 0.222  | 0.022  | 6                      | 0.271   | 0.258   | 0.284   | 0.011  |
| 4                          | 0.159  | 0.153  | 0.166  | 0.006 | 21                              | 0.149  | 0.126 | 0.171  | 0.012  | 12                          | 0.158  | 0.131 | 0.177  | 0.015  | 6                      | 0.197   | 0.189   | 0.205   | 0.006  |
| 4                          | 0.142  | 0.108  | 0.161  | 0.023 | 21                              | 0.129  | 0.097 | 0.170  | 0.021  | 12                          | 0.127  | 0.100 | 0.162  | 0.020  | 6                      | 0.224   | 0.208   | 0.232   | 0.009  |
| 4                          | 0.114  | 0.100  | 0.121  | 0.010 | 21                              | 0.094  | 0.074 | 0.110  | 0.010  | 12                          | 0.104  | 0.090 | 0.121  | 0.010  | 6                      | 0.127   | 0.118   | 0.138   | 0.008  |
| 4                          | 0.000  | 0.000  | 0.000  | 0.000 | 21                              | 0.095  | 0.000 | 1.000  | 0.301  | 12                          | 0.083  | 0.000 | 1.000  | 0.289  | 6                      | 0.000   | 0.000   | 0.000   | 0.000  |
| 4                          | 0.000  | 0.000  | 0.000  | 0.000 | 21                              | 0.143  | 0.000 | 1.000  | 0.359  | 12                          | 0.000  | 0.000 | 0.000  | 0.000  | 6                      | 0.000   | 0.000   | 0.000   | 0.000  |
| 4                          | 16.750 | 16.000 | 17.000 | 0.500 | 21                              | 18.667 | 4.000 | 62.000 | 17.574 | 12                          | 24.750 | 3.000 | 63.000 | 19.008 | 6                      | 0.000   | 0.000   | 0.000   | 0.000  |
| 4                          | 0.331  | 0.307  | 0.353  | 0.019 | 21                              | 0.346  | 0.269 | 0.429  | 0.034  | 12                          | 0.336  | 0.273 | 0.388  | 0.034  | 6                      | 0.000   | 0.000   | 0.000   | 0.000  |
| 4                          | 0.269  | 0.223  | 0.290  | 0.031 | 21                              | 0.251  | 0.187 | 0.314  | 0.032  | 12                          | 0.247  | 0.195 | 0.302  | 0.031  | 6                      | 0.000   | 0.000   | 0.000   | 0.000  |
| 4                          | 0.193  | 0.184  | 0.204  | 0.008 | 21                              | 0.208  | 0.164 | 0.256  | 0.025  | 12                          | 0.195  | 0.172 | 0.230  | 0.016  | 6                      | 0.000   | 0.000   | 0.000   | 0.000  |
| 4                          | 0.112  | 0.108  | 0.117  | 0.004 | 21                              | 0.108  | 0.080 | 0.139  | 0.016  | 12                          | 0.118  | 0.091 | 0.135  | 0.013  | 6                      | 0.000   | 0.000   | 0.000   | 0.000  |
| 4                          | 0.140  | 0.124  | 0.149  | 0.011 | 21                              | 0.143  | 0.110 | 0.189  | 0.022  | 12                          | 0.146  | 0.109 | 0.187  | 0.026  | 6                      | 0.000   | 0.000   | 0.000   | 0.000  |
| 4                          | 0.121  | 0.115  | 0.134  | 0.009 | 21                              | 0.123  | 0.095 | 0.154  | 0.016  | 12                          | 0.118  | 0.084 | 0.153  | 0.020  | 6                      | 0.000   | 0.000   | 0.000   | 0.000  |
| 4                          | 0.099  | 0.077  | 0.111  | 0.016 | 21                              | 0.099  | 0.061 | 0.145  | 0.020  | 12                          | 0.093  | 0.069 | 0.132  | 0.019  | 6                      | 0.000   | 0.000   | 0.000   | 0.000  |
| 4                          | 0.077  | 0.075  | 0.080  | 0.003 | 21                              | 0.075  | 0.052 | 0.097  | 0.010  | 12                          | 0.071  | 0.057 | 0.094  | 0.010  | 6                      | 0.000   | 0.000   | 0.000   | 0.000  |
| 4                          | 0.056  | 0.040  | 0.070  | 0.015 | 21                              | 0.050  | 0.031 | 0.083  | 0.014  | 12                          | 0.127  | 0.085 | 0.160  | 0.027  | 6                      | 0.349   | 0.199   | 0.435   | 0.096  |
| 4                          | 2.485  | 2.107  | 3.481  | 0.665 | 21                              | 4.230  | 2.634 | 6.114  | 0.935  | 12                          | 9.535  | 4.646 | 14.275 | 3.192  | 6                      | 14.004  | 7.062   | 20.195  | 4.354  |
| 4                          | 1.000  | 1.000  | 1.000  | 0.000 | 21                              | 0.000  | 0.000 | 0.000  | 0.000  | 12                          | 0.000  | 0.000 | 0.000  | 0.000  | 6                      | 0.000   | 0.000   | 0.000   | 0.000  |

CHEETHAM, A. H. AND J. B. C. JACKSON. 1996. Speciation, extinction, and the decline of arborescent growth in Neogene and Quaternary Cheilostome Bryozoa of tropical America, p. 205–203. In J. B. C. Jackson and A. G. Coates (eds.), *Evolution and Environment in Tropical America*. University of Chicago Press, Chicago.

CHEETHAM, A. H. AND J. B. C. JACKSON. 1998. The fossil record of Cheilostome Bryozoa in the Neogene and Quaternary of tropical America: adequacy for phylogenetic and evolutionary studies, p. 227–241. In S. K. Donovan and C. R. C. Paul (eds.), *The Adequacy of the Fossil Record*. John Wiley and Sons.

CHEETHAM, A. H. AND J. B. C. JACKSON. 2000. Neogene history of Cheilostome Bryozoa in tropical America, p. 1–16. In A. Herrera-Cubilla and J. B. C. Jackson (eds.), *Proceedings of the 11th International Bryozoology Association Conference*. Smithsonian Institution, Panama.

CHEETHAM, A. H., J. B. C. JACKSON, J. SANNER, AND Y. VENTOCILLA. 1999. Neogene Cheilostome Bryozoa of tropical America: comparison and contrast between the central American Isthmus (Panama, Costa Rica) and the North-central Caribbean (Dominican Republic), p. 158–192. In L. S. Collins and A. G. Coates (eds.), *A paleobiotic survey of Caribbean faunas from the Neogene of the Isthmus of Panama*. *Bulletins of American Paleontology*, 357.

CHEETHAM, A. H., J. SANNER, P. D. TAYLOR, AND A. N. OSTROVSKY. 2006. Morphological differentiation of avicularia and the proliferation of species in mid-Cretaceous *Wilbertopora* Cheetham, 1954 (Bryozoa: Cheilostomata). *Journal of Paleontology*, 80:49–71.

CHEETHAM, A. H., J. SANNER, AND J. B. C. JACKSON. 2007. *Metrarabdotos* and related genera (Bryozoa: Cheilostomata) in the late Paleogene and Neogene of tropical America. *The Paleontological Society Memoir* 67, supplement to volume 81, 96 p.

COATES, A. G. 1999a. Maps, p. 287–298. In L. S. Collins and A. G. Coates (eds.), *A paleobiotic survey of Caribbean faunas from the Neogene of the Isthmus of Panama*. *Bulletins of American Paleontology*, 357.

COATES, A. G. 1999b. Stratigraphic sections, p. 300–348. In L. S. Collins and A. G. Coates (eds.), *A paleobiotic survey of Caribbean faunas from the Neogene of the Isthmus of Panama*. *Bulletins of American Paleontology*, 357.

COATES, A. G., D. F. McNEILL, M.-P. AUBRY, W. A. BERGGREN, AND L. S. COLLINS. 2005. An introduction to the geology of the Bocas del Toro archipelago, Panama. *Caribbean Journal of Science*, 41:374–391.

COLLINS, L. S. 2005. Panama Paleontology Project. <<http://www.fiu.edu/~collins/pppimagemapnew.htm>>.

COOK, P. L. 1963. Observations on live lunulitiform zoaria of Polyzoa. *Cahiers de Biologie Marine*, 4:407–413.

COOK, P. L. 1965a. Notes on the Cupuladriidae (Polyzoa, Anasca). *The Bulletin of the British Museum of Natural History (Zoology)*, 13(5):151–187.

COOK, P. L. 1965b. Polyzoa from West Africa. *The Cupuladriidae* (Cheilostomata, Anasca). *The Bulletin of the British Museum of Natural History (Zoology)*, 13(6):189–227.

COOK, P. L. 1968. Polyzoa from West Africa. *The Malacostega*, Part I. *The Bulletin of the British Museum of Natural History (Zoology)*, 16(3):116–167.

COOK, P. L. AND P. J. CHIMONIDES. 1978. Observations on living colonies of *Selenaria* (Bryozoa, Cheilostomata) I. *Cahiers de Biologie Marine, Roscoff*, 19:147–158.

COOK, P. L. AND P. J. CHIMONIDES. 1994. Notes on the family Cupuladriidae (Bryozoa), and on *Cupuladria remota* sp. n. from the Marquesas Islands. *Zoologica Scripta*, 23(3):251–268.

DICK, M. H., A. HERRERA-CUBILLA, AND J. B. C. JACKSON. 2003. Molecular phylogeny and phylogeography of free-living Bryozoa (Cupuladriidae) from both sides of the Isthmus of Panama. *Molecular Phylogenetics and Evolution*, 27:355–371.

FOOTE, M. 1996. On the probability of ancestors in the fossil record. *Paleobiology*, 22:141–151.

GRAHAM, A. 1976. Studies in Neotropical paleobotany. II. The Miocene communities of Veracruz, Mexico. *Annals of the Missouri Botanical Garden*, 63:787–842.

HASTINGS, A. B. 1930. Cheilostomatous Polyzoa from the vicinity of the Panama Canal collected by Dr. C. Crossland on the cruise of the S. Y. "St. George". *Proceedings of the Zoological Society of London*, 4:697–740.

HERRERA-CUBILLA, A., M. H. DICK, J. SANNER, AND J. B. C. JACKSON. 2006. Neogene Cupuladriidae of tropical America. I: Taxonomy of Recent *Cupuladria* from opposite sides of the Isthmus of Panama. *Journal of Paleontology*, 80:245–263.

HERRERA-CUBILLA, A., M. H. DICK, J. SANNER, AND J. B. C. JACKSON. 2008. Neogene Cupuladriidae of tropical America. II: Taxonomy of Recent *Discoporella* from opposite sides of the Isthmus of Panama. *Journal of Paleontology*, 82:279–298.

JACKSON, J. B. C. AND A. H. CHEETHAM. 1990. Evolutionary significance of morphospecies: a test with Cheilostome Bryozoa. *Science*, 248:521–636.

JACKSON, J. B. C. AND A. H. CHEETHAM. 1994. Phylogeny reconstruction and the tempo of speciation in Cheilostome Bryozoa. *Paleobiology*, 20:407–423.

JAGADEESHAN, S. AND A. O'DEA. 2012. Integrating fossils and molecules to study cupuladriid evolution in an emerging Isthmus. *Evolutionary Ecology*, 26:337–355.

KNOWLTON, N. 1993. Sibling species in the sea. *Annual Review of Ecology and Systematics*, 24:189–216.

KNOWLTON, N. AND J. B. C. JACKSON. 1994. New taxonomy and niche partitioning on coral reefs: jack of all trades or master of some? *Trends in Ecology and Evolution*, 9:7–9.

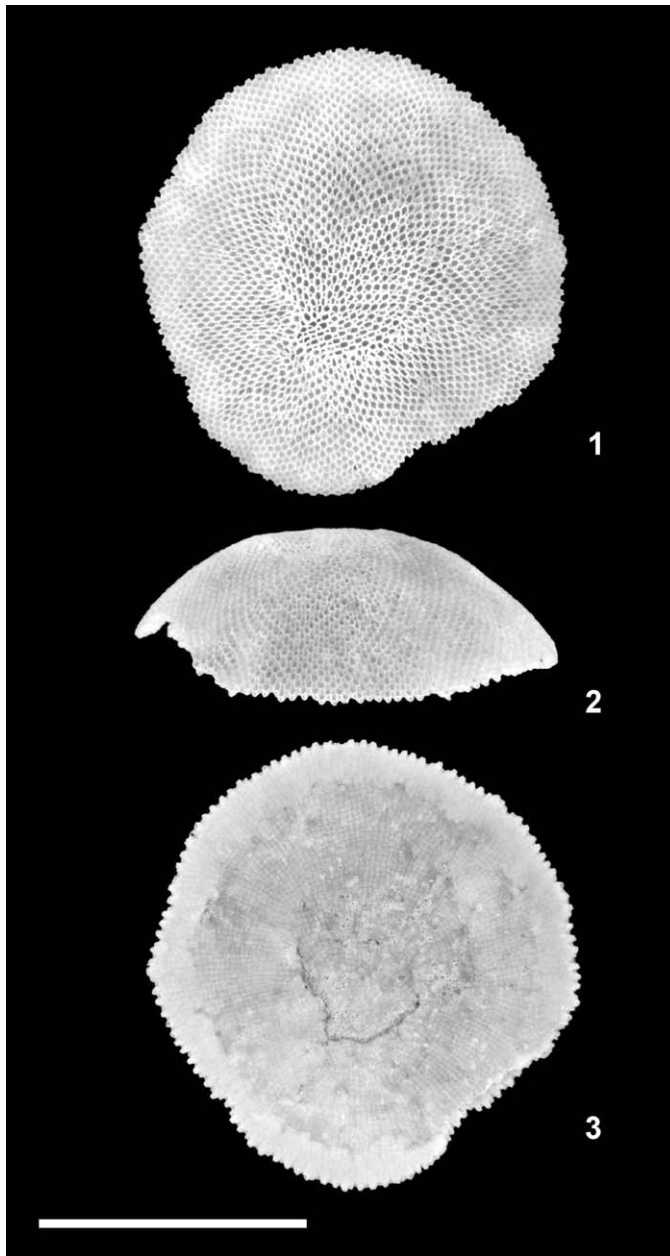


FIGURE 22—*Cupuladria floridensis* n. sp. 1–3, holotype, USNM542571, Recent, New Orleans off coast, Louisiana, U.S.A.: 1, colony frontal view; 2, colony side view; 3, colony basal view. Scale bar=1 mm.

LAGAAIL, R. 1952. The Pliocene Bryozoa of the low countries and their bearing on the marine stratigraphy of the north sea region. *Mededelingen van de Geologische Stichting*, 5(5):1–233.

- LAGAAIL, R. 1963. *Cupuladria canariensis* (Busk): portrait of a bryozoan. *Paleontology*, 6(1):172–217.
- MARCUS, E. 1937. Bryozoários marinhos brasileiros I. *Boletim da Faculdade de filosofia, ciências e letras, Universidade di Sao Paolo, Zoologia*, 1:5–224.
- McKINNEY, F. AND J. B. C. JACKSON. 1989. *Bryozoan evolution*. Unwin Hyman, Boston.
- McNEILL, D. F., J. S. KLAUS, A. F. BUDD, B. P. LUTZ, AND S. E. ISHMAN. 2012. Late Neogene chronology and sequence stratigraphy of mixed carbonate-siliciclastic deposits of the Cibao Basin, Dominican republic. *GSA Bulletin*, 124(1/2):35–58.
- NORMAN, A. M. 1903. Notes on the natural history of East Finmark Polyzoa. *Annals and Magazine of Natural History*, ser. 7, 11:567–598.
- O'DEA, A. 2006. Asexual propagation in the marine bryozoan *Cupuladria exfragminis*. *Journal of Experimental Marine Biology and Ecology*, 335:312–322.
- O'DEA, A. AND J. B. C. JACKSON. 2002. Bryozoan growth mirrors contrasting seasonal regimes across the Isthmus of Panama. *Palaeogeography, Palaeoclimatology, Palaeoecology*, 185:77–94.
- O'DEA, A. AND J. B. C. JACKSON. 2009. Environmental change drove macroevolution in cupuladriid bryozoans. *Proceedings of the Royal Society (B)*, 276:3,629–3,634.
- O'DEA, A., A. HERRERA-CUBILLA, H. FORTUNATO, AND J. B. C. JACKSON. 2004. Life history variation in cupuladriid bryozoans from either side of the isthmus of Panama. *Marine Ecology Progress Series*, 280:145–161.
- O'DEA, A., F. RODRIGUEZ, AND T. ROMERO. 2007. Response of zooid size in *Cupuladria exfragminis* (Bryozoa) to simulated upwelling temperatures. *Marine Ecology*, 28:1–9.
- O'DEA, A., J. B. C. JACKSON, P. D. TAYLOR, AND F. RODRIGUEZ. 2008. Modes of reproduction in recent and fossil cupuladriid bryozoans. *Palaeontology*, 51:847–864.
- OSBURN, R. 1950. *Bryozoa of the Pacific coast of America. Part 1, Cheilostomata-Anasca*. Allan Hancock Pacific Expeditions, 14(1), 269 p. The University of Southern California Press.
- OSTROVSKY, A. N., A. O'DEA, AND F. RODRIGUEZ. 2009. Comparative anatomy of internal incubational sacs in cupuladriid bryozoans and the evolution of brooding in free-living cheilostomes. *Journal of Morphology*, 270:1,413–1,430.
- SAUNDERS, J. B., P. JUNG, AND B. BIJU-DUVAL. 1986. Neogene paleontology in the northern Dominican Republic. I. Field surveys, lithology, environment and age. *Bulletins of American Paleontology*, 323, 79 p.
- SMITT, F. A. 1867. Kritisk förteckning öfver kandinaviens Hafs-Bryozoeer, III. Öfversigt af Kongliga Vetenskaps-Akademiens Förhandlingar Stockholm, 24:279–429.
- SPSS Inc. 2009. PASW Statistics 17.0 for Windows.
- SWOFORD, D. L. 2000. PAUP\*, Phylogenetic Analysis Using Parsimony (\* and Other Methods), Version 4.0b10. Sinauer Associates, Sunderland, Massachusetts.
- TILBROOK, K. J. 1998. The species of *Antropora* Norman, 1903 (Bryozoa: Cheilostomatida), with the description of a new genus in the Calloporoidea. *Records of the South Australian Museum* 30(2):25–49
- WINSTON, J. E. 1982. Marine bryozoans (Ectoprocta) of the Indian River area (Florida). *Bulletin of the American Museum of Natural History*, 173:99–176.
- WINSTON, J. E. 1984. Why Bryozoans have avicularia: a review of the evidence. *American Museum Novitates*, 2789:1–26.
- WINSTON, J. E. 1988. Life histories of free-living bryozoans. *National Geographic Research*, 4:528–539.
- ZIKO, A. 1985. Eocene Bryozoa from Egypt, a paleontological and paleoecological study. *Tübinger Mikropaläontologische Mitteilungen*, 4, 243 p.

ACCEPTED 6 JANUARY 2014

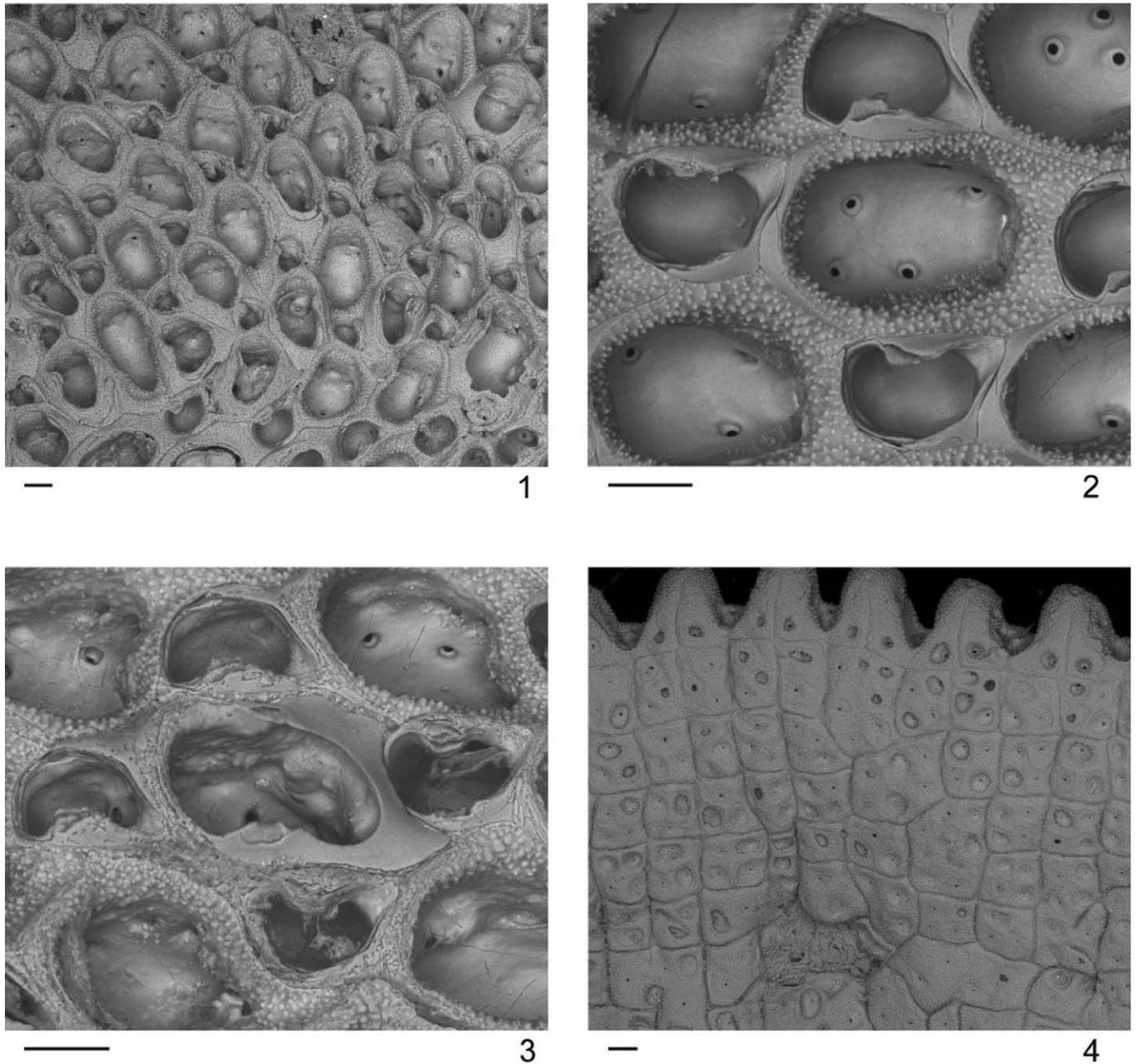


FIGURE 23—*Cupuladria floridensis* n. sp. 1–4, holotype, USNM542571, Recent, New Orleans off coast, Louisiana, U.S.A.: 1, colony center showing its clonal origin, autozooids and vicarious avicularia; 2, view of the autozooid and autozooid vibraculum; 3, closer view of vicarious avicularium and vicarious avicularium vibraculum; 4, view of the basal sectors and pores. Scale bar=100 μm.



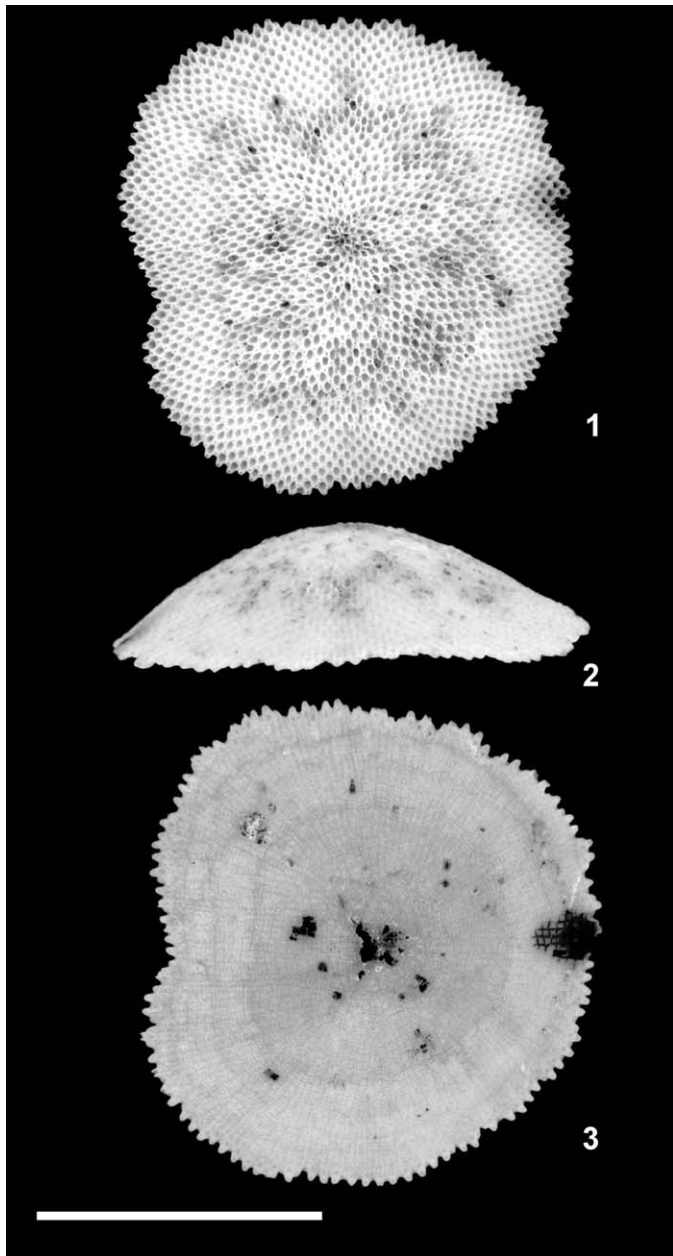


FIGURE 24—*Cupuladria colonensis* n. sp. 1–3, holotype, USNM542575, Recent, Colon, Panama: 1, colony frontal view; 2, colony side view; 3, colony basal view. Scale bar=1 mm.

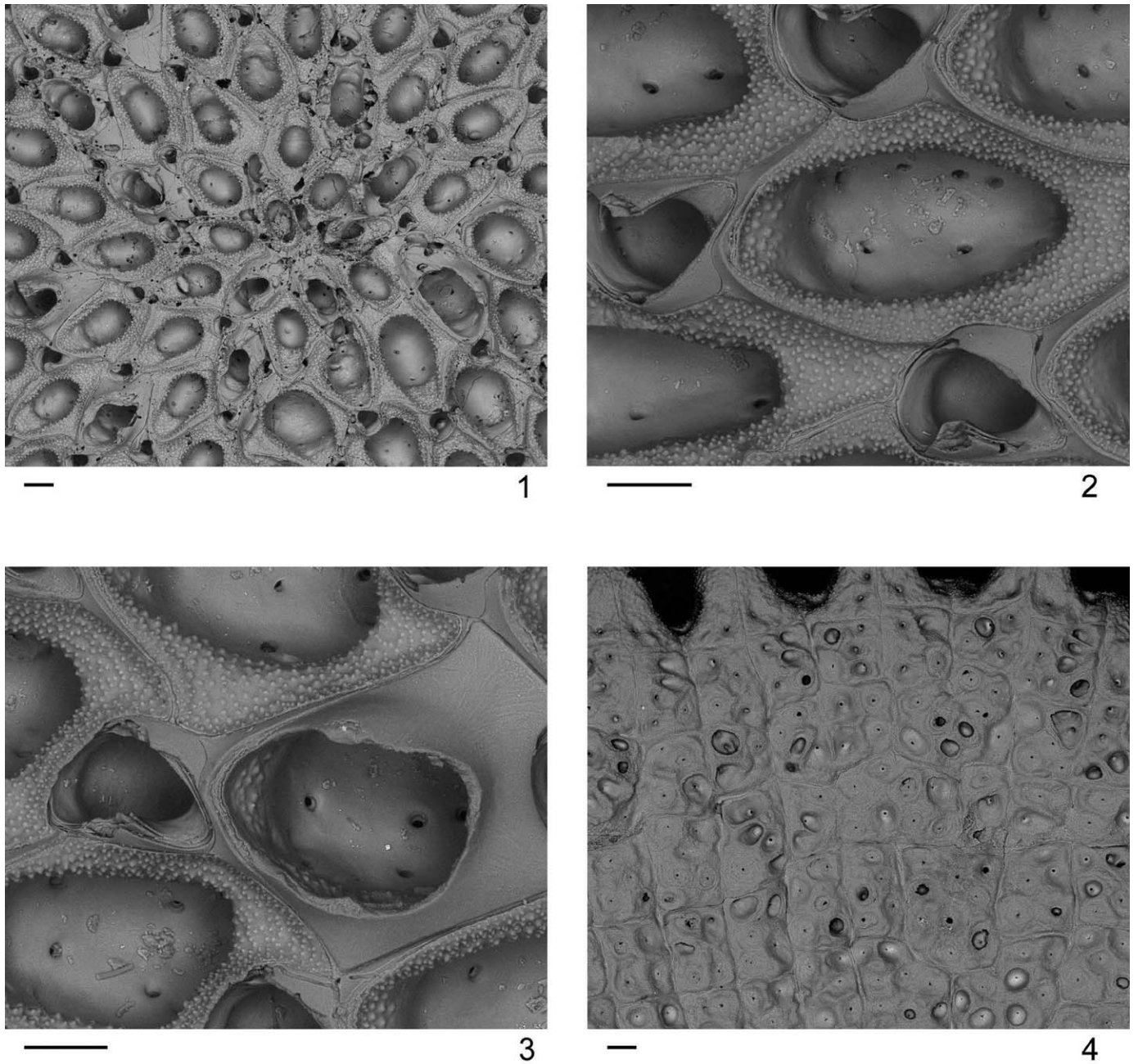


FIGURE 25—*Cupuladria colonensis* n. sp. 1–4, holotype, USNM542575, Recent, Colon, Panama: 1, colony center showing autozooids and vicarious avicularia; 2, view of the autozooid and autozooid vibraculum; 3, view of vicarious avicularium and vicarious avicularium vibraculum; 4, view of the basal sectors and pores. Scale bar=100  $\mu$ m.

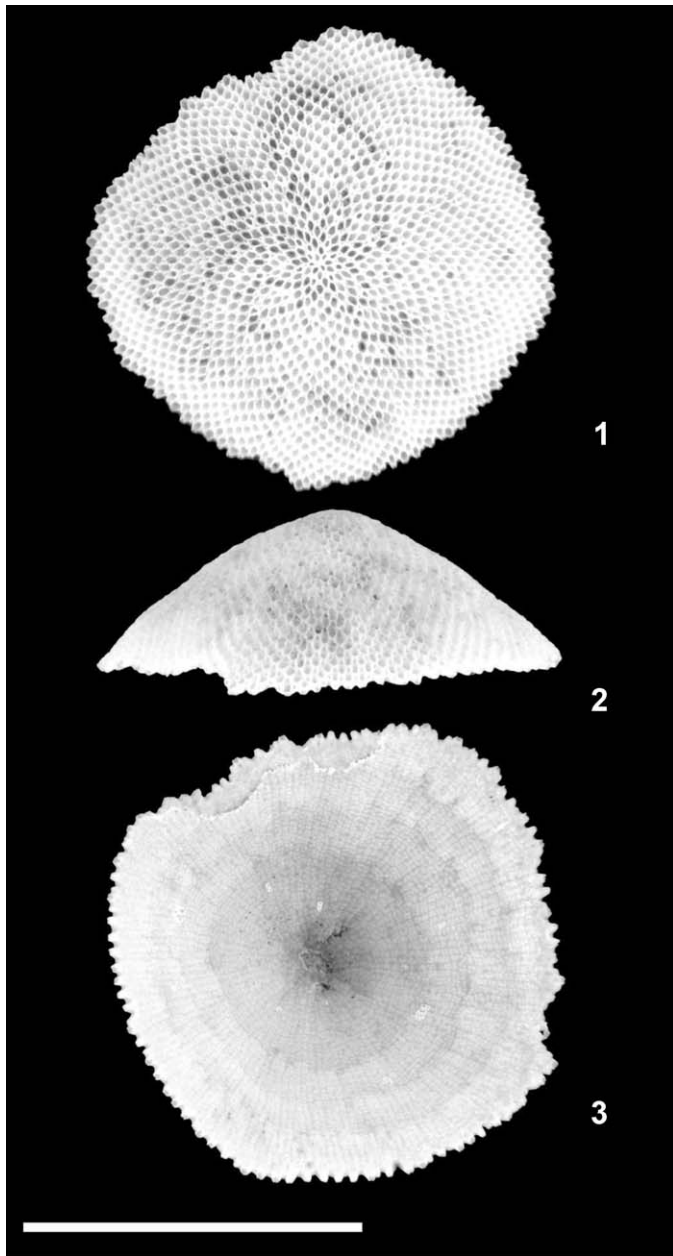


FIGURE 26—*Cupuladria dominicana* n. sp. 1–3, holotype USNM542578, Recent, North East coast Santo Domingo, Dominican Republic: 1, colony frontal view; 2, colony side view; 3, colony basal view. Scale bar=1 mm.



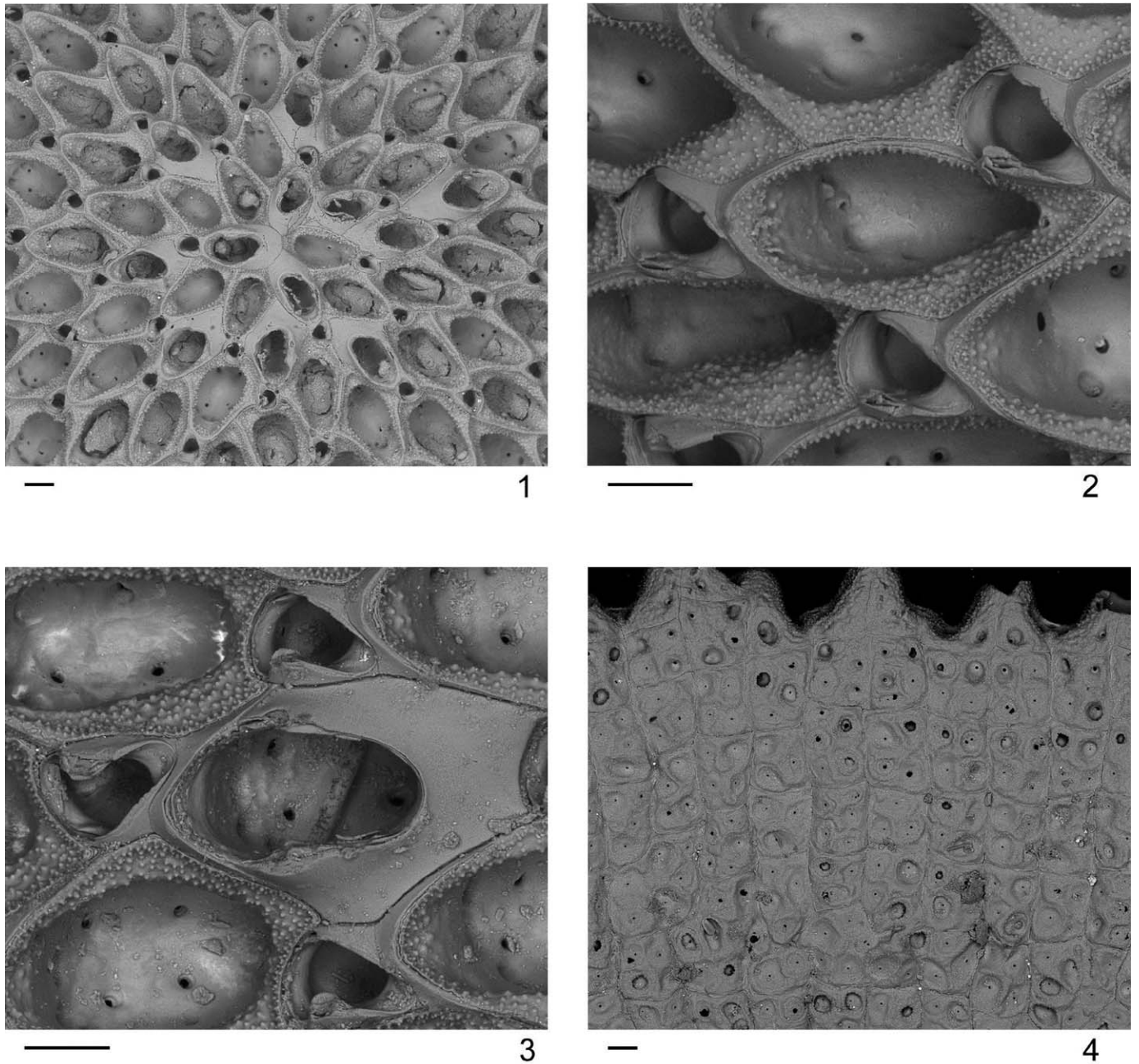


FIGURE 27—*Cupuladria dominicana* n. sp. 1–4, holotype, USNM542578, Recent, North East coast Santo Domingo, Dominican Republic: 1, colony center showing autozooids and vicarious avicularia; 2, view of the autozooid and autozooid vibraculum; 3, view of vicarious avicularium and vicarious avicularium vibraculum; 4, view of the basal sectors and pores. Scale bar=100  $\mu$ m.

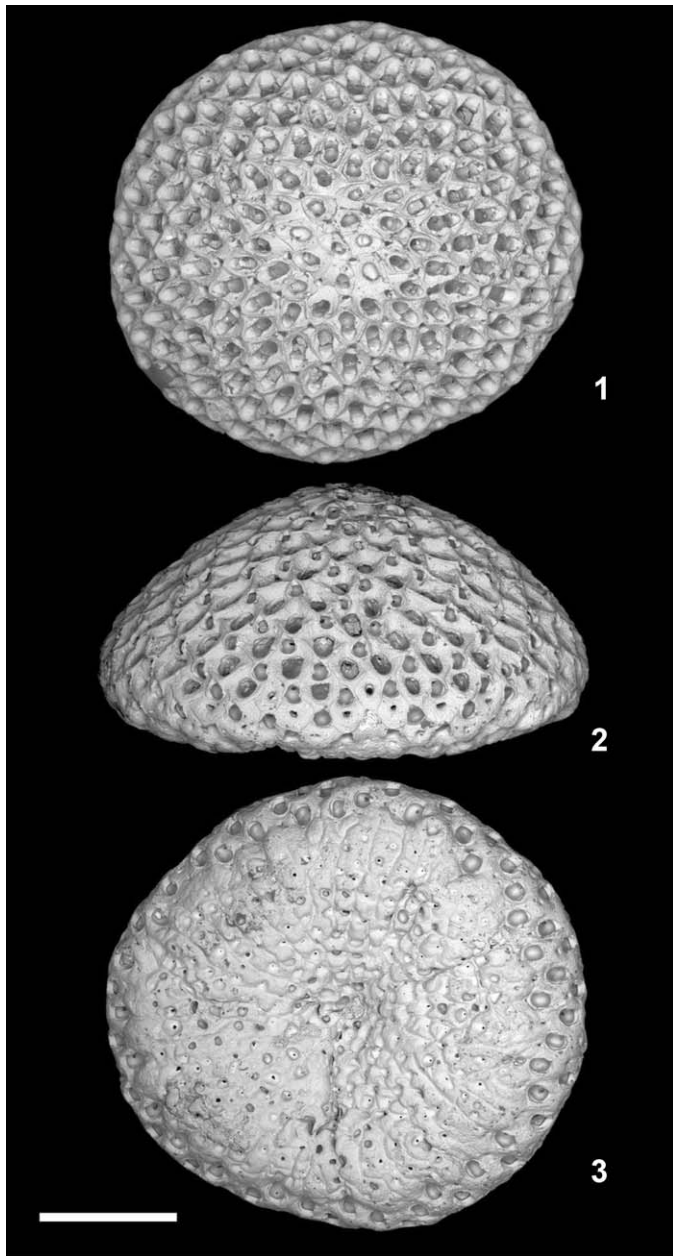


FIGURE 28—*Cupuladria collyrida* n. sp. 1–3, holotype, USNM542561, Bowden Formation, Pliocene, Jamaica: 1, colony frontal view; 2, colony side view; 3, colony basal view. Scale bar=1 mm.



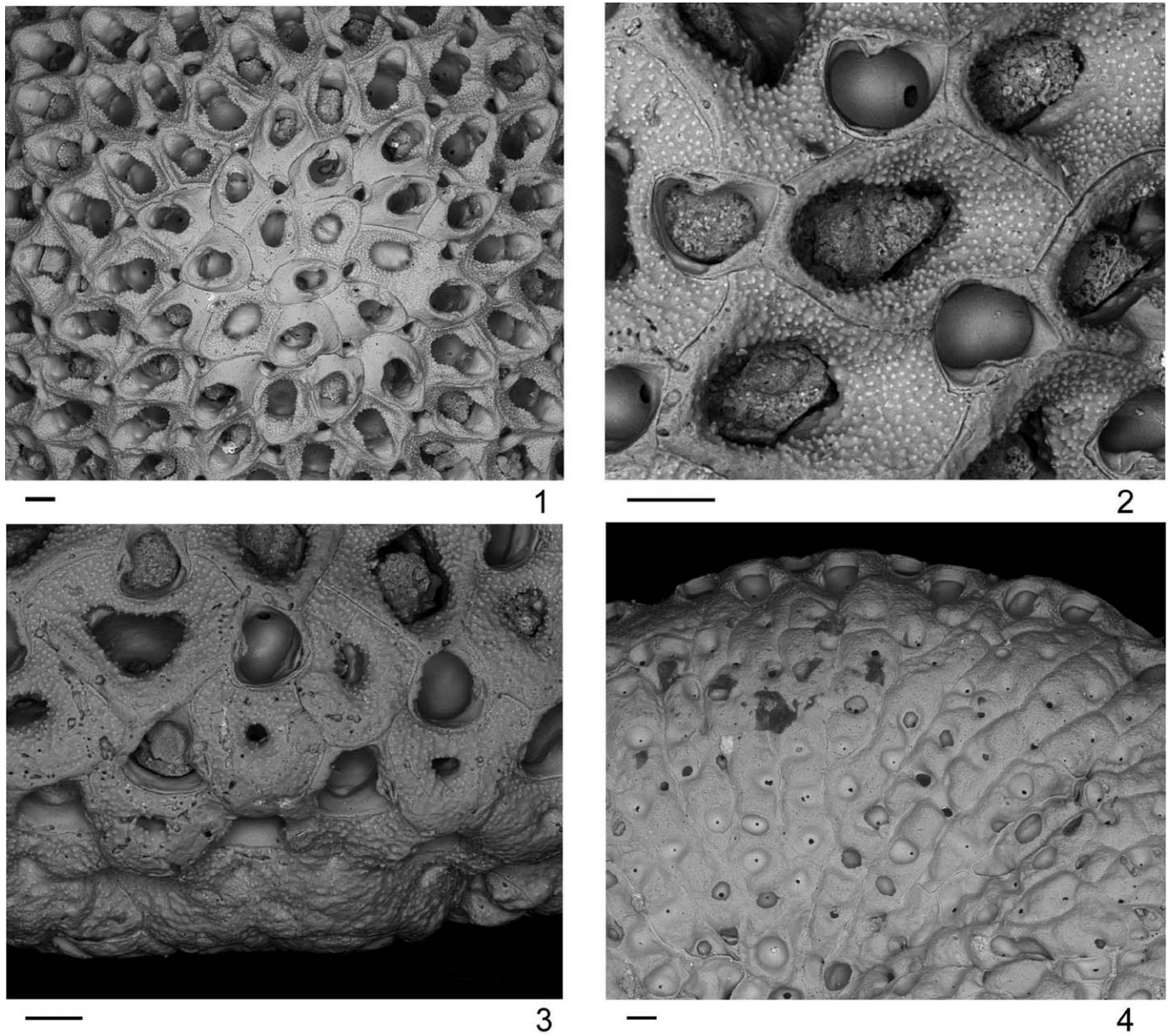


FIGURE 29—*Cupuladria collyrida* n. sp. 1–4, holotype, USNM542561, Bowden Formation, Pliocene, Jamaica: 1, colony center showing vicarious avicularia; 2, view of the autozoid and autozoid vibraculum; 3, view of kenozooids at the colony margin; 4, view of the basal sectors and pores. Scale bar=100  $\mu$ m.



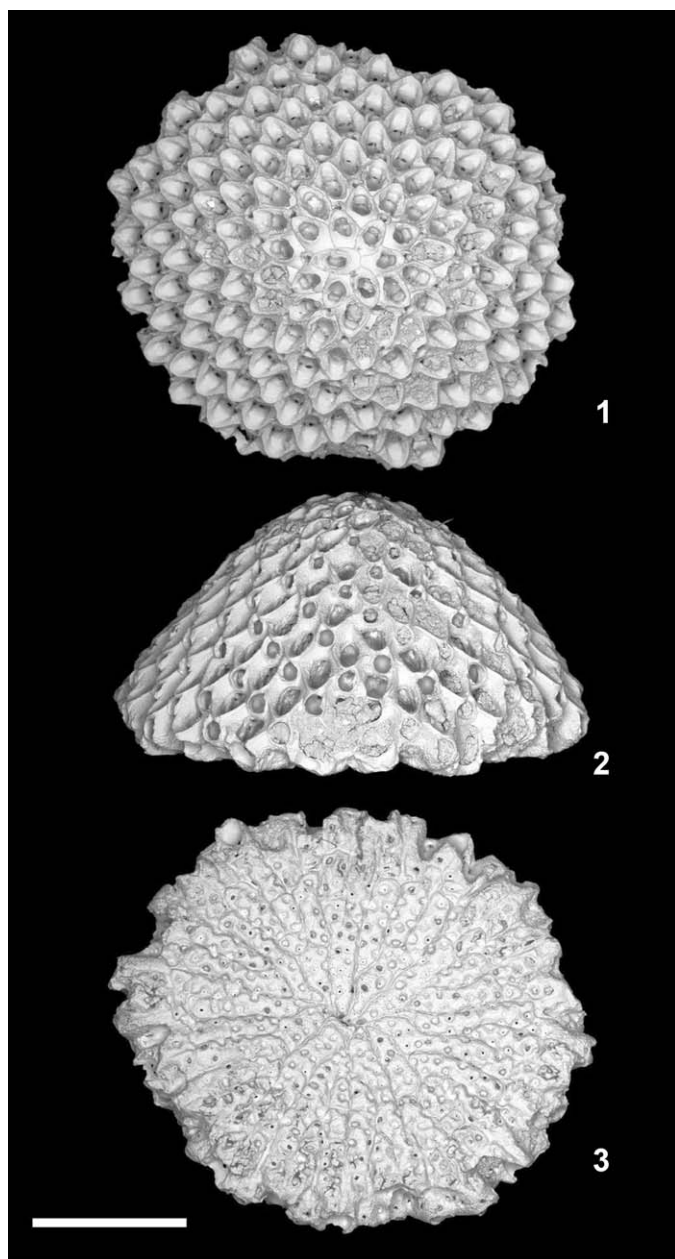


FIGURE 30—*Cupuladria planissima* n. sp. 1–3, holotype, USNM542581, Bastimentos island, late Pliocene, Bocas del Toro, Panama: 1, colony frontal view; 2, colony side view; 3, colony basal view. Scale bar=1 mm.

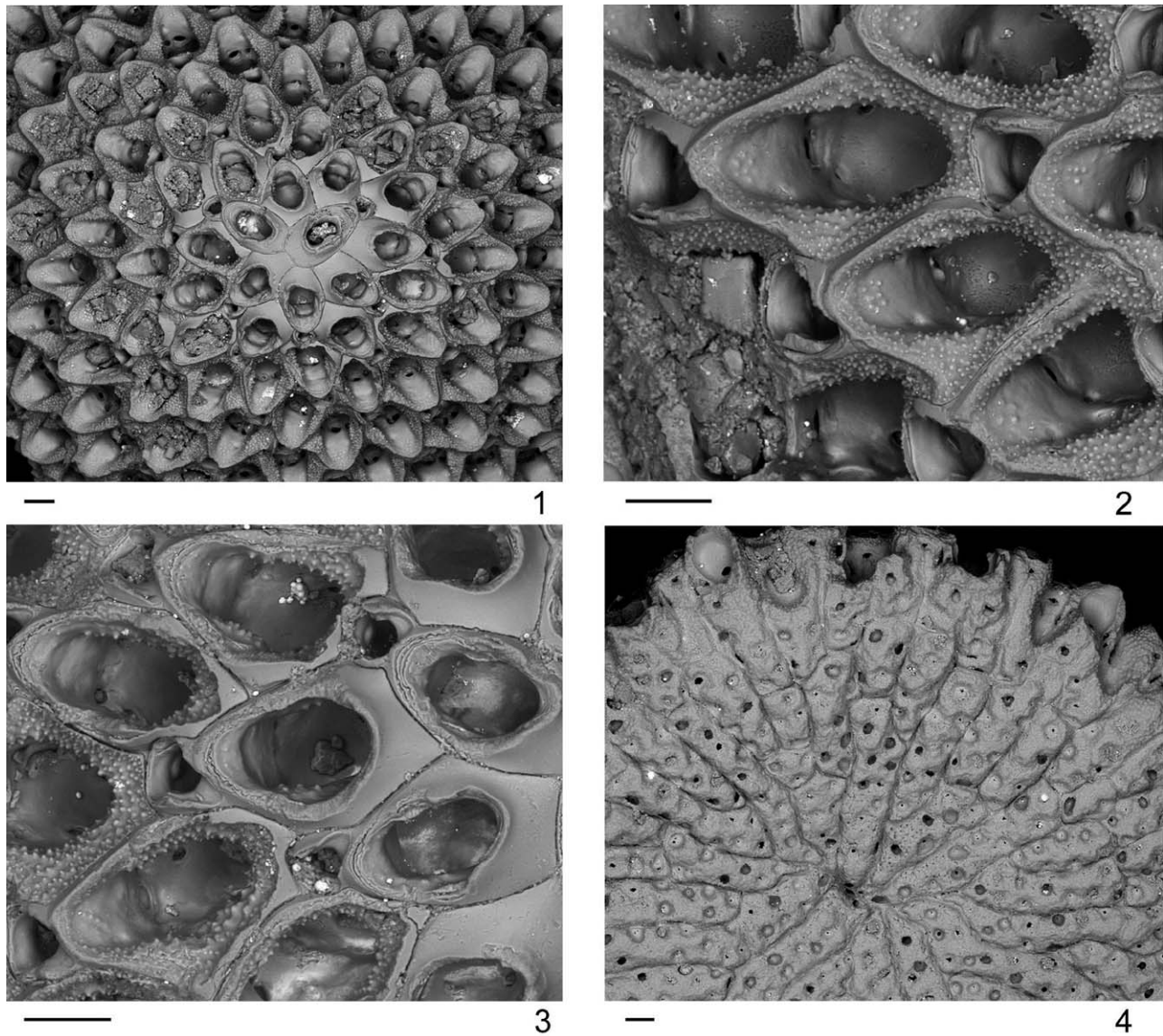


FIGURE 31—*Cupuladria planissima* n. sp. 1–4, holotype, USNM542581, Bastimentos island, late Pliocene, Bocas del Toro, Panama: 1, colony center showing vicarious avicularia; 2, view of the autozooid and autozooid vibraculum; 3, closer view of vicarious avicularium and vicarious avicularium vibraculum; 4, view of the basal sectors and pores. Scale bar=100  $\mu$ m.

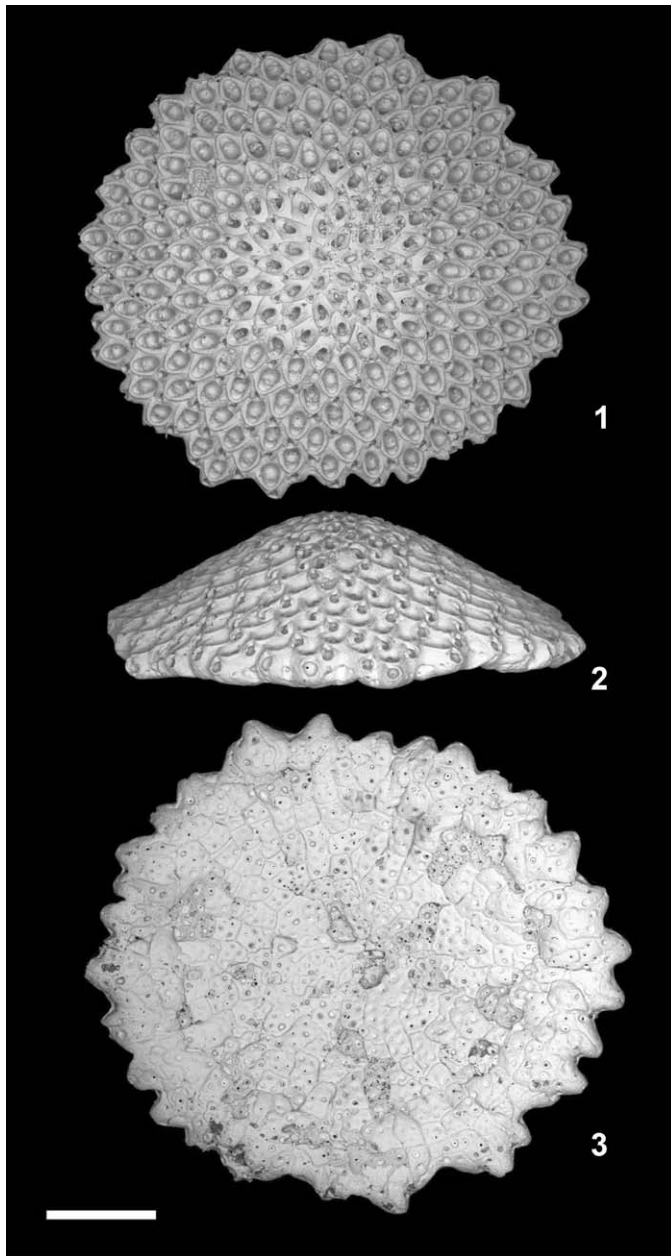


FIGURE 32—*Cupuladria veracruxiensis* n. sp. 1–3, holotype, USNM542562, PPP2171, Escudo de Veraguas Formation, late Pliocene, Bocas del Toro, Panama: 1, colony frontal view; 2, colony side view; 3, colony basal view. Scale bar=1 mm.



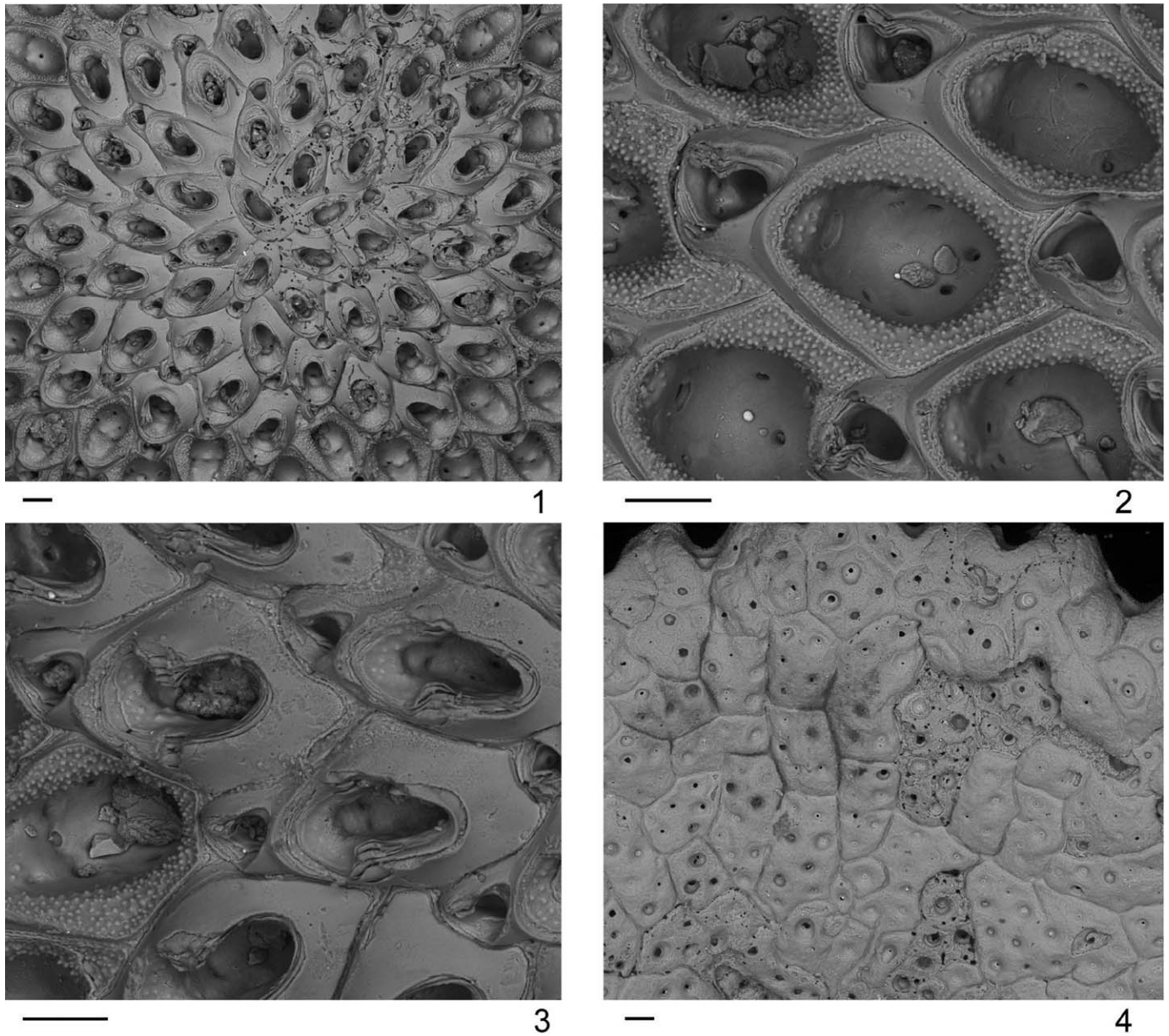


FIGURE 33—*Cupuladria veracruxiensis* n. sp. 1–4, holotype, USNM542562, PPP2171, Escudo de Veraguas Formation, late Pliocene, Bocas del Toro, Panama: 1, colony center showing vicarious avicularia; 2, view of the autozooid and autozooid vibraculum; 3, closer view vicarious avicularium and vicarious avicularium vibraculum; 4, view of the basal sectors and pores. Scale bar=100  $\mu$ m.

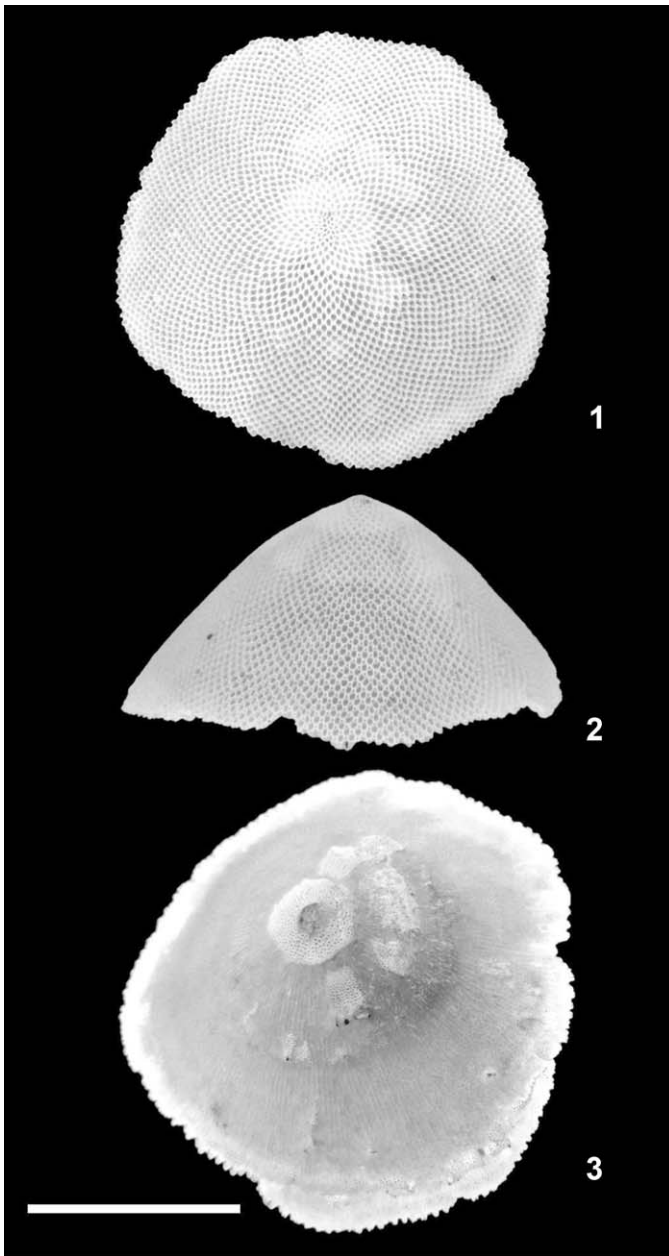


FIGURE 34—*Cupuladria gigas* n. sp. 1–3, holotype USNM542584, Recent, Bahía de Almirante, Bocas del Toro, Panama: 1, colony frontal view; 2, colony side view; 3, colony basal view. Scale bar=1 mm.

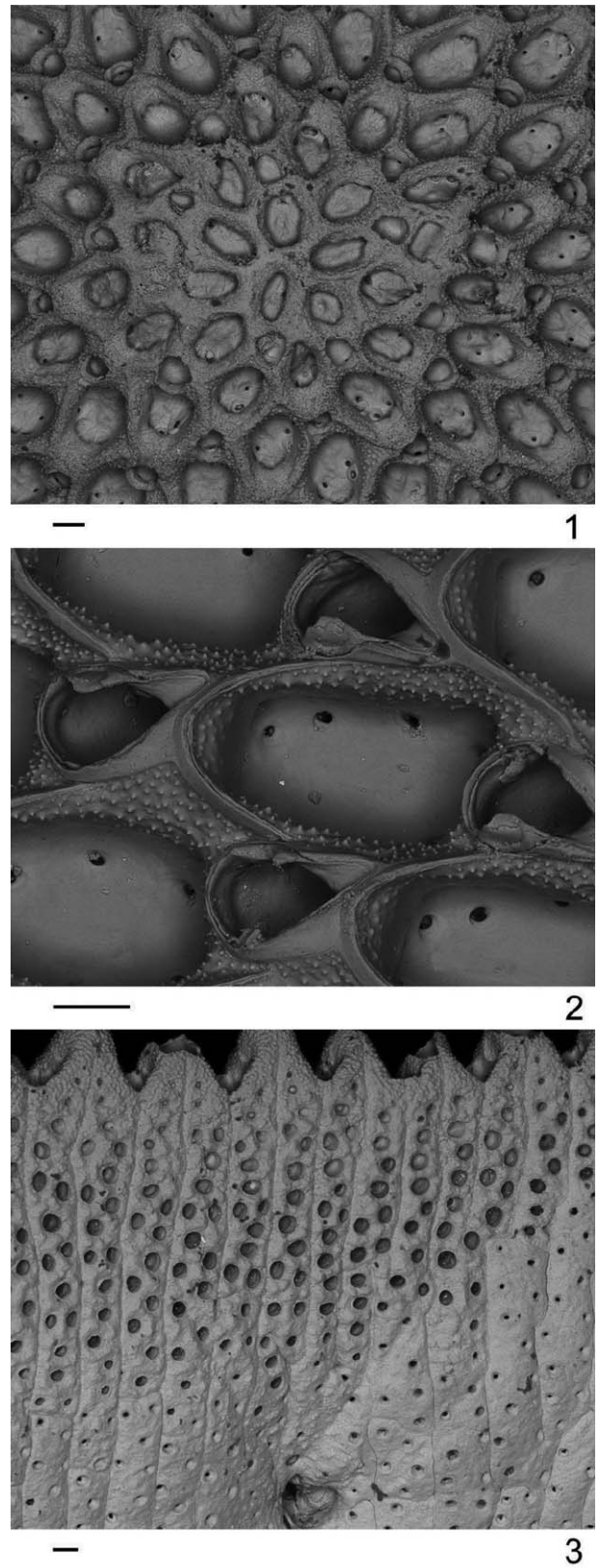


FIGURE 35—*Cupuladria gigas* n. sp. 1–3, holotype USNM542584, Recent, Bahía de Almirante, Bocas del Toro, Panama: 1, colony center showing autozooids; 2, view of the autozooid and autozooid vibraculum; 3, view of the basal sectors and pores. Scale bar=100  $\mu$ m.

Appendix 1—Characters and character states used in cladistic analysis of extant and fossil vicarious and non-vicarious *Cupuladria* species, plus extant *Discoporella* species. Coding was performed on re-scaled values, see text.

|           |   |
|-----------|---|
| Cw        | Coded states: 0=0.606–0.902, 1=0.935, 2=0.985–1.024, 4=1.149, 6=1.252–1.315   |
| Ch        | Coded states: 0=0.048, 2=0.233–0.474, 4=0.555–0.566, 5=0.627, 6=0.646–0.737, 8=0.951  |
| Rahw      | Coded states: 0=0.006, 2=0.068–0.115, 3=0.122, 4=0.142–0.157, 5=0.174, 6=0.184–0.187, 8=0.219   |
| Csur      | Coded states: 0=0.974–1.167, 2=1.346–1.739, 3=1.758, 4=1.918, 5=1.944–1.952, 7=2.191, 9=2.405, b=2.593                                  |
| Ci        | Coded states: 0=0.000, 2=0.022–0.057, 4=0.081   |
| RaZV      | Coded states: 0=0.034–0.041, 1=0.061, 2=0.097–0.102, 4=0.187–0.224, 6=0.301–0.325, 8=0.389–0.423, a=0.477, c=0.602                      |
| Zl        | Coded states: 0=0.132–0.174, 1=0.184, 2=0.193, 3=0.199–0.203  |
| Zw        | Coded states: 0=0.102–0.137, 1=0.144, 2=0.149   |
| ZwZl      | Coded states: 0=0.197, 2=0.219–0.283  |
| Ol        | Coded states: 0=0.038–0.053, 2=0.087–0.105, 4=0.116–0.123, 5=0.132, 6=0.137, 7=0.142, 9=0.158   |
| Ow        | Coded states: 0=0.044–0.074, 1=0.078, 2=0.082, 4=0.090–0.092  |
| OwOl      | Coded states: 0=0.169–0.218, 2=0.306, 4=0.334–0.359, 6=0.405  |
| Al        | Coded states: 0=0.000, 2=0.060, 3=0.061, 4=0.069–0.090, 6=0.103–0.104   |
| Aw        | Coded states: 0=0.000, 2=0.052–0.080  |
| AwAl      | Coded states: 0=0.000, 2=0.237–0.287  |
| Alo       | Coded states: 0=0.000, 2=0.039, 3=0.043, 4=0.049, 5=0.052–0.070, 7=0.078, 9=0.088   |
| Awo       | Coded states: 0=0.000, 2=0.027, 4=0.032, 5=0.037, 6=0.038–0.053   |
| AwoAlo    | Coded states: 0=0.000, 2=0.196, 4=0.218–0.278   |
| RaOIZl    | Coded states: 0=0.088–0.107, 2=0.212–0.245  |
| RaOwZw    | Coded states: 0=0.140–0.168, 1=0.179, 2=0.184–0.216   |
| RaAlZl    | Coded states: 0=0.000, 2=0.131–0.198  |
| RaAwZw    | Coded states: 0=0.000, 2=0.162–0.202  |
| RaAloAl   | Coded states: 0=0.000, 2=0.205–0.262  |
| RaAwoAw   | Coded states: 0=0.000, 2=0.179, 4=0.200–0.239   |
| RaAloOl   | Coded states: 0=0.000, 2=0.122, 4=0.154–0.214, 6=0.271, 7=0.286, 8=0.303–0.310, 9=0.327, a=0.338, c=0.423                               |
| RaAwoOw   | Coded states: 0=0.000, 2=0.176–0.268  |
| Zcp       | Coded states: 0=0.000–0.030, 2=0.301  |
| Vcp       | Coded states: 0=0.000–0.015, 2=0.043  |
| Nope      | Coded states: 0=0.000, 2=0.797–0.828, 4=0.874–0.885, 6=0.922, 8=0.953   |
| Opew      | Coded states: 0=0.000, 2=0.013, 4=0.016, 6=0.018–0.022  |
| Opesp     | Coded states: 0=0.000–0.059, 2=0.350, 3=0.414, 4=0.470–0.471, 5=0.517, 6=0.551  |
| Npor      | Coded states: 0=0.000–0.112, 2=0.219–0.283  |
| NV        | Coded states: 0=0.000, 2=0.911–1.640, 3=1.742, 4=1.861  |
| VI        | Coded states: 0=0.000, 2=0.124–0.134, 4=0.147–0.155, 5=0.161, 6=0.164, 8=0.190  |
| Vw        | Coded states: 0=0.000, 2=0.096, 3=0.097, 4=0.103–0.111, 5=0.115, 6=0.120  |
| VwVI      | Coded states: 0=0.000, 2=0.201–0.208, 4=0.222–0.245, 6=0.258  |
| VOI       | Coded states: 0=0.000, 2=0.076, 3=0.077, 4=0.082, 5=0.083, 6=0.084, 7=0.089, 8=0.090, 9=0.092, a=0.096, b=0.100, c=0.104, d=0.106–0.109 |
| VOw       | Coded states: 0=0.000, 2=0.044–0.063  |
| VOwVOI    | Coded states: 0=0.000, 2=0.178–0.181, 3=0.183, 4=0.193, 5=0.195–0.206   |
| VAl       | Coded states: 0=0.000, 2=0.057–0.059, 4=0.064–0.069, 5=0.072, 6=0.075, 7=0.078–0.083  |
| VAw       | Coded states: 0=0.000, 2=0.048–0.050, 4=0.054–0.066   |
| VAwVAl    | Coded states: 0=0.000, 2=0.240–0.280  |
| VAlo      | Coded states: 0=0.000, 2=0.039–0.0460, 4=0.051–0.054, 6=0.061–0.064   |
| VAwo      | Coded states: 0=0.000, 2=0.030–0.039, 4=0.042–0.045   |
| VAwo VAlo | Coded states: 0=0.000, 2=0.222–0.253  |
| RaVOIVl   | Coded states: 0=0.000, 2=0.175, 3=0.183, 4=0.189, 5=0.196–0.205, 6=0.210, 7=0.217   |
| RaVOwVw   | Coded states: 0=0.000, 2=0.144, 3=0.153, 4=0.156–0.175, 5=0.179, 6=0.186  |
| RaVAIVl   | Coded states: 0=0.000, 2=0.129, 4=0.150–0.173   |
| RaVAwVw   | Coded states: 0=0.000, 2=0.163–0.195  |
| RaVAloVAl | Coded states: 0=0.000, 2=0.213–0.244  |
| RaVAwoVAw | Coded states: 0=0.000, 2=0.196–0.226  |
| RaVAloVOI | Coded states: 0=0.000, 2=0.167–0.200  |
| RaVAwoVOw | Coded states: 0=0.000, 2=0.197–0.240, 4=0.261   |
| Asec      | Coded states: 0=0.000, 2=0.021–0.030, 4=0.052–0.064, 6=0.085–0.098, 8=0.127–0.129   |
| Psec      | Coded states: 0=0.000, 2=0.362, 4=0.537, 6=0.622–0.712, 8=0.900, a=1.003, b=1.050, c=1.112–1.159  |
| Graden    | Coded states: 0=0.000, 2=0.190, 4=0.221–0.232, 6=0.296, 8=0.329–0.347, a=0.400  |
| Ken       | Coded states: 0=0.000–0.006, 2=0.301  |



Appendix 2—Measurements of zoarial and zooidal characters (in mm) for *A. leucocypha*, *C. monotrema* and the eight species described in Herrera Cubilla et al. (2006) including additional fossil and extant specimens. Refer to Table 1 for character names.

| Characters | <i>A. leucocypha</i> |        |        |        |        | <i>C. monotrema</i> |        |        |        |        | <i>C. pacificiensis</i> |        |        |        |       |
|------------|----------------------|--------|--------|--------|--------|---------------------|--------|--------|--------|--------|-------------------------|--------|--------|--------|-------|
|            | N                    | Mean   | Min    | Max    | SD     | N                   | Mean   | Min    | Max    | SD     | N                       | Mean   | Min    | Max    | SD    |
| Cw         | 3                    | 8.667  | 8.000  | 9.000  | 0.577  | 7                   | 5.821  | 4.200  | 6.750  | 0.978  | 20                      | 5.494  | 4.225  | 7.625  | 0.865 |
| Ch         | 3                    | 0.116  | 0.098  | 0.126  | 0.016  | 7                   | 1.486  | 0.400  | 2.200  | 0.540  | 20                      | 1.365  | 0.400  | 2.300  | 0.420 |
| Rahw       | 3                    | 0.013  | 0.012  | 0.014  | 0.001  | 7                   | 0.249  | 0.095  | 0.338  | 0.077  | 20                      | 0.246  | 0.089  | 0.330  | 0.054 |
| Csur       | 3                    | 56.972 | 47.664 | 69.151 | 11.028 | 7                   | 30.856 | 14.105 | 40.076 | 10.070 | 20                      | 27.167 | 16.126 | 53.336 | 9.499 |
| Ci         | 3                    | 0.000  | 0.000  | 0.000  | 0.000  | 7                   | 0.105  | 0.087  | 0.132  | 0.018  | 20                      | 0.082  | 0.037  | 0.163  | 0.034 |
| RaZV       | 3                    | 3.000  | 3.000  | 3.000  | 0.000  | 7                   | 0.643  | 0.375  | 1.000  | 0.244  | 20                      | 0.600  | 0.125  | 0.875  | 0.184 |
| Zl         | 3                    | 0.410  | 0.323  | 0.494  | 0.086  | 7                   | 0.420  | 0.386  | 0.468  | 0.032  | 20                      | 0.462  | 0.381  | 0.554  | 0.048 |
| Zw         | 3                    | 0.287  | 0.228  | 0.338  | 0.056  | 7                   | 0.303  | 0.275  | 0.321  | 0.016  | 20                      | 0.321  | 0.271  | 0.383  | 0.032 |
| Ol         | 3                    | 0.313  | 0.239  | 0.378  | 0.070  | 7                   | 0.273  | 0.247  | 0.331  | 0.030  | 20                      | 0.327  | 0.286  | 0.378  | 0.026 |
| Ow         | 3                    | 0.186  | 0.135  | 0.216  | 0.044  | 7                   | 0.163  | 0.131  | 0.188  | 0.020  | 20                      | 0.168  | 0.143  | 0.195  | 0.013 |
| Al         | 3                    | 0.000  | 0.000  | 0.000  | 0.000  | 7                   | 0.202  | 0.174  | 0.253  | 0.027  | 20                      | 0.206  | 0.171  | 0.231  | 0.016 |
| Aw         | 3                    | 0.000  | 0.000  | 0.000  | 0.000  | 7                   | 0.178  | 0.147  | 0.233  | 0.029  | 20                      | 0.159  | 0.110  | 0.192  | 0.016 |
| Alo        | 3                    | 0.000  | 0.000  | 0.000  | 0.000  | 7                   | 0.155  | 0.126  | 0.185  | 0.021  | 20                      | 0.137  | 0.103  | 0.159  | 0.015 |
| Awo        | 3                    | 0.000  | 0.000  | 0.000  | 0.000  | 7                   | 0.109  | 0.091  | 0.141  | 0.018  | 20                      | 0.108  | 0.090  | 0.125  | 0.011 |
| Zcp        | 3                    | 0.000  | 0.000  | 0.000  | 0.000  | 7                   | 0.000  | 0.000  | 0.000  | 0.000  | 20                      | 0.100  | 0.000  | 1.000  | 0.308 |
| Vcp        | 3                    | 0.000  | 0.000  | 0.000  | 0.000  | 7                   | 0.000  | 0.000  | 0.000  | 0.000  | 20                      | 0.050  | 0.000  | 1.000  | 0.224 |
| NV         | 3                    | 0.000  | 0.000  | 0.000  | 0.000  | 7                   | 38.286 | 5.000  | 81.000 | 28.129 | 20                      | 13.908 | 1.000  | 32.000 | 8.540 |
| Vl         | 3                    | 0.000  | 0.000  | 0.000  | 0.000  | 7                   | 0.413  | 0.380  | 0.525  | 0.051  | 20                      | 0.421  | 0.331  | 0.536  | 0.062 |
| Vw         | 3                    | 0.000  | 0.000  | 0.000  | 0.000  | 7                   | 0.287  | 0.248  | 0.355  | 0.035  | 20                      | 0.281  | 0.212  | 0.364  | 0.046 |
| VOl        | 3                    | 0.000  | 0.000  | 0.000  | 0.000  | 7                   | 0.216  | 0.197  | 0.290  | 0.033  | 20                      | 0.237  | 0.214  | 0.273  | 0.017 |
| VOw        | 3                    | 0.000  | 0.000  | 0.000  | 0.000  | 7                   | 0.113  | 0.093  | 0.151  | 0.021  | 20                      | 0.134  | 0.102  | 0.160  | 0.014 |
| VAL        | 3                    | 0.000  | 0.000  | 0.000  | 0.000  | 7                   | 0.170  | 0.153  | 0.201  | 0.017  | 20                      | 0.174  | 0.145  | 0.225  | 0.021 |
| VAw        | 3                    | 0.000  | 0.000  | 0.000  | 0.000  | 7                   | 0.153  | 0.137  | 0.181  | 0.014  | 20                      | 0.137  | 0.120  | 0.178  | 0.014 |
| VAlo       | 3                    | 0.000  | 0.000  | 0.000  | 0.000  | 7                   | 0.125  | 0.094  | 0.157  | 0.021  | 20                      | 0.112  | 0.076  | 0.149  | 0.021 |
| VAwo       | 3                    | 0.000  | 0.000  | 0.000  | 0.000  | 7                   | 0.092  | 0.074  | 0.123  | 0.016  | 20                      | 0.083  | 0.059  | 0.120  | 0.014 |
| Asec       | 3                    | 0.000  | 0.000  | 0.000  | 0.000  | 7                   | 0.051  | 0.040  | 0.087  | 0.017  | 20                      | 0.060  | 0.033  | 0.076  | 0.011 |
| Psec       | 3                    | 0.000  | 0.000  | 0.000  | 0.000  | 7                   | 1.352  | 1.000  | 2.557  | 0.581  | 20                      | 3.884  | 2.776  | 5.542  | 0.746 |
| Ken        | 3                    | 0.000  | 0.000  | 0.000  | 0.000  | 7                   | 0.000  | 0.000  | 0.000  | 0.000  | 20                      | 0.000  | 0.000  | 0.000  | 0.000 |

Appendix 2—Extended.

| <i>C. cheethami</i> |        |        |        |        | <i>C. biporosa</i> |        |        |         |        | <i>C. exfragminis</i> |        |       |        |        |
|---------------------|--------|--------|--------|--------|--------------------|--------|--------|---------|--------|-----------------------|--------|-------|--------|--------|
| N                   | Mean   | Min    | Max    | SD     | N                  | Mean   | Min    | Max     | SD     | N                     | Mean   | Min   | Max    | SD     |
| 5                   | 7.655  | 6.600  | 9.050  | 0.912  | 8                  | 9.429  | 7.200  | 11.775  | 1.938  | 36                    | 6.066  | 3.050 | 9.250  | 1.506  |
| 5                   | 1.600  | 1.000  | 2.250  | 0.486  | 8                  | 4.138  | 2.500  | 6.300   | 1.623  | 36                    | 1.061  | 0.200 | 2.100  | 0.512  |
| 5                   | 0.206  | 0.152  | 0.249  | 0.041  | 8                  | 0.425  | 0.341  | 0.543   | 0.082  | 36                    | 0.171  | 0.044 | 0.317  | 0.065  |
| 5                   | 50.671 | 35.753 | 71.849 | 13.560 | 8                  | 98.019 | 49.576 | 157.493 | 46.805 | 36                    | 32.711 | 7.690 | 69.435 | 15.691 |
| 5                   | 0.053  | 0.031  | 0.110  | 0.032  | 8                  | 0.098  | 0.043  | 0.273   | 0.074  | 36                    | 0.080  | 0.027 | 0.123  | 0.027  |
| 5                   | 1.125  | 0.750  | 2.000  | 0.500  | 8                  | 0.641  | 0.375  | 0.875   | 0.170  | 36                    | 2.000  | 2.000 | 2.000  | 0.000  |
| 5                   | 0.597  | 0.540  | 0.666  | 0.045  | 8                  | 0.436  | 0.387  | 0.463   | 0.026  | 36                    | 0.444  | 0.359 | 0.546  | 0.045  |
| 5                   | 0.340  | 0.309  | 0.378  | 0.031  | 8                  | 0.319  | 0.259  | 0.466   | 0.066  | 36                    | 0.314  | 0.258 | 0.388  | 0.033  |
| 5                   | 0.438  | 0.394  | 0.454  | 0.025  | 8                  | 0.309  | 0.272  | 0.345   | 0.026  | 36                    | 0.311  | 0.272 | 0.389  | 0.025  |
| 5                   | 0.208  | 0.178  | 0.249  | 0.027  | 8                  | 0.181  | 0.156  | 0.212   | 0.022  | 36                    | 0.168  | 0.123 | 0.207  | 0.019  |
| 5                   | 0.215  | 0.197  | 0.231  | 0.012  | 8                  | 0.230  | 0.207  | 0.262   | 0.019  | 36                    | 0.205  | 0.150 | 0.265  | 0.023  |
| 5                   | 0.165  | 0.145  | 0.190  | 0.019  | 8                  | 0.176  | 0.159  | 0.197   | 0.012  | 36                    | 0.168  | 0.127 | 0.212  | 0.018  |
| 5                   | 0.142  | 0.132  | 0.157  | 0.009  | 8                  | 0.158  | 0.143  | 0.182   | 0.012  | 36                    | 0.150  | 0.112 | 0.188  | 0.018  |
| 5                   | 0.103  | 0.092  | 0.119  | 0.011  | 8                  | 0.118  | 0.105  | 0.132   | 0.010  | 36                    | 0.109  | 0.084 | 0.137  | 0.014  |
| 5                   | 0.000  | 0.000  | 0.000  | 0.000  | 8                  | 0.093  | 0.000  | 0.741   | 0.262  | 36                    | 0.000  | 0.000 | 0.000  | 0.000  |
| 5                   | 0.000  | 0.000  | 0.000  | 0.000  | 8                  | 0.000  | 0.000  | 0.000   | 0.000  | 36                    | 0.000  | 0.000 | 0.000  | 0.000  |
| 5                   | 10.200 | 1.000  | 23.000 | 8.701  | 8                  | 29.500 | 4.000  | 75.000  | 24.071 | 36                    | 12.500 | 1.000 | 50.000 | 11.421 |
| 5                   | 0.548  | 0.458  | 0.607  | 0.062  | 8                  | 0.411  | 0.333  | 0.493   | 0.049  | 36                    | 0.404  | 0.285 | 0.494  | 0.055  |
| 5                   | 0.318  | 0.289  | 0.344  | 0.024  | 8                  | 0.290  | 0.259  | 0.341   | 0.026  | 36                    | 0.287  | 0.216 | 0.361  | 0.036  |
| 5                   | 0.272  | 0.208  | 0.307  | 0.038  | 8                  | 0.246  | 0.211  | 0.277   | 0.019  | 36                    | 0.231  | 0.170 | 0.291  | 0.028  |
| 5                   | 0.153  | 0.137  | 0.166  | 0.011  | 8                  | 0.140  | 0.120  | 0.156   | 0.013  | 36                    | 0.133  | 0.097 | 0.190  | 0.021  |
| 5                   | 0.189  | 0.155  | 0.218  | 0.024  | 8                  | 0.198  | 0.175  | 0.240   | 0.024  | 36                    | 0.181  | 0.127 | 0.227  | 0.022  |
| 5                   | 0.144  | 0.130  | 0.161  | 0.012  | 8                  | 0.152  | 0.131  | 0.190   | 0.019  | 36                    | 0.146  | 0.110 | 0.187  | 0.019  |
| 5                   | 0.134  | 0.098  | 0.150  | 0.021  | 8                  | 0.128  | 0.116  | 0.157   | 0.014  | 36                    | 0.130  | 0.087 | 0.167  | 0.018  |
| 5                   | 0.089  | 0.073  | 0.109  | 0.013  | 8                  | 0.093  | 0.074  | 0.111   | 0.012  | 36                    | 0.091  | 0.064 | 0.117  | 0.013  |
| 5                   | 0.071  | 0.057  | 0.092  | 0.015  | 8                  | 0.051  | 0.039  | 0.068   | 0.009  | 36                    | 0.057  | 0.036 | 0.087  | 0.011  |
| 5                   | 3.311  | 2.634  | 4.144  | 0.709  | 8                  | 3.439  | 2.565  | 5.071   | 0.950  | 36                    | 3.498  | 2.302 | 5.082  | 0.819  |
| 5                   | 0.000  | 0.000  | 0.000  | 0.000  | 8                  | 0.000  | 0.000  | 0.000   | 0.000  | 36                    | 0.000  | 0.000 | 0.000  | 0.000  |

## Appendix 2—Extended.

| <i>C. incognita</i> |        |       |         |        | <i>C. multesima</i> |        |        |         |        | <i>C. surinamensis</i> |        |       |        |        | <i>C. panamensis</i> |        |        |         |        |
|---------------------|--------|-------|---------|--------|---------------------|--------|--------|---------|--------|------------------------|--------|-------|--------|--------|----------------------|--------|--------|---------|--------|
| N                   | Mean   | Min   | Max     | SD     | N                   | Mean   | Min    | Max     | SD     | N                      | Mean   | Min   | Max    | SD     | N                    | Mean   | Min    | Max     | SD     |
| 25                  | 4.685  | 3.100 | 6.825   | 0.920  | 12                  | 4.181  | 3.050  | 5.625   | 0.929  | 48                     | 5.324  | 1.050 | 9.900  | 1.953  | 52                   | 6.347  | 3.950  | 10.250  | 1.633  |
| 25                  | 1.816  | 0.800 | 2.700   | 0.532  | 12                  | 2.732  | 1.800  | 3.950   | 0.616  | 48                     | 1.477  | 0.200 | 2.500  | 0.574  | 52                   | 3.290  | 2.100  | 4.800   | 0.670  |
| 25                  | 0.391  | 0.198 | 0.581   | 0.108  | 12                  | 0.658  | 0.541  | 0.824   | 0.093  | 48                     | 0.287  | 0.062 | 0.533  | 0.084  | 52                   | 0.544  | 0.293  | 0.923   | 0.151  |
| 25                  | 22.547 | 8.983 | 43.246  | 8.474  | 12                  | 23.650 | 12.051 | 42.850  | 10.093 | 48                     | 28.826 | 1.196 | 83.033 | 19.531 | 52                   | 47.744 | 19.771 | 108.769 | 20.222 |
| 25                  | 0.115  | 0.069 | 0.177   | 0.033  | 12                  | 0.104  | 0.030  | 0.154   | 0.034  | 48                     | 0.070  | 0.019 | 0.239  | 0.041  | 52                   | 0.083  | 0.033  | 0.157   | 0.033  |
| 25                  | 0.200  | 0.000 | 2.000   | 0.439  | 12                  | 0.115  | 0.000  | 0.625   | 0.203  | 48                     | 1.062  | 0.250 | 2.000  | 0.307  | 52                   | 1.017  | 0.875  | 2.000   | 0.140  |
| 25                  | 0.392  | 0.348 | 0.446   | 0.027  | 12                  | 0.385  | 0.347  | 0.418   | 0.021  | 48                     | 0.529  | 0.404 | 0.688  | 0.058  | 52                   | 0.561  | 0.437  | 0.759   | 0.064  |
| 25                  | 0.321  | 0.261 | 0.413   | 0.044  | 12                  | 0.327  | 0.238  | 0.426   | 0.043  | 48                     | 0.365  | 0.241 | 0.471  | 0.051  | 52                   | 0.410  | 0.323  | 0.565   | 0.053  |
| 25                  | 0.249  | 0.189 | 0.286   | 0.024  | 12                  | 0.256  | 0.225  | 0.300   | 0.021  | 48                     | 0.373  | 0.258 | 0.497  | 0.051  | 52                   | 0.389  | 0.275  | 0.667   | 0.064  |
| 25                  | 0.144  | 0.119 | 0.170   | 0.012  | 12                  | 0.149  | 0.130  | 0.170   | 0.011  | 48                     | 0.207  | 0.120 | 0.264  | 0.032  | 52                   | 0.236  | 0.168  | 0.381   | 0.033  |
| 25                  | 0.209  | 0.161 | 0.271   | 0.027  | 12                  | 0.222  | 0.187  | 0.249   | 0.021  | 48                     | 0.230  | 0.159 | 0.345  | 0.039  | 52                   | 0.269  | 0.189  | 0.408   | 0.037  |
| 25                  | 0.181  | 0.145 | 0.215   | 0.022  | 12                  | 0.185  | 0.151  | 0.214   | 0.017  | 48                     | 0.171  | 0.119 | 0.250  | 0.027  | 52                   | 0.202  | 0.150  | 0.387   | 0.035  |
| 25                  | 0.156  | 0.121 | 0.214   | 0.023  | 12                  | 0.146  | 0.112  | 0.194   | 0.020  | 48                     | 0.175  | 0.105 | 0.269  | 0.037  | 52                   | 0.197  | 0.108  | 0.252   | 0.028  |
| 25                  | 0.120  | 0.091 | 0.169   | 0.018  | 12                  | 0.112  | 0.098  | 0.147   | 0.014  | 48                     | 0.113  | 0.068 | 0.157  | 0.019  | 52                   | 0.129  | 0.098  | 0.166   | 0.016  |
| 25                  | 0.040  | 0.000 | 1.000   | 0.200  | 12                  | 0.000  | 0.000  | 0.000   | 0.000  | 48                     | 0.083  | 0.000 | 1.000  | 0.279  | 52                   | 0.019  | 0.000  | 1.000   | 0.139  |
| 25                  | 0.000  | 0.000 | 0.000   | 0.000  | 12                  | 0.000  | 0.000  | 0.000   | 0.000  | 48                     | 0.000  | 0.000 | 0.000  | 0.000  | 52                   | 0.000  | 0.000  | 0.000   | 0.000  |
| 25                  | 48.960 | 5.000 | 102.000 | 31.085 | 12                  | 39.250 | 7.000  | 139.000 | 36.849 | 48                     | 0.000  | 0.000 | 0.000  | 0.000  | 52                   | 0.000  | 0.000  | 0.000   | 0.000  |
| 25                  | 0.363  | 0.279 | 0.440   | 0.040  | 12                  | 0.361  | 0.305  | 0.403   | 0.029  | 48                     | 0.000  | 0.000 | 0.000  | 0.000  | 52                   | 0.000  | 0.000  | 0.000   | 0.000  |
| 25                  | 0.274  | 0.206 | 0.336   | 0.030  | 12                  | 0.270  | 0.210  | 0.327   | 0.030  | 48                     | 0.000  | 0.000 | 0.000  | 0.000  | 52                   | 0.000  | 0.000  | 0.000   | 0.000  |
| 25                  | 0.210  | 0.157 | 0.257   | 0.024  | 12                  | 0.211  | 0.183  | 0.238   | 0.017  | 48                     | 0.000  | 0.000 | 0.000  | 0.000  | 52                   | 0.000  | 0.000  | 0.000   | 0.000  |
| 25                  | 0.119  | 0.095 | 0.149   | 0.015  | 12                  | 0.123  | 0.093  | 0.152   | 0.018  | 48                     | 0.000  | 0.000 | 0.000  | 0.000  | 52                   | 0.000  | 0.000  | 0.000   | 0.000  |
| 25                  | 0.159  | 0.134 | 0.193   | 0.017  | 12                  | 0.161  | 0.125  | 0.210   | 0.022  | 48                     | 0.000  | 0.000 | 0.000  | 0.000  | 52                   | 0.000  | 0.000  | 0.000   | 0.000  |
| 25                  | 0.132  | 0.095 | 0.164   | 0.015  | 12                  | 0.140  | 0.118  | 0.183   | 0.019  | 48                     | 0.000  | 0.000 | 0.000  | 0.000  | 52                   | 0.000  | 0.000  | 0.000   | 0.000  |
| 25                  | 0.110  | 0.074 | 0.137   | 0.018  | 12                  | 0.103  | 0.081  | 0.124   | 0.012  | 48                     | 0.000  | 0.000 | 0.000  | 0.000  | 52                   | 0.000  | 0.000  | 0.000   | 0.000  |
| 25                  | 0.080  | 0.058 | 0.098   | 0.011  | 12                  | 0.079  | 0.070  | 0.101   | 0.011  | 48                     | 0.000  | 0.000 | 0.000  | 0.000  | 52                   | 0.000  | 0.000  | 0.000   | 0.000  |
| 25                  | 0.216  | 0.159 | 0.347   | 0.048  | 12                  | 0.161  | 0.055  | 0.234   | 0.054  | 48                     | 0.255  | 0.026 | 0.456  | 0.078  | 52                   | 0.344  | 0.167  | 0.599   | 0.101  |
| 25                  | 12.428 | 7.082 | 22.538  | 3.839  | 12                  | 7.066  | 4.518  | 9.459   | 1.596  | 48                     | 10.837 | 2.915 | 16.660 | 3.549  | 52                   | 12.763 | 5.082  | 23.450  | 4.374  |
| 25                  | 0.000  | 0.000 | 0.000   | 0.000  | 12                  | 0.000  | 0.000  | 0.000   | 0.000  | 48                     | 0.021  | 0.000 | 1.000  | 0.144  | 52                   | 0.000  | 0.000  | 0.000   | 0.000  |